

Thermophysical Investigation of Asteroid Surfaces I: Characterization of Thermal Inertia

Eric M. MacLennan^{a,b,*}, Joshua P. Emery^{a,c}

^a*Earth and Planetary Sciences Department, Planetary Geosciences Institute, The University of Tennessee,
Knoxville, TN 37996, USA*

^b*Department of Physics, P.O. Box 64, 00560 University of Helsinki, Finland*

^c*Department of Physics and Astronomy, Northern Arizona University, NAU Box 6010, Flagstaff, AZ
86011, USA*

Abstract

The thermal inertia of an asteroid is an indicator of the thermophysical properties of the regolith and is determined by the size of grains on the surface. Previous thermophysical modeling studies of asteroids have identified or suggested that object size, rotation period, and heliocentric distance (a proxy for temperature) are important factors that separately influence thermal inertia. In this work we present new thermal inertia values for 239 asteroids and model all three factors in a multi-variate model of thermal inertia. Using multi-epoch infrared data of this large set of objects observed by WISE, we derive the size, albedo, thermal inertia, surface roughness, and sense of spin using a thermophysical modelling approach that doesn't require *a priori* knowledge of an object's shape or spin axis direction. Our thermal inertia results are consistent with previous values from the literature for similarly sized asteroids, and we identify an excess of retrograde rotators among main-belt asteroids $< 8\text{ km}$. We then combine our results with thermal inertias of 220 objects from the literature to construct a multi-variate model and quantify the dependency on asteroid diameter, rotation period, and surface temperature. This multi-variate model, which accounts for co-dependencies between the three independent variables, identifies asteroid diameter and surface temperature as strong controls on thermal inertia.

Keywords:

1. Introduction

The thermophysical characterization of regolith—the unconsolidated, heterogeneous, rocky material covering the surface of other planetary bodies—is an important part of understanding the processes and evolution of airless bodies of the Solar System. By comparing

*corresponding author

Email addresses: eric.maclennan@helsinki.fi (Eric M. MacLennan),
mv.helsinki.fi/home/maceric/home.html (Eric M. MacLennan)

thermal observations to thermophysical models, the regoliths of asteroids can be characterized by their thermal inertia (Γ). Thermal inertia is defined as $\Gamma = \sqrt{k\rho c_s}$, where k is the effective thermal conductivity of the regolith, ρ is the bulk density, and c_s is the bulk specific heat capacity. Thermophysical models (TPMs) are often used to derive thermal inertia of a body by comparing the observed fluxes to those estimated from the model.

The largest asteroids (ranging from $\sim 500 - 1000$ km) in the Solar System—e.g., (1) Ceres, (2) Pallas, and (4) Vesta—exhibit global¹ thermal inertias (Mueller and Lagerros, 1998; Capria et al., 2014; Alí-Lagoa et al., 2020; Rognini et al., 2020) that are comparable to the Moon ($\approx 50 \text{ J m}^{-2} \text{ K}^{-1} \text{ s}^{-1/2}$; Wesselink, 1948; Cremers, 1975; Bandfield et al., 2011; Hayne et al., 2017). On the other hand, smaller asteroids such as (433) Eros, (162173) Ryugu, (101955) Bennu, and (25143) Itokawa have approximate, estimated thermal inertias of, respectively 150, 225, 350, and $700 \text{ J m}^{-2} \text{ K}^{-1} \text{ s}^{-1/2}$ (Mueller, 2007; Dellagiustina et al., 2019; Shimaki et al., 2020). The observed correlation among asteroids of thermal inertia with size (Delbo' et al., 2015; Hanuš et al., 2018; Rozitis et al., 2018) suggests that only larger asteroids harbor a fine-grained regolith, whereas smaller asteroid regoliths are comprised of coarse sand-sized particles and/or a higher fraction of blocky material. This general trend suggest that asteroid size is a large factor in determining the state of asteroid regolith.

In addition to asteroid size, the rotation period has been suggested as a factor that controls asteroid thermal inertia. Harris and Drube (2016) used a thermal inertia estimator based on the near-Earth Asteroid Thermal Model (NEATM; Harris, 1998) and found a positive correlation between rotation period, P_{rot} , and thermal inertia. This correlation was attributed to deeper penetration of the thermal wave into subsurface material that was higher in thermal conductivity and/or bulk density (caused by smaller porosities). The thermal wave can be expressed in terms of the thermal skin depth, l_s , which is the length scale over which the diurnal temperature variation changes by a factor of $e \approx 2.71828$: $l_s = \sqrt{kP_{\text{rot}}/2\pi\rho c_s}$. On the other hand, Marciak et al. (2019) used a TPM to derive thermal inertias of slow-rotators and found no correlation between the two variables.

For airless bodies, the effective thermal conductivity is comprised of a solid and radiative component that correspond to different heat transport mechanisms in a regolith (e.g., Piqueux and Christensen, 2009). If radiation is the dominant form of heat propagation then thermal inertia is expected to vary as $T^{3/2}$ (Delbo' et al., 2015) because the radiative conductivity is proportional to T^3 (Vasavada et al., 1999). Rozitis et al. (2018) characterized the thermal inertia variation with heliocentric distance (as a proxy for temperature) for three individual asteroids and found a wide range of scaling dependencies for each. In particular, they found that the thermal inertia of two of the studied asteroids had stronger dependencies on heliocentric distance than the $T^{3/2}$ scaling law. On the other hand, the thermal inertia of Bennu as measured by the OSIRIS-REx spacecraft showed no evidence of temperature dependence (Rozitis et al., 2020).

Generally speaking, the temperature distribution of a surface is influenced by the thermal inertia. All other factors kept constant, higher thermal inertia surfaces have a smaller difference in sunlit and nighttime temperature, while low thermal inertia surfaces exhibit a

¹Anomalously high thermal inertias have been measured for some localized areas on Ceres, for example.

greater diurnal temperature differences. As demonstrated in [MacLennan and Emery \(2019\)](#), thermal emission observations taken at pre- and post-opposition (multi-epoch) are sensitive to differences in the temperature distribution and thus can be used to estimate the thermal inertia. This technique is effective at estimating the thermal inertia when no shape or spin axis information about an asteroid is known *a priori*.

The sense of spin (i.e. retrograde or prograde) for an asteroid can also be estimated using multi-epoch observations ([Mueller, 2007](#); [MacLennan and Emery, 2019](#)). Because there exists a time-lag between the period of maximum heating at local noon and when the maximum surface temperature is reached, a morning-afternoon dichotomy is present on surfaces with a non-zero thermal inertia. Thus, the morning and afternoon sides will correspond, respectively, or inversely, to pre- and post-opposition viewing aspects, depending on the object's sense of rotation.

In this work we use multi-epoch observations and the methods of [MacLennan and Emery \(2019\)](#) to derive thermal inertia and size estimates for 239 asteroids. In some cases, we constrain the roughness and object's sense of spin. Comparing our results to the benchmark study of [MacLennan and Emery \(2019\)](#) and other literature works, we assess the ability of this technique to estimate these TPM parameters. We then incorporate diameter, rotation period, and temperature into a unifying multi-factor thermal inertia model that simultaneously accounts for these variables. In a follow-up work, we produce grain size estimates from the thermal inertia values presented here and investigate compositional differences in regolith properties.

2. Observations & Thermophysical Modeling

Data from the Wide-field Infrared Survey Explorer (WISE) are used for model fitting. Absolute magnitude (H_V) and slope parameter (G_V) from [Oszkiewicz et al. \(2011\)](#), and P_{rot} from the Asteroid Lightcurve Database (ALCDB; [Warner et al., 2009](#)) are used as TPM input values for each object ([Table 1](#)) along with mean and peak-to-trough fluxes calculated from sparse lightcurve data. The thermophysical modeling approach presented in [MacLennan and Emery \(2019\)](#) is used, as briefly summarized below, and we thus select objects that were observed by WISE at pre- and post-opposition. In [MacLennan and Emery \(2019\)](#) we extracted and used the mean and peak-to-trough flux quantities from thermal light curves via simple geometric averaging and subtracting the maximum and minimum values, respectively. Although those simplistic calculations are useful for dense lightcurve data, they can be problematic when used on sparsely sampled lightcurves for reasons discussed in Sec. 2.2.

2.1. Data Description

In 2010, WISE mapped the entire sky at four photometric filters: referred to as W1, W2, W3, and W4 with wavelength centers near 3.4, 4.6, 12, and 22 μm , respectively ([Wright et al., 2010](#)). WISE was designed as an astrophysics all-sky mapping mission, but its infrared sensors detected the thermal emission from warm asteroids in the inner solar system. A data-processing enhancement (NEOWISE; [Mainzer et al., 2011a](#)) to the nominal pipeline

was thus designed and implemented to identify and measure the emission from these solar system objects. Since the initial mapping phase in which all four bands were operational (the cryogenic phase) the WISE telescope operated at shorter wavelengths and was later reactivated (NEOWISE-R). In this work, we only use the cryogenic phase of the mission.

Since WISE does not target moving objects, the asteroids were only observed for a relatively brief (typically less than a couple days) period of time, referred to as an epoch. Each epoch of observations nominally yielded between 10 to 20 individual measurements that were separated by ≈ 1.6 hr—the orbital period of the spacecraft. NEOWISE flux data are stored at the Infrared Processing and Analysis Center² (IPAC) and each detection of a moving solar system object was reported to the Minor Planet Center³ (MPC), where the information regarding the sky position and time of observation can be retrieved. In downloading the data, we used the MPC observation file to parse the WISE All-Sky Single Exposure (L1b) catalog on IPAC’s Infrared Science Archive (IRSA) and select detections acquired within 10 s of that reported to the MPC, with a search cone of $10''$. We shift the isophotal wavelengths of the filters and perform a color-correction to the fluxes (Wright et al., 2010) using a spectrum calculated from NEATM temperatures, as per the recommendation of the WISE Explanatory supplement Cutri et al. (2012). Since the criteria used to parse IPAC can potentially return contaminated (i.e., by a background star or galaxy) or unwanted (non-asteroid) infrared sources from the catalog, we employ Peirce’s Criterion (Peirce, 1852; Gould, 1855) on the infrared color, W4–W3, as detailed in MacLennan and Emery (2019), to better ensure the inclusion of only uncontaminated observations of asteroids.

2.2. Sparse Lightcurve Sampling

Due to the nature of WISE’s orbit and survey cadence, a given asteroid will be observed an average of a dozen times during each epoch. This sparse sampling does not allow for the construction of a well-characterized rotational lightcurve. Since observations are taken at irregularly-spaced rotational phases—depending both on the number of observations and the object’s rotation period—information may be missing for crucial points of an object’s lightcurve, such as the minima and maxima. The WISE telescope orbital cadence may over-sample certain rotational phases, which poses a challenge for extracting scientifically-important characteristics such as the mean and peak-to-trough range of the lightcurve. We present here a technique for extracting these parameters from a statistically-scant photometric set, given *a priori* knowledge of the object’s rotation period. We note that applying this approach to the objects in MacLennan and Emery (2019) does not significantly change the results of that work. The formulations below are similar to the analytical solution of a least-squares sinusoidal fit to lightcurve data, with some differences. We show the results of this technique on (91) Aegina in Fig. 1 and report the fluxes computed from this method for all asteroids studied in this work, along with observing circumstances, in Table 2.

First, we step through each possible pair of flux measurement points and compute their average and difference so that for the i th and j th point the mean and range (absolute differ-

²<http://irsa.ipac.caltech.edu/Missions/wise.html>

³<http://www.minorplanetcenter.net/>

ence) are m_{ij} and r_{ij} , respectively. The flux uncertainties (δf) are summed in quadrature, so that the errors in each mean (δm_{ij}) and range (δr_{ij}) are given by:

$$2\delta m_{ij} = \delta r_{ij} = \sqrt{\delta f_i^2 + \delta f_j^2} \quad (1)$$

Note the factor of 2 associated with the mean, as per the rules of error propagation. Proceeding, we calculate a weighting factor, s_{ij} , based on the separation in rotational phase (normalized to 2π radians) of the two points, $\phi_i - \phi_j$. In this weighting scheme, pairs that sample around the same rotational phase or half a turn ($\phi_i - \phi_j = 0, 1/2$), are given a weight of $s_{ij} = 0$, and pairs separated by a quarter turn ($\phi_i - \phi_j = 1/4, 3/4$) have $s_{ij} = 1$, with linear scaling of the weights between these two extremes (top right panel of Fig. 1).

The weighted flux mean (\bar{F}) and error ($\delta \bar{F}$) are then given by:

$$\bar{F} = \frac{\sum_i \sum_{j>i} m_{ij} \delta m_{ij}^{-2} s_{ij}^2}{\sum_i \sum_{j>i} \delta m_{ij}^{-2} s_{ij}^2} \quad (2)$$

and

$$\delta \bar{F} = \sqrt{\frac{\sum_i \sum_{j>i} \delta m_{ij}^2 s_{ij}^2}{\sum_i \sum_{j>i} s_{ij}^2}} \quad (3)$$

Pair means are shown in the bottom left panel of Fig. 1, along with the result of applying Eq. 3 to the data.

In order to formulate the lightcurve range ($\diamond F$) and error ($\delta \diamond F$) we employ a slightly different approach than that used for the mean. For the i th point, we iterate across every combination of differences between points, to select the j th point that which maximizes the range between the two: r_{ij} . Difference pairs that are separated by a quarter-turn of the asteroid are given more weight based off the pair weight, s_{ij} , from above (i.e., the factor $(1 - \cos(4\pi s_{ij}))^2$):

$$\diamond F = 2 \frac{\sum r_{ij} \delta r_{ij}^{-2} (1 - \cos(4\pi s_{ij}))}{\sum \delta r_{ij}^{-2} (1 - \cos(4\pi s_{ij}))^2} \quad (4)$$

and

$$\delta \diamond F = \sqrt{\frac{\sum \delta r_{ij}^2 s_{ij}^2}{\sum s_{ij}^2}} \quad (5)$$

The factor, $1 - \cos(4\pi s_{ij})$, is used to scale the s_{ij} factor in Eq. 4 in order to create a weight function based off a sinusoid, as opposed to a linear relationship, because we wish to add weights to the error estimation that are appropriate for a rotating non-spherical object. However, this factor is not used in Eq. 5 since doing so would create a penalty for data that do not resemble a sine function, such as for shapes that significantly deviate from an ellipsoid. Employing Eq. 4 is essentially the same as extracting the peak-to-trough range of the the best-fit sinusoid to the original lightcurve. Pair ranges are shown in the bottom right panel of Fig. 1 with the function given in Eq. 5 in red.

2.3. TPM Implementation

The TPM and data-fitting approach used here is identical to that presented in MacLennan and Emery (2019) and is summarized briefly here. First, the surface temperatures are modeled across the surface of a spherical object constructed of discrete facets. The one-dimensional heat transfer equation (Fourier's Law) is numerically solved using the estimated insolation (incoming solar radiation) as the energy input. The discrete facets are characterized as planar faces and divided into latitude bins. A diurnal cycle is simulated by rotating the facets about the object's spin axis. Two types of surfaces are modeled: a perfectly smooth surface in which only direct insolation is considered, and a rough surface that is comprised of spherical-section craters, for which direct and multiply-scattered insolation and thermally re-radiated energy from other facets are calculated. Surface roughness is characterized by the mean surface slope ($\bar{\theta}$; Hapke, 1984), which is varied by differing both the opening angle of the crater (γ) and the proportion of surface area that is covered by those craters (f_R); the latter is implemented when calculating the flux contribution of rough and smooth surfaces.

We use parameterized forms of the energy balance equation and heat diffusion equation (see MacLennan and Emery, 2019, for further details), which reduces the number of TPM variables that are necessary to calculate a unique surface temperature distribution, in order to construct temperature reference tables and reduce the computational time. In this scheme, the necessary information required for rough surface temperature calculation is the bond albedo (A_b), thermal parameter,

$$\Theta = \frac{\Gamma}{\varepsilon_B \sigma_0 T_{eq}^3} \sqrt{\frac{2\pi}{P_{rot}}}, \quad (6)$$

and sub-solar latitude; whereas the smooth surface only requires the thermal parameter and sub-solar latitude. In Eq. 6, σ_0 is the Stefan-Boltzmann constant, ε_B is the bolometric emissivity, and T_{eq} is the sub-solar equilibrium temperature:

$$\varepsilon_B \sigma_0 T_{eq}^4 = \frac{S_\odot (1 - A)}{R_{au}^2}. \quad (7)$$

In the case of smooth surfaces A_b is implicitly accounted for in the T_{eq} term and we thus do not need to specify it to run the TPM. In the case of rough surfaces, A_b explicitly determines the amount of multiple-scattering within a crater. Thus we run the rough surface for various values of A_b , as detailed in the next paragraph. The surface temperatures for both the smooth and rough surface TPMs are stored in reference tables, expressed as $T' = T/T_{eq}$.

The smooth-surface TPM was run for 46 values of sub-solar latitude (0° to 90° in 2° increments) and 116 values of the thermal parameter (spaced equally in \log_{10} space, from 0 to 450) whereas the rough-surface TPM was iterated across 3 values of $\gamma = \{45^\circ, 68^\circ, 90^\circ\}$ and run for 46 values of sub-solar latitude (0° to 90° in 2° increments), 116 values of the thermal parameter (spread out in \log_{10} space, from 0 to 450), and 7 values of $A_{grid} = \{0, 0.1, 0.2, 0.3, 0.4, 0.5, 1\}$. These parameters are chosen to ensure an accuracy within 1%

between the surface temperature values interpolated from the grid and those calculated using the exact model parameters.

Surface temperatures calculated for spheres are mapped to prolate ellipsoids ($b/c = 1$, where $a \geq b \geq c$) using closed-form algebraic expressions (i.e., Appendix B in [MacLennan and Emery, 2019](#)) in order to model elongated bodies of differing a/b axis ratio. Fluxes are calculated for the given observing circumstances by interpolation of the flux calculated using the tabulated temperatures. The flux calculated from the interpolated grid are within 1% of the flux calculated by running the TPM with the exact thermophysical and observing parameters. Finally, thermal flux is calculated by a summation of the individual flux contributions from smooth surface (B_{smooth}) and crater elements (B_{rough}) and using a grey-body approximation, with spectral emissivity ($\varepsilon_\lambda = 0.9$):

$$F(\lambda) = \frac{\varepsilon_\lambda}{\Delta_{au}^2} \sum_S \{(1 - f_R)B_{smooth}(\lambda, T) \cos(e) + f_R a_R v \Lambda B_{rough}(\lambda, T) \cos(e_R)\} a_f \quad (8)$$

e_\angle and $e_{R\angle}$ are the emission angle of the flat facet and crater element. The facet area is a_f , and the crater element areas are $a_R = 2/(m(1 + \cos \gamma))$ where $m = 40$ is the number of crater elements ([Emery et al., 2014](#)). We note that the flux calculation formula stated in [MacLennan and Emery \(2019\)](#) neglects the latter two parameters for a rough surface and that the one presented here is correct. For rough (crater) elements, v is used to indicate if it is visible ($v = 1$) or not ($v = 0$) to the observer, and Λ is a correction factor used to adjust fluxes that deviate from the pre-computed A_{grid} values (for more details, see [MacLennan and Emery, 2019](#)).

In our data-fitting approach, the shape, spin vector ($\lambda_{eclip}, \beta_{eclip}$), roughness, and thermal inertia are left as free parameters that we select from a pre-defined sample space. A sphere and prolate ellipsoids with a/b axis ratios of 1.25, 1.75, 2.5, and 3.5 are used. For each of these shapes, we sample 25 predefined thermal inertia values, 3 default roughness (mean surface slope; $\bar{\theta}$) values, and 235 spin vectors. We search for the best-fit D_{eff} for each combination of these parameters. Each individual value of γ is paired with a value of $f_R = \{1/2, 4/5, 1\}$ that correspond to default mean surface slopes of $\bar{\theta} = \{10^\circ, 29^\circ, \text{ and } 58^\circ\}$. The thermal inertia points are uniformly distributed in \log_{10} space from 0 to 3000 $J m^{-2} K^{-1} s^{-1/2}$, and the spin vectors are spread evenly throughout the celestial sphere, which is achieved by constructing a Fibonacci lattice in spherical coordinates (e.g., [Swinbank and Purser, 2006](#)). For each shape/spin vector/ $\bar{\theta}/\Gamma$ combination we use a routine to find the D_{eff} value which minimizes χ^2 . To place confidence limits on each of the fitted parameters, we use the reduced χ^2 statistic ($\tilde{\chi}^2 = \chi^2/\nu$) to express the solutions within a 1σ range as $\tilde{\chi}^2 < \tilde{\chi}_{min}^2(1 + \sqrt{2\nu}/\nu)$ and consider solutions with $\tilde{\chi}_{min}^2 < 8$ to be acceptable.

2.4. Characteristic Temperature Calculation

Estimating the temperature of an asteroid at the time of observation is necessary to perform our multivariate analysis. Calculating a single value for the characteristic surface temperature of an asteroid, which exhibits wide temperature variations across the surface, can be approached in a few different ways. One approach is to rely on the estimation of the

sub-solar temperature, based on the theoretical energy balance formulation (Eq. 7). This approach has two problems: the assumptions made in the energy balance equation will often lead to the overestimation of the true sub-solar temperature, and there is a low likelihood that the sub-observer point is close to the sub-solar point.

In order to overcome these possible problems we calculate the color temperature, T_c , by independently fitting a blackbody curve (via least-squares minimization) to the asteroid's W3 and W4 thermal fluxes. This approach implicitly accounts for the spatial variation in surface temperatures and explicitly calculated from the data itself, as opposed to using the sub-solar temperature, T_{ss} . We found that a blackbody assumption ($\varepsilon_B = 1$) does not introduce uncertainty in the temperature, as any non-zero value would not shift the peak of a blackbody emission curve, which is related to the temperature through Wein's Law. Fitting a blackbody function directly to the WISE dataset is straightforward, but retroactively applying this approach to thermal inertias found in the literature is less so. To estimate T_c for asteroids in the literature we calculate the relationship between the NEATM sub-solar temperature T_{ss} ⁴ (Eq. 9) and T_c for our set of asteroids: $T_{ss} = 0.777 \times T_c^{1.063(\pm 0.005)}$. This best-fit equation, along with the data, is depicted in Fig. 2 by the dotted red line and blue dot-dash lines showing the 1σ uncertainty bounds in the exponent. We invert this equation and use it on the TPM results from previous works, since it is often not the case that a temperature is reported with the thermal inertia. For these objects we use,

$$T_{ss} = \left[\frac{S_\odot(1 - A)}{\eta \varepsilon_B \sigma_0 R_{\text{au}}^2} \right]^{1/4}, \quad (9)$$

and assume a beaming parameter of $\eta = 1.1$ (the approximate mean for main-belt objects Mainzer et al., 2011b), to compute T_{ss} and then T_c .

3. Results and Analysis

The TPM was run for 239 objects: 3 near-Earth asteroids (NEAs), 2 Mars-crossers (MCs), and 234 main-belt asteroids (MBAs). Table 3 shows the best-fit and 1σ uncertainties for the effective diameter (D_{eff}), geometric albedo (p_V), thermal inertia (Γ), surface roughness ($\bar{\theta}$), elongation (a/b ; prolate ellipsoid axis ratio), and sense of spin (\uparrow for prograde and \downarrow for retrograde) for all 239 objects, with the results of the 21 object from MacLennan and Emery (2019) included at the top. Diameter errors for $D_{\text{eff}} > 10$ km are below 15% of the diameter value, but can be as high as 40% for objects smaller than 10 km. Upper and lower thermal inertia uncertainties are, on average, 180% and 67% of the reported value, respectively. Surface roughness could only be estimated for 97 of the 239 (41%) objects. Informed by the model validation tests of MacLennan and Emery (2019), we use spherical shapes to make an estimate of the sense of spin, which could be unambiguously estimated for all but 17 of the 239 (93%) objects. In some cases, TPM fits only allowed for a lower or

⁴This was calculated during the calibration of WISE data for each observation and then averaged for each object.

upper bound on the surface roughness. Note that objects with TPM fits having $\tilde{\chi}_{min}^2 > 8$ are marked in [Table 3](#) and should be used with caution.

We combine our sense of spin results with that in [MacLennan and Emery \(2019\)](#) and compare to the spin poles of object shapes that are in the DAMIT⁵ database (Database of Asteroid Models from Inversion Techniques; [Durech, 2010](#)). In total, there are 101 objects both datasets and 77 of them have sense of spin estimate that agree. If we assume that the DAMIT spin axis estimates have 100% accurate sense of spin, then the TPM has a $76.2\% \pm 4.3\%$ success rate, based on binomial probability distribution. [MacLennan and Emery \(2019\)](#) demonstrated that the sense of spin success rate is dependent on the thermal inertia, with a success rate of 65 – 80% in the range $\Gamma = 40 - 150 \text{ J m}^{-2} \text{ K}^{-1} \text{ s}^{-1/2}$ when using spheres. The fact that this agrees with our comparison in this work is encouraging, yet more investigation into model development should be performed in an effort to improve the success rate of constraining the sense of spin using TPMs.

Based on the TPM results, we observe a correlation between the retrograde/prograde ratio and asteroid size. We bin our set of objects by diameter in [Fig. 3](#) and assign the uncertainty (shown as vertical lines) of the bins to be the number of objects with indeterminate spins in that diameter bin, or the $\sim 76\%$ success rate based on our check with DAMIT spins—whichever is larger. The horizontal lines that transect some of the spin/diameter bins indicate the number of NEAs in that bin. The fraction of prograde to retrograde rotators in most of the bins in our sample are statistically-indistinguishable. Only asteroids with $D_{eff} < 8 \text{ km}$ show a statistically-significant excess of retrograde rotators, which we discuss in [Sec. 4](#).

The diameter estimates from NEATM fits presented by the WISE team (i.e., [Mainzer et al., 2011b](#); [Masiero et al., 2011](#)) are reported for each sighting, or epoch, which can have pre- or post-opposition geometry. Because the NEATM assumes a spherical shape, it is most-useful to compare the volume-equivalent, effective diameters of the ellipsoid to their values. We present a comparison of these diameter pairs (D_{eff}^{WISE}) to the diameter values (one per object; D_{eff}^{TPM}) obtained here, and plot them (colored by observing geometry) in [Fig. 4](#). There is a general agreement of within $\pm 15\%$ between the two datasets, with a few important notes. Firstly, for objects $\sim 30 \text{ km}$ and above, our TPM diameters are slightly higher than the NEATM model estimates of the WISE team. This discrepancy is likely due to the inherent model differences between our TPM approach and the NEATM used by the WISE team. Secondly, objects smaller than 20 km exhibit, on average, 5% lower diameters from our TPM analysis than from the WISE NEATM analysis. Lastly, we highlight an interesting trend seen in [Fig. 4](#) for different observing geometries: pre-opposition (upright triangles) NEATM diameters are more similar to the TPM-derived diameters for objects smaller than $\sim 8 \text{ km}$ while the post-opposition (downward triangles) diameters remain consistently offset from our TPM diameters at smaller sizes. From this result we can conclude that the majority (over 50%) of small diameter asteroids are retrograde rotators—which serves as an independent check on our sense of spin results ([Sec. 3](#)).

A handful of asteroids with thermal inertias presented here have previous estimates from

⁵<http://astro.troja.mff.cuni.cz/projects/asteroids3D/web.php>

the works of Hanuš et al. (2018), Marciniak et al. (2019), and Pravec et al. (2019). We depict all these estimates in Fig. 5. In several instances, two thermal inertias were reported because two shape/spin solutions were used, for which we show both values. In nearly all cases there is good agreement between our estimate and the previously-reported value (i.e., the error bars overlap). Only (1741) Giclas shows a significant difference between our estimate and the previous estimates (Pravec et al., 2019)—our estimate is smaller by around a factor of three and there is no overlap at the 1σ level. We note that our retrograde sense of spin estimate for Giclas is opposite to that of the prograde shape solution in Pravec et al. (2019), and our roughness estimate is much higher ($\approx 58^\circ$ compared to 38.8°). If we were to only use the prograde solutions from our fitting, our estimate would not change, but if we consider higher roughness values that have a higher $\tilde{\chi}^2_{min}$ then the uncertainty in our estimate would overlap with Pravec et al. (2019). This difference in thermal inertia may most likely be caused by the ellipsoidal shape assumption used in TPM fitting.

In addition to comparing the diameters and thermal inertias of individual objects from our dataset to the findings from the WISE team, we compare thermal inertia results of 220 asteroids from previous TPM works. Combined with the results from MacLennan and Emery (2019), we present thermal inertia estimates for 250 asteroids (19 of which have previous determinations in other works), an approximate doubling over the tally of literature values (Table 4)—mostly in the 5–50 km size range. We highlight previous authors and works that have presented thermal inertia estimates for 5 objects or more, notably Alí-Lagoa et al. (2020); Hanuš et al. (2015); Hanuš et al. (2016); Hanuš et al. (2018); Marciniak et al. (2018, 2019). Alí-Lagoa et al. (2020) targets some of the largest asteroids in the Main-Belt. Similar to this work and MacLennan and Emery (2019), Hanuš et al. (2015) and Hanuš et al. (2018) have collectively modeled dozens of asteroids that were observed by WISE. Marciniak et al. (2018) and Marciniak et al. (2019) specifically targeted asteroids with longer rotation periods ($P_{rot} > 24$ hrs); a group of objects that have lacked thermal inertia estimations. We refer to object thermal inertias presented in papers with less than 5 objects as “miscellaneous literature”.

3.1. Multivariate Regression Model

We implement a forward stepwise multivariate regression model (Draper and Smith, 1998) on the thermal inertias presented here and in previous works (Table 3 and Table 4) in order to characterize the controlling factors. The independent factors in this model are color temperature (T_c)—an approximation of the surface temperature; Sec. 2.4—object diameter (D_{eff}) and rotation period (P_{rot}). All variables, including Γ are transformed into \log_{10} space when included in the model. We use the inverse of the uncertainty in Γ as a weighting factor for each object in the model. The forward stepwise regression algorithm permits a factor to enter the model when the relationship with the dependent variable is statistically-significant ($p < .05$).

The regression model selected all input variables as statistically-significant explanatory variables. The equation is given by,

$$\log_{10} \Gamma = W + X(\log_{10} T_c) + Y(\log_{10} D_{eff}) + Z(\log_{10} P_{rot}), \quad (10)$$

with best-fit intercept and coefficient values: $W = -4.65 \pm 0.70$, $X = 2.74 \pm 0.29$, $Y = -0.17 \pm 0.03$, and $Z = 0.12 \pm 0.05$. This best-fit model and data are shown in Fig. 6. Previous studies quantified the thermal inertia dependence on diameter (e.g. Delbo' and Tanga, 2009), rotation period (Harris and Drube, 2016), and heliocentric distance (as a proxy for temperature; Rozitis et al., 2018) separately, but no study to-date has attempted to *simultaneously* account for the effect of all three of these variables on thermal inertia. Performing a multivariate regression, as we have done here, accounts for confounding effects between variables, such as the codependency between diameter and surface temperature. This is particularly important because the smallest objects tend to be observed at smaller heliocentric distances and thus have larger surface temperatures.

3.2. Noteworthy Objects

Notably, two objects in this study have higher estimated thermal inertias than any other asteroid to-date:

(3554) *Amun*. Discovered in 1986, this Venus-crossing, Aten NEA has an estimated size of $D_{\text{eff}} = 2.71 \pm 0.02$ km. Its rotation period of 2.53 hr places it close to the theoretical spin barrier limit, and near-infrared reflectance observations show a red and featureless spectrum yielding an ambiguous classification as a X- or D-type (Thomas et al., 2014). Our moderate albedo ($p_V \approx 0.241$) estimate and its very high thermal inertia are highly suggestive of a metal-rich surface, which may help explain the thermal inertia of $\sim 1400 \text{ J m}^{-2} \text{ K}^{-1} \text{ s}^{-1/2}$ estimated here. Additionally, our low roughness estimate is interesting to note, as it suggests a surface that is relatively smooth at the cm scale (i.e., on the order of l_s).

(5604) *1992 FE*. This V-type NEA is also an Aten and has been flagged as a Potentially Hazardous Asteroid (PHA) by the MPC. This sub-kilometer object has a very high thermal inertia, but with large error bars: $1100^{+2200}_{-600} \text{ J m}^{-2} \text{ K}^{-1} \text{ s}^{-1/2}$. Its high optical albedo and radar circular polarization ratio⁶ are consistent with its V-type taxonomic classification and having surface properties similar to Vesta (Benner et al., 2008).

4. Discussion

Our results show a slight excess of prograde spins at larger sizes (Fig. 3), which is generally consistent with previous findings of spin vector distributions estimated from lightcurve inversion methods (Kryszczynska et al., 2007; Hanuš et al., 2011; Ďurech et al., 2016). The estimated success rate of our sense of spin determinations places some uncertainty on this claim, however. We can be most confident about an prograde/retrograde difference in the > 60 km size bin, which is consistent with the findings of Hanuš et al. (2011); Ďurech et al. (2016). But the large, overlapping uncertainties in the 16–30 km and 30–60 km places doubt on any claim of excess prograde rotators. The prograde excess for these large objects is likely a remnant of the primordial spins of large protoplanets due to the accretion direction of pebbles into planetesimals (Johansen and Lacerda, 2010).

⁶https://echo.jpl.nasa.gov/asteroids/1992FE/1992FE_planning.2017.html

Our results show a curious overabundance of small (< 8 km) retrograde rotators. An overabundance of retrograde rotators among NEAs was presented by Spina et al. (2004), with the cause attributed to a dynamical selection effect: retrograde MBAs are more likely to feed into resonances, via the Yarkovsky effect, that alter their orbits into near-Earth space (Bottke et al., 2002). Properly investigating and explaining this result is beyond the scope of this work, but we suspect that modeling of YORP spin obliquity evolution (e.g., Vokrouhlický et al., 2003) and/or the spin alteration due to collisions (Ševeček et al., 2019) should be used to investigate this topic. Yet, the MBAs studied here have not yet been subjected to this dynamical selection effect. We also note that, because we only consider asteroids with rotation periods in the ALCDB, our object set is subject to the observational biases inherent in the determination of rotation periods. This includes, but is not limited to, the skew of known rotation periods to less than Earth’s rotation period and object shapes that depart from spherical shapes.

The multivariate model of asteroid thermal inertia indicates that temperature is a strong controlling factor ($p < .001$). The best-fit coefficient in Eq. 10 can be written as the proportionality: $\Gamma \propto T_c^{2.74 \pm 0.29}$. Because surface temperatures generally scale with the inverse square of heliocentric distance (Eq. 7), it follows that $\Gamma \propto r^\alpha$. Our results can be expressed in terms of this proportionality by using $T_c^X = R_{\text{au}}^{-2\alpha}$, which gives: $\alpha = -1.37 \pm 0.14$. If only the radiative component of thermal conductivity on thermal inertia is considered, the expected coefficient would be $\alpha = -0.75$. Rozitis et al. (2018) calculated α for three objects ranging from -2.5 to -1 , with each object having a different best-fit α . Our result is remarkably consistent with all three objects (see Fig. 8 in Rozitis et al., 2018), although the asteroids studied in that work exhibited vastly different thermal inertia dependence on heliocentric distance. Similar to Harris and Drube (2016), Rozitis et al. (2018) suggested that increased solar heating would allow the thermal wave to sample higher thermal inertia material in the sub-surface due to an increase in l_s . This would result in an increase in thermal inertia for warmer objects if the thermal conductivity and/or bulk density increases with depth—as is the case for the Moon (Keihm and Langseth, 1973).

In the 200–350 K range—the approximate range for most asteroids—the heat capacity is also temperature-dependent ($c_s \propto T$; Opeil et al., 2012; Macke et al., 2019) and should also contribute to the thermal inertia temperature-dependence. The overall dependence of thermal inertia on temperature should be stronger than that predicted using only the radiative component of thermal conductivity, namely $\Gamma \propto T^2$. When combining the temperature-dependence of the radiative component of thermal conductivity and heat capacity together into the thermal inertia dependency of temperature, the expected relationship is still weaker than the observed dependence presented here.

Our multivariate regression model for thermal inertia also selected the diameter ($p < .001$) and rotation period ($p = .011$) as statistically significant factors. The trend of increasing thermal inertia with smaller asteroid size was established by Delbo’ et al. (2007) and has been supported by subsequent works that increase the overall number of thermal inertia estimates (Delbo’ et al., 2015). Delbo’ and Tanga (2009) found a power-law exponent of -0.21 ± 0.4 between diameter and thermal inertia for NEAs and MBAs with sizes < 100 km. The Delbo’ and Tanga (2009) value is consistent with, but somewhat smaller than, our value

of -0.17 ± 0.03 , implying a stronger relationship. It is not unexpected that our estimate is larger because we account for the temperature-dependency. For example, Rozitis et al. (2018) found that the diameter and temperature power-law exponents are inversely correlated, and that $\alpha = -1.32$ corresponds to a power-law diameter exponent of -0.18 , which is consistent with our estimate of -0.17 ± 0.03 .

Whereas the dependency on diameter is statistically robust, our findings show that the relationship between thermal inertia and rotation period is barely distinguishable from a slope of zero ($Z = 0.12 \pm 0.05$). In the work of Harris and Drube (2016), who used a NEATM-based thermal inertia estimator, found a significant correlation between thermal inertia and rotation period for asteroids with rotation periods spanning 2–200 hrs. However, the works of Marciak et al. (2018, 2019) found an abundance of low- Γ slow-rotators ($P_{rot} > 12$ hrs) using a TPM that explicitly accounts for thermal inertia. Considering the results in this paper and from these previous works we claim that the relationship between thermal inertia and rotation period, if present, is very weak.

Future thermophysical modeling efforts should target more slow rotators to better characterize their thermal inertia and understand the its relationship (or lack thereof) with asteroid rotation period. Higher thermal inertias could be indicative of the increase in thermal conductivity (or bulk density due to compression) for objects with large l_s values. These objects with large l_s , which include asteroids with high surface temperatures (Rozitis et al., 2018), can be used to investigate possible changes in regolith properties as a function of depth (i.e., Harris and Drube, 2016).

5. Conclusions and Follow-Up Work

In this work, we applied the method of MacLennan and Emery (2019) to WISE multi-epoch observations in order to estimate the effective diameter, geometric albedo, thermal inertia, and surface roughness for 239 asteroids (Table 3). Additionally, we report the shape and sense of spin for a large fraction of these objects Sec. 3. Our thermal inertia estimates are consistent with previous literature values for individual objects (Fig. 5) and for objects with similar size and rotation period. From our results, we conclude that surface temperature, asteroid size (inverse relationship), and rotation period are controls of thermal inertia of asteroids. We find that the relationship between thermal inertia and size is present, but less pronounced than suggested in previous works that do not also consider the influence of temperature (Sec. 3.1). The temperature dependence ($\Gamma \propto T_c^{2.74 \pm 0.29}$) is larger than the theoretical prediction of $\Gamma \propto T^{1.5}$ if only the temperature-dependence of the radiative component of thermal conductivity is considered, and of $\Gamma \propto T^2$ if the temperature-dependence of heat capacity is additionally considered. Instead, this relationship between thermal inertia and temperature is consistent with temperature-dependency of both the heat capacity and thermal conductivity (Sec. 4). The thermal inertia dependence on object rotation period is weak and increased statistics of slow-rotator thermal inertias in the future could either support or negate this finding.

In a follow-up work, we will utilize a thermal conductivity model to estimate characteristic grain sizes for each object in this thermal inertia dataset. These grain sizes will then be

used to investigate plausible regolith development mechanisms such as impact erosion and thermal fatigue cycling. We will then run the grain sizes through a multi-variate regression model similar to that performed here in order to explore the controlling factors of regolith evolution on asteroids.

Acknowledgements

We thank two anonymous reviewers for their thoughtful critiques which improved the presentation of this paper. E.M.M. is supported by the NASA Earth and Space Science Fellowship #NNX14AP21H.

References

- Alí-Lagoa, V., Müller, T., Kiss, C., Szakáts, R., Marton, G., Farkas-Takács, A., Bartczak, P., Butkiewicz-Bak, M., Dudziński, G., Marcinia, A., Podlewska-Gaca, E., Duffard, R., Santos-Sanz, P., and Ortiz, J. (2020). Thermal properties of large main-belt asteroids observed by herschel pacs. *A&A*, 638:A84.
- Bandfield, J. L., Ghent, R. R., Vasavada, A. R., Paige, D. A., Lawrence, S. J., and Robinson, M. S. (2011). Lunar surface rock abundance and regolith fines temperatures derived from LRO Diviner Radiometer data. *Journal of Geophysical Research*, 116:E00H02.
- Benner, L. A. M., Ostro, S. J., Magri, C., Nolan, M. C., Howell, E. S., Giorgini, J. D., Jurgens, R. F., Margot, J.-L., Taylor, P. A., Busch, M. W., and Shepard, M. K. (2008). Near-Earth asteroid surface roughness depends on compositional class. *Icarus*, 198(2):294–304.
- Bottke, Jr., W. F., Morbidelli, A., Jedicke, R., Petit, J.-M., Levison, H. F., Michel, P., and Metcalfe, T. S. (2002). Debiased Orbital and Absolute Magnitude Distribution of the Near-Earth Objects. *Icarus*, 156:399–433.
- Capria, M. T., Tosi, F., Sanctis, M. C. D., Capaccioni, F., Ammannito, E., Frigeri, A., Zambon, F., Fonte, S., Palomba, E., Turrini, D., Titus, T. N., Schröder, S. E., Toplis, M., Li, J.-Y., Combe, J.-P., Raymond, C. A., and Russell, C. T. (2014). Vesta surface thermal properties map. *Geophysical Research Letters*, 41:1438–1443.
- Cremers, C. J. (1975). Thermophysical properties of Apollo 14 fines. *J. Geophys. Research*, 80:4466–4470.
- Cutri, R. M., Wright, E. L., Conrow, T., Bauer, J., Benford, D., Brandenburg, H., Dailey, J., Eisenhardt, P. R. M., Evans, T., Fajardo-Acosta, S., Fowler, J., Gelino, C., Grillmair, C., Harbut, M., Hoffman, D., Jarrett, T., Kirkpatrick, J. D., Leisawitz, D., Liu, W., Mainzer, A., Marsh, K., Masci, F., McCallon, H., Padgett, D., Ressler, M. E., Royer, D., Skrutskie, M. F., Stanford, S. A., Wyatt, P. L., Tholen, D., Tsai, C.-W., Wachter, S., Wheelock, S. L., Yan, L., Alles, R., Beck, R., Grav, T., Masiero, J., McCollum, B., McGehee, P., Papin, M., and Wittman, M. (2012). Explanatory Supplement to the WISE All-Sky Data Release Products. <http://wise2.ipac.caltech.edu/docs/release/allsky/expsup/>.
- Delbo', M., dell'Oro, A., Harris, A. W., Mottola, S., and Mueller, M. (2007). Thermal Inertia of near-Earth Asteroids and Implications for the Magnitude of the Yarkovsky Effect. *Icarus*, 190:236–249.
- Delbo', M., Mueller, M., Emery, J. P., Rozitis, B., and Capria, M. T. (2015). Asteroid Thermophysical Modeling. In Michel, P., DeMeo, F. E., and Bottke Jr., W. F., editors, *Asteroids IV*, pages 107–128. University of Arizona Press.
- Delbo', M. and Tanga, P. (2009). Thermal Inertia of Main Belt Asteroids Smaller than 100 km from IRAS Data. *Planetary and Space Science*, 57:259–265.
- Dellagiustina, D. N., Emery, J. P., Golish, D. R., Rozitis, B., Bennett, C. A., Burke, K. N., Ballouz, R. L., Becker, K. J., Christensen, P. R., Drouet D'Aubigny, C. Y., Hamilton, V. E., Reuter, D. C., Rizk, B., Simon, A. A., Asphaug, E., Bandfield, J. L., Barnouin, O. S., Barucci, M. A., Bierhaus, E. B., Binzel, R. P., Bottke, W. F., Bowles, N. E., Campins, H., Clark, B. C., Clark, B. E., Connolly, H. C., Daly, M. G., Leon, J. D., Delbo', M., Deshapriya, J. D. P., Elder, C. M., Fornasier, S., Hergenrother, C. W.,

- Howell, E. S., Jawin, E. R., Kaplan, H. H., Karefa, T. R., Le Corre, L., Li, J. Y., Licandro, J., Lim, L. F., Michel, P., Molaro, J., Nolan, M. C., Pajola, M., Popescu, M., Garcia, J. L. R., Ryan, A., Schwartz, S. R., Shultz, N., Siegler, M. A., Smith, P. H., Tatsumi, E., Thomas, C. A., Walsh, K. J., Wolner, C. W. V., Zou, X. D., Lauretta, D. S., and Osiris-Rex Team (2019). Properties of rubble-pile asteroid (101955) Bennu from OSIRIS-REx imaging and thermal analysis. *Nature Astronomy*, 3:341–351.
- Devogèle, M., MacLennan, E., Gustafsson, A., Moskovitz, N., Chatelain, J., Borisov, G., Abe, S., Arai, T., Fedorets, G., Ferrais, M., Granvik, M., Jehin, E., Siltala, L., Pöntinen, M., Mommert, M., Polishook, D., Skiff, B., Tanga, P., and Yoshida, F. (2020). New Evidence for a Physical Link between Asteroids (155140) 2005 UD and (3200) Phaethon. *The Planetary Science Journal*, 1(1):15.
- Draper, N. R. and Smith, H. (1998). *Applied Regression Analysis*. John Wiley & Sons, Inc.
- Ďurech, J. (2010). DAMIT: A Database of Asteroid Models. *Astronomy and Astrophysics*, 513:A46.
- Ďurech, J., Hanuš, J., Oszkiewicz, D., and Vanco, R. (2016). Asteroid models from the Lowell Photometric Database. *Astronomy & Astrophysics*, 587:A48.
- Emery, J. P., Fernández, Y. R., Kelley, M. S. P., Warden, K. T., Hergenrother, C., Lauretta, D. S., Drake, M. J., Campins, H., and Ziffer, J. (2014). Thermal Infrared Observations and Thermophysical Characterization and OSIRIS-REx Target Asteroid (101955) Bennu. *Icarus*, 234:17–35.
- Gould, B. A. (1855). On Peirce's Criterion for the Rejection of Doubtful Observations, with Tables for Facilitating its Application. *Astronomical Journal*, 4:81–87.
- Hanuš, J., Delbó, M., Ďurech, J., and Alí-Lagoa, V. (2015). Thermophysical Modeling of Asteroids from WISE Thermal Infrared Data – Significance of the Shape Model and the Pole Orientation Uncertainties. *Icarus*, 256:101–116.
- Hanuš, J., Delbo', M., Ďurech, J., and Alí-Lagoa, V. (2018). Thermophysical Modeling of Main-Belt Asteroids from WISE Thermal Data. *Icarus*, 309:297–337.
- Hanuš, J., Ďurech, J., Broz, M., Warner, B. D., Pilcher, F., Stephens, R., Oey, J., Bernasconi, L., Casulli, S., Behrend, R., Polishook, D., Henych, T., Lehky, M., Yoshida, F., and Ito, T. (2011). A study of asteroid pole-latitude distribution based on an extended set of shape models derived by the lightcurve inversion method. *Astronomy & Astrophysics*, 530:A134.
- Hanuš, J., Delbo', M., Vokrouhlický, D., Pravec, P., Emery, J. P., Alí-Lagoa, V., Bolin, B., Devogèle, M., Dyvig, R., Galád, A., Jedicek, R., Kornoš, L., Kušnírák, P., Licandro, J., Reddy, V., Rivet, J. P., Világí, J., and Warner, B. D. (2016). Near-Earth asteroid (3200) Phaethon: Characterization of its orbit, spin state, and thermophysical parameters. *A&A*, 592:A34.
- Hapke, B. (1984). Bidirectional Reflectance Spectroscopy 3. Correction for Macroscopic Roughness. *Icarus*, 59:41–59.
- Harris, A. W. (1998). A Thermal Model for Near-Earth Asteroids. *Icarus*, 131:291–301.
- Harris, A. W. and Drube, L. (2016). Thermal Tomography of Asteroid Surface Structure. *Astrophysical Journal*, 832:127.
- Hayne, P. O., Bandfield, J. L., Siegler, M. A., Vasavada, A. R., Ghent, R. R., Williams, J.-P., Greenhagen, B. T., Aharonson, O., Lucey, C. M. E. P. G., and Paige, D. A. (2017). Global Regolith Thermophysical Properties of the Moon From the Diviner Lunar Radiometer Experiment. *Journal of Geophysical Research: Planets*, 22:2371–2400.
- Jiang, H., Ji, J., and Yu, L. (2020). Determination of Size, Albedo, and Thermal Inertia of 10 Vesta Family Asteroids with WISE/NEOWISE Observations. *AJ*, 159(6):264.
- Johansen, A. and Lacerda, P. (2010). Prograde rotation of protoplanets by accretion of pebbles in a gaseous environment. *Monthly Notices of the Royal Astronomical Society*, 404:475–485.
- Keihm, S., Tosi, F., Kamp, L., Capaccioni, F., Gulkis, S., Grassi, D., Hofstadter, M., Filacchione, G., Lee, S., Giuppi, S., Janssen, M., and Capria, M. (2012). Interpretation of combined infrared, submillimeter, and millimeter thermal flux data obtained during the Rosetta fly-by of Asteroid (21) Lutetia. *Icarus*, 221(1):395–404.
- Keihm, S. J. and Langseth, M. G., J. (1973). Surface brightness temperatures at the Apollo 17 heat flow site: Thermal conductivity of the upper 15 cm of regolith. *Lunar and Planetary Science Conference Proceedings*, 4:2503.

- Kryszczynska, A., Spina, A. L., Paolicchi, P., Harris, A. W., Breiter, S., and Pravec, P. (2007). New findings on asteroid spin-vector distributions. *Icarus*, 192:223–237.
- Leyrat, C., Coradini, A., Erard, S., Capaccioni, F., Capria, M. T., Drossart, P., de Sanctis, M. C., Tosi, F., and Virtis Team (2011). Thermal properties of the asteroid (2867) Steins as observed by VIRTIS/Rosetta. *A&A*, 531:A168.
- Macke, R. J., Opeil, C., and Consolmagno, G. J. (2019). Heat capacities of ordinary chondrite falls below 300 k. *Meteoritics and Planetary Science*, 54(11):2729–2743.
- MacLennan, E. M. and Emery, J. P. (2019). Thermophysical modeling of asteroid surfaces using ellipsoid shape models. *The Astronomical Journal*, 157(1):2.
- Mainzer, A., Bauer, J., Grav, T., Masiero, J., Cutri, R. M., Dailey, J., Eisenhardt, P., McMillan, R. S., Wright, E., Walker, R., Jedicke, R., Spahr, T., Tholen, D., Alles, R., Beck, R., Brandenburg, H., Conrow, T., Evans, T., Fowler, J., Jarrett, T., Marsh, K., Masci, F., McCallon, H., Wheelock, S., Wittman, M., Wyatt, P., DeBaun, E., Elliott, G., Elsbury, D., Gautier, T., Gomillion, S., Leisawitz, D., Maleszewski, C., Micheli, M., and Wilkins, A. (2011a). PRELIMINARY RESULTS FROM NEOWISE: AN ENHANCEMENT TO THE WIDE-FIELD INFRARED SURVEY EXPLORERFOR SOLAR SYSTEM SCIENCE. *Astrophysical Journal*, 731:53.
- Mainzer, A., Grav, T., Bauer, J., Masiero, J., McMillan, R. S., Cutri, R. M., Walker, R., Wright, E., Eisenhardt, P., Tholen, D. J., Spahr, T., Jedicke, R., Denneau, L., DeBaun, E., Elsbury, D., Gautier, T., Gomillion, S., Hand, E., Mo, W., Watkins, J., Wilkins, A., Bryngelson, G. L., Molina, A. D. P., Desai, S., Camus, M. G., Hidalgo, S. L., Konstantopoulos, I., Larsen, J. A., Maleszewski, C., Malkan, M. A., Mauduit, J.-C., Mullan, B. L., Olszewski, E. W., Pforr, J., Saro, A., Scotti, J. V., and Wasserman, L. H. (2011b). NEOWISE Observations of near-Earth Objects: Preliminary Results. *The Astrophysical Journal*, 743:156.
- Marciniak, A., Alí-Lagoa, V., Müller, T. G., Szakáts, R., Molnár, L., Pál, A., Podlewska-Gaca, E., Parley, N., Antonini, P., Barbotin, E., Behrend, R., Bernasconi, L., Butkiewicz-Bak, M., Crippa, R., Duffard, R., Ditteon, R., Feuerbach, M., Fauvaud, S., Garlitz, J., Geier, S., Goncalves, R., Grice, J., Grześkowiak, I., Hirsch, R., Horbowicz, J., Kamiński, K., Kamińska, M. K., Kim, D. H., Kim, M. J., Konstanciak, I., Kudak, V., Kulczak, P., Maestre, J. L., Manzini, F., Marks, S., Monteiro, F., Ogloza, W., Oszkiewicz, D., Pilcher, F., Perig, V., Polakis, T., Polńska, M., Roy, R., Sanabria, J. J., Santana-Ros, T., Skiff, B., Skrzypek, J., Sobkowiak, K., Sonbas, E., Thizy, O., Trela, P., Urakawa, S., Żejmo, M., and Żukowski, K. (2019). Thermal properties of slowly rotating asteroids: results from a targeted survey. *A&A*, 625:A139.
- Marciniak, A., Bartczak, P., Müller, T., Sanabria, J. J., Alí-Lagoa, V., Antonini, P., Behrend, R., Bernasconi, L., Bronikowska, M., Butkiewicz-Bak, M., Cikota, A., Crippa, R., Ditteon, R., Dudziński, G., Duffard, R., Dziadura, K., Fauvaud, S., Geier, S., Hirsch, R., Horbowicz, J., Hren, M., Jerosimic, L., Kamiński, K., Kankiewicz, P., Konstanciak, I., Korlevic, P., Kosturkiewicz, E., Kudak, V., Manzini, F., Morales, N., Murawiecka, M., Ogloza, W., Oszkiewicz, D., Pilcher, F., Polakis, T., Poncy, R., Santana-Ros, T., Siwak, M., Skiff, B., Sobkowiak, K., Stoss, R., Żejmo, M., and Żukowski, K. (2018). Photometric survey, modelling, and scaling of long-period and low-amplitude asteroids. *A&A*, 610:A7.
- Marsset, M., Carry, B., Dumas, C., Hanus, J., Viikinkoski, M., Vernazza, P., Müller, T. G., Delbo, M., Jehin, E., Gillon, M., Grice, J., Yang, B., Fusco, T., Berthier, J., Sonnett, S., Kugel, F., Caron, J., and Behrend, R. (2017). 3d shape of asteroid (6) hebe from vlt/sphere imaging: Implications for the origin of ordinary h chondrites. *A&A*, 604:A64.
- Masiero, J. R., Mainzer, A. K., Grav, T., Bauer, J. M., Cutri, R. M., Dailey, J., Eisenhardt, P. R. M., McMillan, R. S., Spahr, T. B., Skrutskie, M. F., Tholen, D., Walker, R. G., Wright, E. L., DeBaun, E., Elsbury, D., Gautier, T., Gomillion, S., and Wilkins, A. (2011). Main Belt Asteroids with WISE/NEOWISE. I. Preliminary Albedos and Diameters. *The Astrophysical Journal*, 741:68–88.
- Matter, A., Delbó, M., Carry, B., and Ligori, S. (2013). Evidence of a metal-rich surface for the asteroid (16) Psyche from interferometric observations in the thermal infrared. *Icarus*, 226:419–427.
- Mueller, M. (2007). *Surface Properties of Asteroids from Mid-Infrared Observations and Thermophysical Modeling*. PhD thesis, Freie Universitaet Berlin.
- Mueller, T. G. and Lagerros, J. S. V. (1998). Asteroids as far-infrared photometric standards for isophot.

- Astronomy & Astrophysics*, 338:340–352.
- Müller, T. G. and Blommaert, J. A. D. L. (2004). *iASTROBJ*: Cybele/ASTROBJ in the thermal infrared: Multiple observations and thermophysical analysis. *A&A*, 418:347–356.
- Müller, T. G., Sterzik, M. F., Schütz, O., Pravec, P., and Siebenmorgen, R. (2004). Thermal infrared observations of near-earth asteroid 2002 ny40*. *A&A*, 424(3):1075–1080.
- Opeil, C. P., Consolmagno, G. J., Safarik, D. J., and Britt, D. T. (2012). Stony meteorite thermal properties and their relationship with meteorite chemical and physical states. *Meteoritics & Planetary Science*, 47(3):319–329.
- Oszkiewicz, D. A., Muinonen, K., Bowell, E., Trilling, D., Penttilä, A., Pieniluoma, T., Wasserman, L. H., and Enga, M.-T. (2011). Online multi-parameter phase-curve fitting and application to a large corpus of asteroid photometric data. *Journal of Quantitative Spectroscopy & Radiative Transfer*, 112:1919–1929.
- Peirce, B. (1852). Criterion for the Rejection of Doubtful Observations. *Astronomical Journal*, 2:161–163.
- Piqueux, S. and Christensen, P. R. (2009). A model of thermal conductivity for planetary soils: 1. theory for unconsolidated soils. *Journal of Geophysical Research: Planets*, 114:E9.
- Pravec, P., Fatka, P., Vokrouhlický, D., Scheirich, P., Ďurech, J., Scheeres, D. J., Kušnírák, P., Hornoch, K., Galád, A., Pray, D. P., Krugly, Y. N., Burkhanov, O., Ehgamberdiev, S. A., Pollock, J., Moskovitz, N., Thirouin, A., Ortiz, J. L., Morales, N., Husárik, M., Inasaridze, R. Y., Oey, J., Polishook, D., Hanuš, J., Kučáková, H., Vraštil, J., Világí, J., Gajdoš, Š., Kornoš, L., Vereš, P., Gaftonyuk, N. M., Hromakina, T., Sergeyev, A. V., Slyusarev, I. G., Ayvazian, V. R., Cooney, W. R., Gross, J., Terrell, D., Colas, F., Vachier, F., Slivan, S., Skiff, B., Marchis, F., Ergashev, K. E., Kim, D. H., Aznar, A., Serra-Ricart, M., Behrend, R., Roy, R., Manzini, F., and Molotov, I. E. (2019). Asteroid pairs: A complex picture. *Icarus*, 333:429–463.
- Rognini, E., Capria, M. T., Tosi, F., De Sanctis, M. C., Ciarniello, M., Longobardo, A., Carrozzo, F. G., Raponi, A., Frigeri, A., Palomba, E., Fonte, S., Giardino, M., Ammannito, E., Raymond, C. A., and Russell, C. T. (2020). High thermal inertia zones on ceres from dawn data. *Journal of Geophysical Research: Planets*, 125(3):e2018JE005733. e2018JE005733 2018JE005733.
- Rozitis, B., Duddy, S. R., Green, S. F., and Lowry, S. C. (2013). A Thermophysical Analysis of the (1862) Apollo Yarkovsky and YORP Effects. *Astronomy and Astrophysics*, 555:A20.
- Rozitis, B., Green, S. F., MacLennan, E., and Emery, J. P. (2018). Observing the Variation of Asteroid Thermal Inertia with Heliocentric Distance. *Monthly Notices of the Royal Astronomical Society*, 477(2):1782–1802.
- Rozitis, B., Ryan, A. J., Emery, J. P., Christensen, P. R., Hamilton, V. E., Simon, A. A., Reuter, D. C., Al Asad, M., Ballouz, R.-L., Bandfield, J. L., Barnouin, O. S., Bennett, C. A., Bernacki, M., Burke, K. N., Cambioni, S., Clark, B. E., Daly, M. G., Delbo, M., DellaGiustina, D. N., Elder, C. M., Hanna, R. D., Haberle, C. W., Howell, E. S., Golish, D. R., Jawin, E. R., Kaplan, H. H., Lim, L. F., Molaro, J. L., Munoz, D. P., Nolan, M. C., Rizk, B., Siegler, M. A., Susorney, H. C. M., Walsh, K. J., and Lauretta, D. S. (2020). Asteroid (101955) bennu’s weak boulders and thermally anomalous equator. *Science Advances*, 6(41).
- Shimaki, Y., Senshu, H., Sakatani, N., Okada, T., Fukuhara, T., Tanaka, S., Taguchi, M., Arai, T., Demura, H., Ogawa, Y., Suko, K., Sekiguchi, T., Kouyama, T., Hasegawa, S., Takita, J., Matsunaga, T., Imamura, T., Wada, T., Kitazato, K., Hirata, N., Hirata, N., Noguchi, R., Sugita, S., Kikuchi, S., Yamaguchi, T., Ogawa, N., Ono, G., Mimasu, Y., Yoshikawa, K., Takahashi, T., Takei, Y., Fujii, A., Takeuchi, H., Yamamoto, Y., Yamada, M., Shirai, K., Iijima, Y.-i., Ogawa, K., Nakazawa, S., Terui, F., Saiki, T., Yoshikawa, M., Tsuda, Y., and Watanabe, S.-i. (2020). Thermophysical properties of the surface of asteroid 162173 Ryugu: Infrared observations and thermal inertia mapping. *Icarus*, 348:113835.
- Spina, A. L., Paolicchi, P., Kryszczynska, A., and Pravec, P. (2004). Retrograde spins of near-Earth asteroids from the Yarkovsky effect. *Nature*, 428:400.
- Swinbank, R. and Purser, R. J. (2006). Fibonacci Grids: A Novel Approach to Global Modelling. *Quarterly Journal of the Royal Meteorological Society*, 132:1769–1763.
- Thomas, C. A., Emery, J. P., Trilling, D. E., Delbó, M., Hora, J. L., and Mueller, M. (2014). Physical characterization of Warm Spitzer-observed near-Earth objects. *Icarus*, 228:217–246.

- Vasavada, A. R., Paige, D. A., and Wood, S. E. (1999). Near-surface temperatures on mercury and the moon and the stability of polar ice deposits. *Icarus*, 141(2):179–193.
- Vokrouhlický, D., Nesvorný, D., and Bottke, W. F. (2003). The vector alignments of asteroid spins by thermal torques. *Nature*, 425(6954):147–151.
- Ševeček, P., Brož, M., and Jutzi, M. (2019). Impacts into rotating targets: angular momentum draining and efficient formation of synthetic families. *A&A*, 629:A122.
- Warner, B. D., Harris, A. W., and Pravec, P. (2009). The Asteroid Lightcurve Database. *Icarus*, 202:134–146.
- Wesselink, A. J. (1948). Heat conductivity and nature of the lunar surface material. *Bull. Astron. Inst. Netherlands*, 10:351–363.
- Wright, E. L., Eisenhardt, P. R. M., Mainzer, A. K., Ressler, M. E., Cutri, R. M., Jarrett, T., Kirkpatrick, J. D., Padgett, D., McMillan, R. S., Skrutskie, M., Stanford, S. A., Cohen, M., Walker, R. G., Mather, J. C., Leisawitz, D., Gautier, T. N., McLean, I., Benford, D., Lonsdale, C. J., Blain, A., Mendez, B., Irace, W. R., Duval, V., Liu, F., Royer, D., Heinrichsen, I., Howard, J., Shannon, M., Kendall, M., Walsh, A. L., Larsen, M., Cardon, J. G., Schick, S., Schwalm, M., Abid, M., Fabinsky, B., Naes, L., and Tsai, C.-W. (2010). The Wide-Field Infrared Survey Explorer (WISE): Mission Description and Initial On-Orbit Performance. *Astronomical Journal*, 140:1868–1881.
- Yu, L. L., Yang, B., Ji, J., and Ip, W.-H. (2017). Thermophysical characteristics of the large main-belt asteroid (349) Dembowska. *MNRAS*, 472(2):2388–2397.

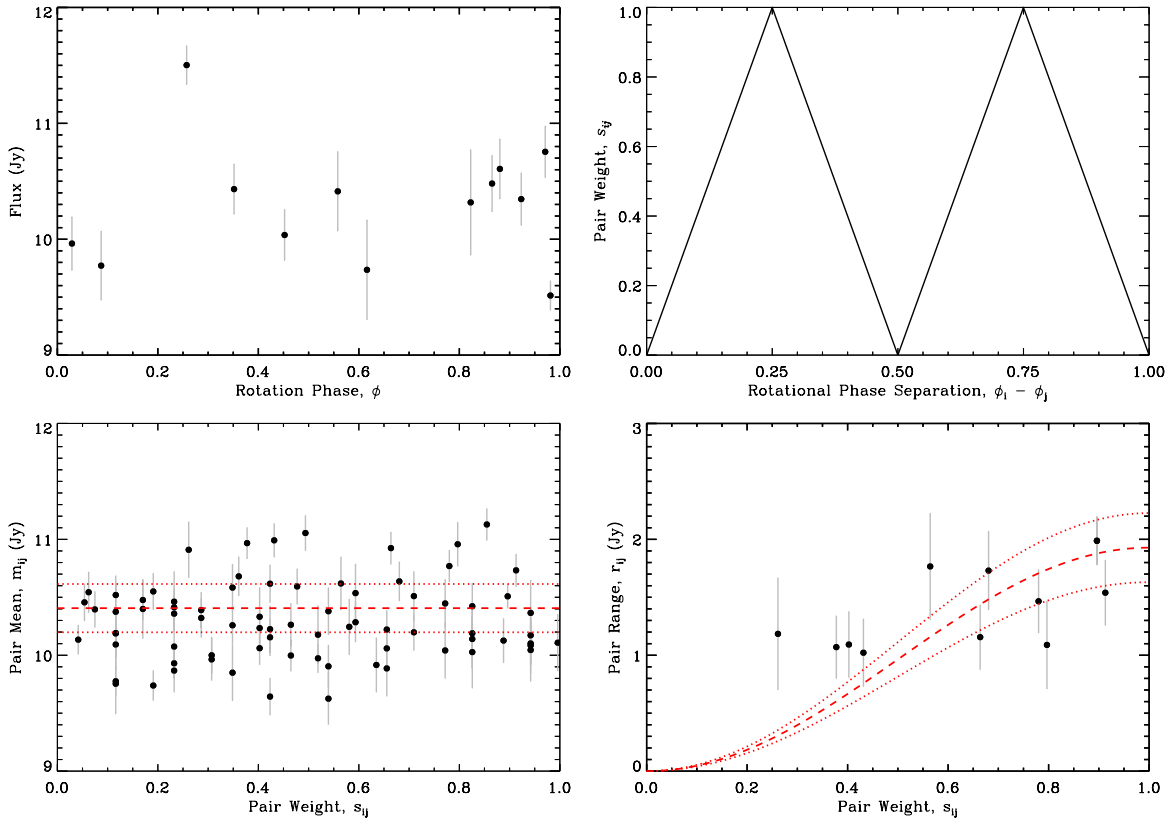


Figure 1: Graphical depiction of applying Eq. 2 and Eq. 4 toward computing the mean (lower left) and flux range (lower right) of W4 data for (91) Aegina. The upper left panel shows the W4 fluxes as a function of rotation phase and the upper right panel depicts the weights applied to pairs of fluxes as a function of their phase separation. The red dashed line and dotted lines give the best-fit and 1σ uncertainty for the mean and amplitude of $\bar{F} = 10.4 \pm 2.2$ Jy and $\diamond F = 1.9 \pm 0.3$ Jy.

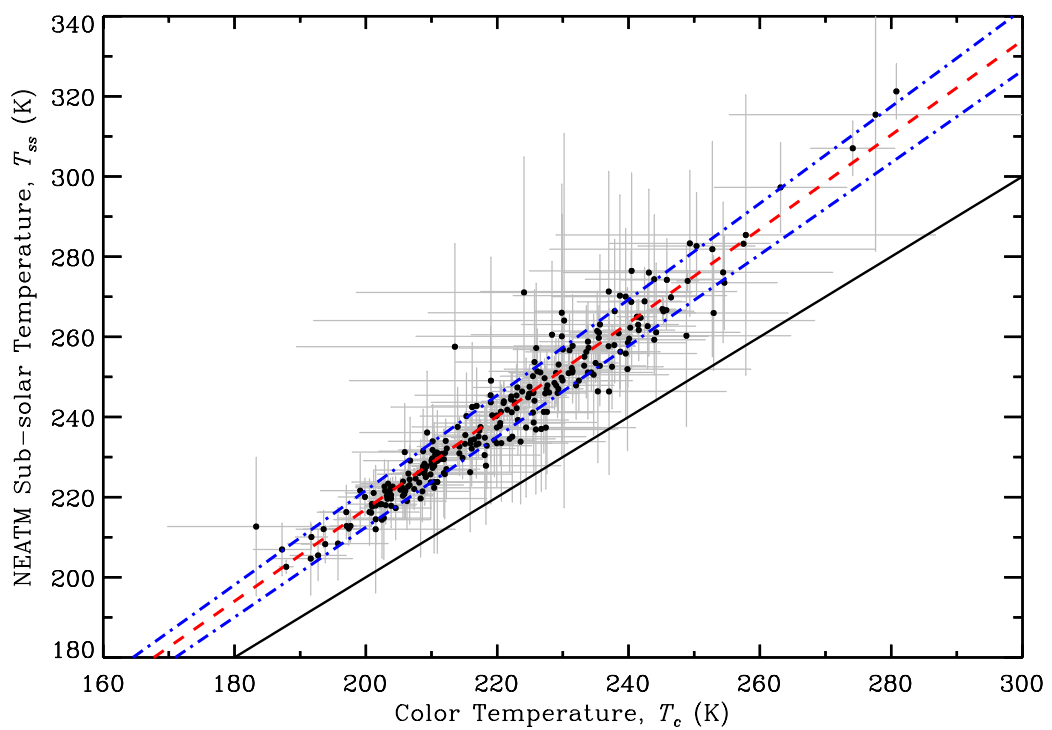


Figure 2: NEATM T_{ss} as a function of color temperature, fit by the red dashed line (equation given in the text) with the blue dash-dot lines showing the 1σ uncertainty in the fit parameters. The black solid line shows the identity function.

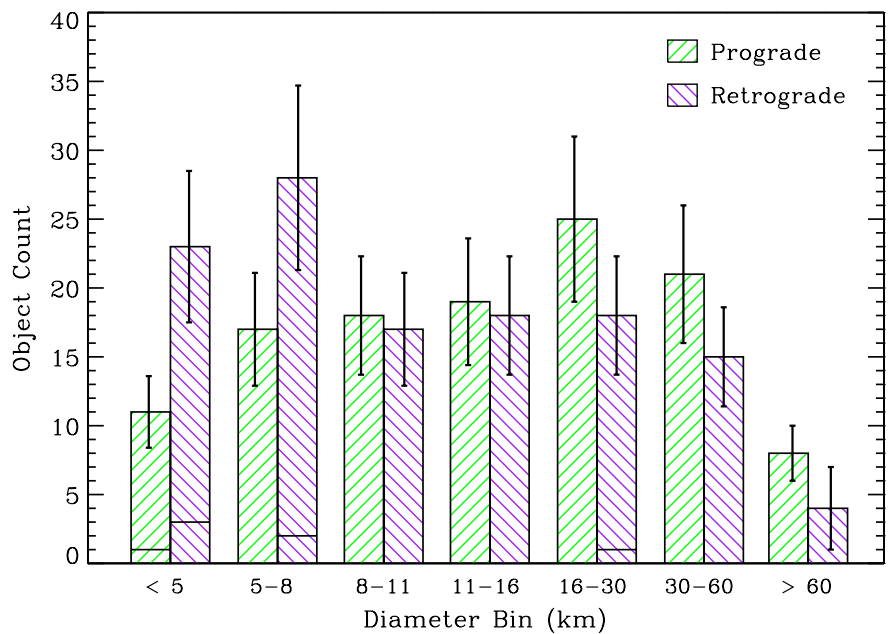


Figure 3: The number of prograde and retrograde rotators as a function of diameter bin. Horizontal lines indicate the number of NEAs within each bin. Vertical lines indicate the number of objects with indeterminate sense of spin within that size range, or one; whichever is greater.

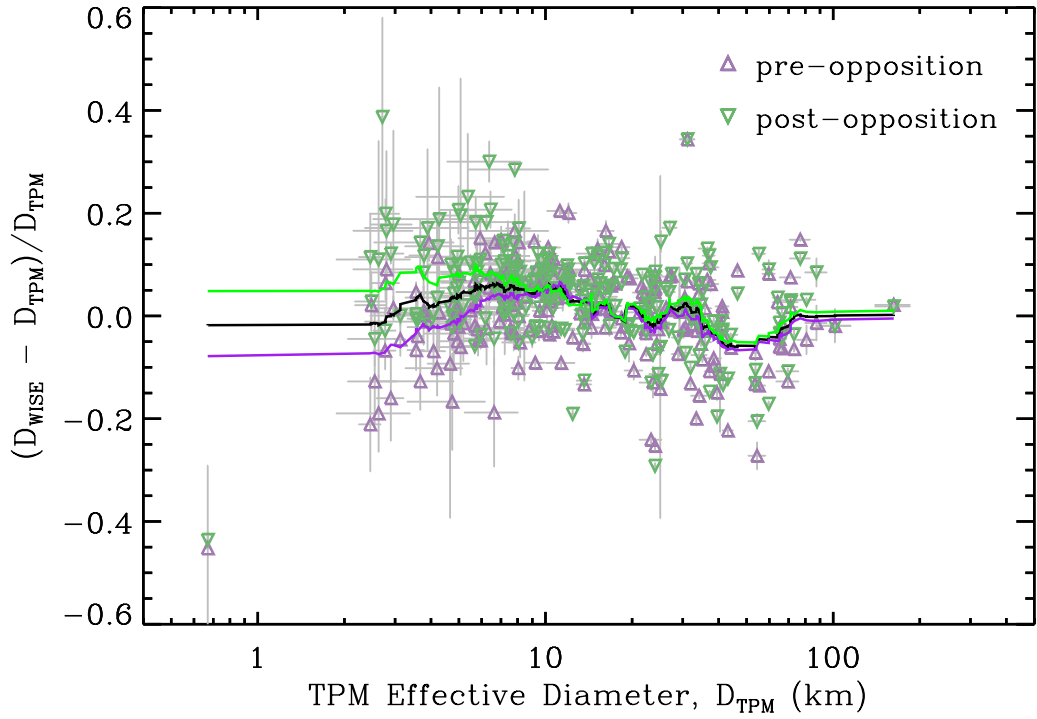


Figure 4: Comparison of the effective diameter values obtained by [Masiero et al. \(2011\)](#) and [Mainzer et al. \(2011b\)](#) to our reported TPM values. We plot the difference between the individual pre- and post-opposition diameters of the WISE team and our TPM diameter as a function of the diameter from our TPM. Purple, upward-facing and green, downward-facing triangles are data collected at pre- and post-opposition, respectively. the green line shows a running mean of the post-opposition data, the purple line shows a running mean of the pre-opposition data, and the black line shows a running mean of the relative diameter difference for all objects.

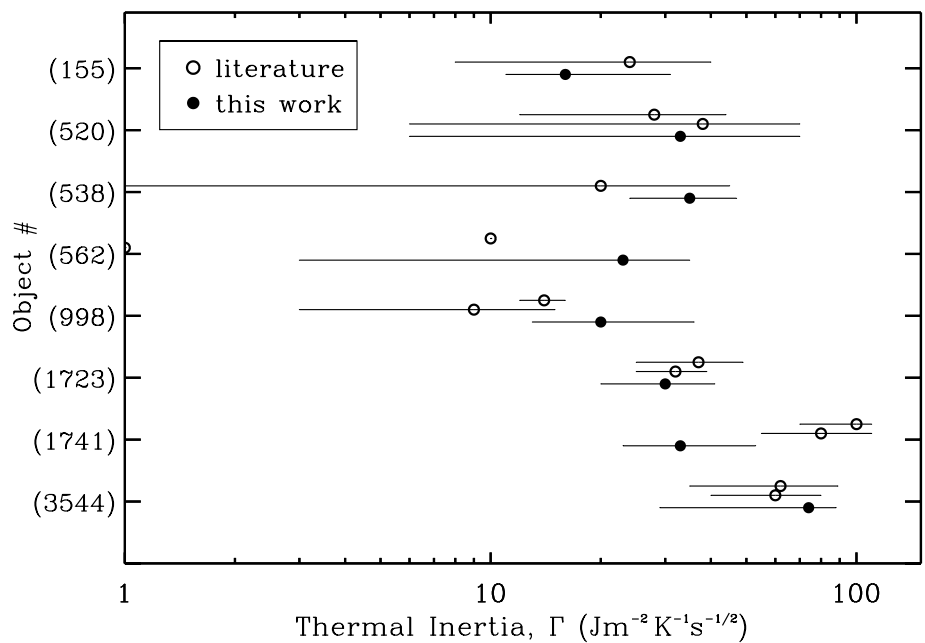


Figure 5: Comparison of literature thermal inertia values (open circles; Table 4) for individual objects to estimates in this work (filled circles; Table 3). All objects with previous estimates are from Hanuš et al. (2015), except (538) Fredicke (Marciniak et al., 2019) and (1741) Giclas (Pravec et al., 2019).

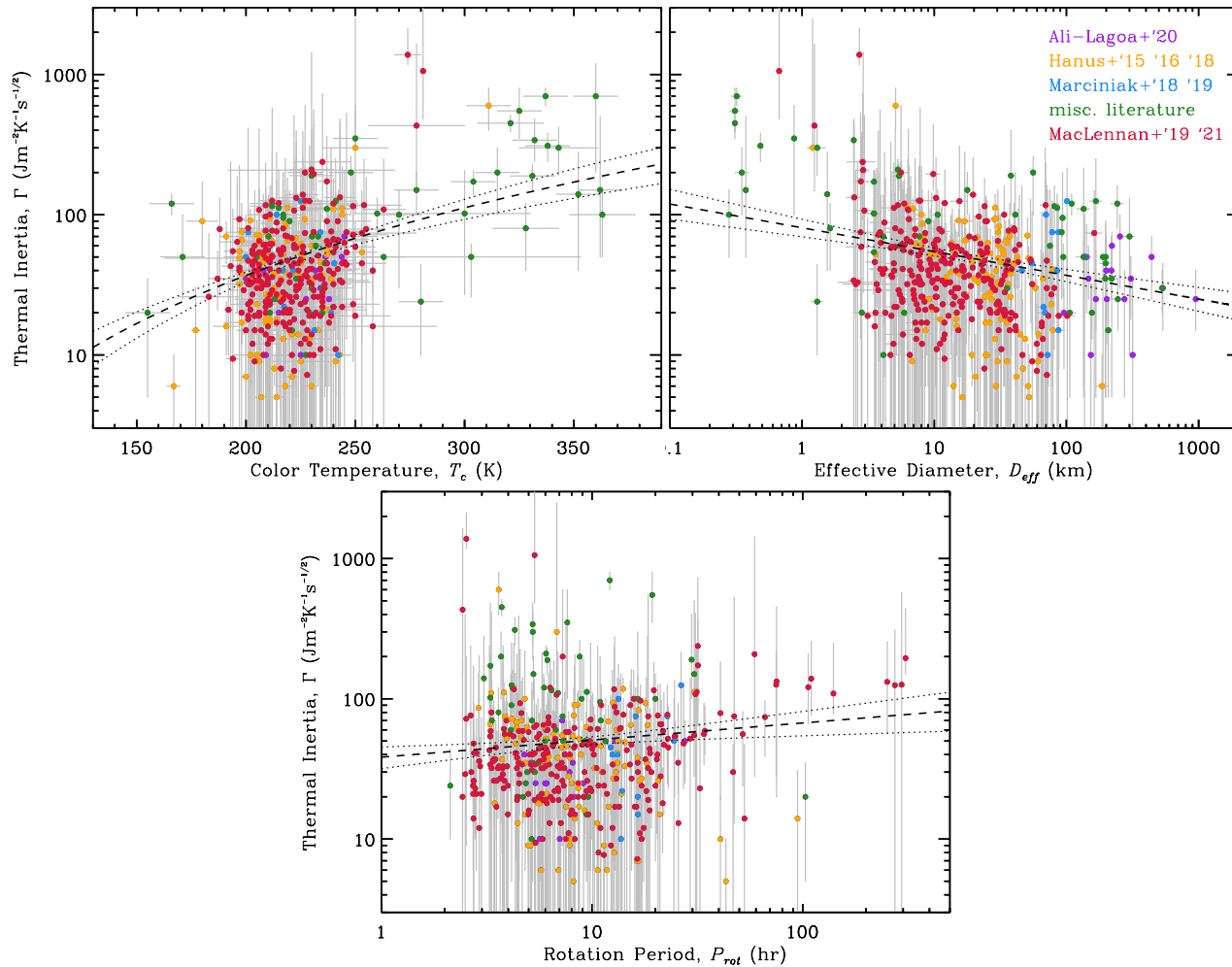


Figure 6: Thermal inertia dependence on surface (color) temperature, object diameter, and rotation period. The black lines show the best-fit multivariate regression model to the data (dashed) and 1σ uncertainty (dotted). Red points are objects from this work (MacLennan’21; Table 3) and MacLennan and Emery (2019). Other colors indicate the source from other works (Table 4), as indicated in the upper right panel, where misc. literature refers to papers that present less than 5 thermal inertias.

Table 1: Absolute Magnitudes, Slope Parameters, and Rotation Periods used as TPM Input

Object	H_V	G_V	P_{rot} (hr)	Object	H_V	G_V	P_{rot} (hr)	Object	H_V	G_V	P_{rot} (hr)
(91) Aegina	8.795	0.200	6.0250 [†]	(1759) Kienle	13.01	0.277	29.25	(4908) Ward	13.61	0.206	10.96
(155) Scylla	10.87	0.087	7.9597	(1768) Appenzella	12.33	0.056	5.1839	(5035) Swift	12.25	0.236	9.4752
(271) Penthesilea	9.724	0.134	18.787	(1807) Slovakia	12.25	0.162	308.0	(5052) Nancyruth	14.21	0.134	17.204
(295) Theresia	9.841	0.185	10.730	(1896) Beer	13.69	0.251	3.3278	(5080) Oja	12.64	0.280	7.2220
(322) Phaeo	8.986	0.211	17.5845	(1936) Lugano	11.41	0.046	19.651	(5088) Tancredi	12.51	0.181	5.0591
(343) Ostara	11.51	0.148	109.87	(1979) Sakharov	13.63	0.485	7.5209	(5104) Skripnichenko	11.93	0.162	2.8270 [†]
(444) Gyptis	7.837	0.193	6.214	(2005) Hencke	12.10	0.224	10.186	(5226) Pollack	13.12	0.284	2.725
(463) Lola	11.43	0.105	6.206	(2072) Kosmodemyanskaya	12.69	0.343	4.4	(5333) Kanaya	12.86	0.066	3.8022
(464) Megaira	9.586	0.119	12.726	(2106) Hugo	12.18	0.096	6.9297	(5378) Ellyett	13.68	0.207	47.32
(493) Griseldis	10.72	0.183	51.940	(2111) Tselina	10.48	0.283	6.563	(5427) Jensmartin	13.65	0.287	5.810
(500) Selinur	9.316	0.316	8.0111	(2123) Vltava	11.46	0.170	34.0	(5527) 1991 UQ ₃	13.57	0.209	4.2554
(520) Franziska	10.49	0.252	16.5045 [†]	(2140) Kemerovo	11.24	0.143	9.2	(5574) Seagrave	12.29	0.319	4.6629
(538) Friederike	9.342	0.085	46.728	(2144) Marietta	11.16	0.254	5.489	(5592) Oshima	11.68	0.119	12.54
(558) Carmen	9.065	0.354	11.387	(2177) Oliver	11.84	0.226	6.1065	(5604) 1992 FE	17.35	0.309	5.3375
(562) Salome	9.870	0.188	6.351	(2203) van Rhijn	11.52	0.201	30.55	(5682) Beresford	13.54	0.238	3.769
(567) Eleutheria	9.047	0.263	7.717	(2204) Lylly	11.93	0.141	11.063	(5712) Funke	12.75	0.217	3.950
(583) Klotilde	9.009	0.143	9.2116	(2214) Carol	11.55	0.082	4.987	(6091) Mitsuru	13.08	0.074	5.853
(651) Antikleia	9.952	0.229	20.299	(2239) Paracelsus	10.92	0.344	6.101	(6121) Plachinda	13.29	0.266	4.0863
(656) Beagle	9.833	0.145	7.035	(2268) Szmytowna	11.51	0.119	11.260	(6139) Naomi	12.18	0.284	21.35
(662) Newtonia	10.40	0.402	16.46	(2275) Cuitlahuac	12.46	0.208	6.2891	(6170) Levasseur	13.44	0.357	2.6529
(668) Dora	11.81	0.123	22.914	(2297) Daghestan	11.28	0.203	7.75	(6185) Mitsuma	12.90	0.087	21.05
(670) Ottegebe	9.362	0.255	10.045	(2306) Bauschinger	12.05	0.110	21.64	(6261) Chione	14.07	0.218	5.3334
(688) Melanie	10.58	0.120	18.87	(2332) Kalm	10.85	0.180	22.8	(6361) Koppel	13.18	0.230	9.1122
(734) Benda	9.888	0.285	7.110	(2347) Vinata	11.21	0.175	4.4835	(6572) Carson	12.41	0.125	2.8235
(735) Marghanna	9.558	0.151	15.95	(2365) Interkosmos	11.29	0.218	6.1548	(6838) Okuda	12.07	0.287	8.983
(793) Arizona	10.03	0.376	7.399	(2375) Radek	10.35	0.168	16.875	(6870) 1991 OM ₁	13.85	0.240	4.487
(826) Henrika	11.34	0.083	5.9846	(2446) Lunacharsky	12.91	0.134	3.613	(6901) Roybishop	13.27	0.084	4.682
(829) Academia	10.77	0.107	7.891	(2463) Sterpin	11.87	0.324	13.44	(6905) Miyazaki	11.47	0.180	2.7418
(883) Matterania	12.50	0.228	5.64	(2500) Alascattalo	12.49	0.254	2.754	(6911) Nancycgreen	14.02	0.233	59.1
(906) Repsolda	9.244	0.180	15.368	(2556) Louise	13.23	0.308	3.809	(7476) Ogilsbie	11.37	0.104	3.92
(918) Itha	10.58	0.310	3.4739 [†]	(2567) Elba	11.69	0.148	9.7785	(7783) 1994 JD	14.23	0.265	31.83
(972) Cohnia	9.436	0.137	18.472	(2687) Tortali	11.82	0.207	21.75	(7829) Jaroff	14.50	0.560	4.398
(977) Philippa	9.672	0.107	15.405	(2786) Grinevia	11.95	0.352	2.911	(7832) 1993 FA ₂₇	13.74	0.183	8.295
(987) Wallia	9.430	0.240	10.0813	(2855) Bastian	12.95	0.102	3.5160	(7949) 1992 SU	12.25	0.038	17.91
(998) Bodea	11.35	0.152	8.574	(2870) Haupt	12.78	0.135	274.0	(8213) 1995 FE	13.56	0.237	2.911
(1018) Arnolda	11.01	0.373	14.617	(2947) Kippenhahn	12.58	0.163	10.5	(8862) Takayukiota	12.76	0.150	3.2549
(1047) Geisha	11.87	0.241	25.62	(2985) Shakespeare	11.94	0.144	6.06	(8887) Scheeres	12.62	0.253	2.9827
(1051) Merope	9.935	0.172	27.2	(3036) Krat	10.14	0.061	9.61	(9297) Marchuk	12.17	0.102	18.09
(1076) Viola	12.05	0.215	7.336	(3051) Nantong	12.22	0.080	3.690	(10936) 1998 FN ₁₁	12.50	0.123	25.70
(1077) Campanula	12.18	0.194	3.8508 [†]	(3144) Brosche	13.86	0.181	3.300	(11549) 1992 YY	12.07	0.289	2.671
(1083) Salvia	12.06	0.273	4.23	(3162) Nostalgia	11.29	0.185	6.412	(11780) Thunder Bay	12.82	0.134	295.0
(1095) Tulipa	10.27	0.193	2.7872 [†]	(3249) Musashino	13.40	0.241	4.5527 [†]	(12376) Cochabamba	13.28	0.238	6.3206 [†]
(1109) Tata	9.861	0.161	8.277	(3267) Glo	12.73	0.166	6.8782	(12753) Povenmire	12.61	0.177	12.854

Table 1 — continued

Object	<i>H_V</i>	<i>G_V</i>	<i>P_{rot}</i> (hr)	Object	<i>H_V</i>	<i>G_V</i>	<i>P_{rot}</i> (hr)	Object	<i>H_V</i>	<i>G_V</i>	<i>P_{rot}</i> (hr)
(1123) Shapleya	11.51	0.220	52.92	(3305) Ceadams	12.19	0.238	2.729	(13474) V'yus	13.59	0.167	6.587
(1125) China	11.52	0.156	5.367	(3411) Debetencourt	13.37	0.197	9.93	(13856) 1999 XZ ₁₀₅	12.84	0.133	4.4475
(1136) Mercedes	10.93	0.207	24.64	(3438) Inarradas	11.69	0.183	24.82	(14342) Iglika	12.31	0.154	3.9867
(1142) Aetolia	10.18	0.273	10.730	(3483) Svetlov	14.02	0.465	6.790	(14950) 1996 BE ₂	13.59	0.183	3.2791 [†]
(1152) Pawona	11.13	0.349	3.4154	(3509) Sanshui	12.17	0.254	13.68	(15362) 1996 ED	13.54	0.199	31.4
(1162) Larissa	9.594	0.490	6.516	(3536) Schleicher	13.85	0.243	5.79	(15430) 1998 UR ₃₁	14.04	0.162	2.5273 [†]
(1224) Fantasia	11.43	0.233	4.995	(3544) Borodino	12.32	0.186	5.442	(15499) Cloyd	12.77	0.128	6.878
(1258) Sicilia	10.44	0.065	13.500	(3554) Amun	15.58	0.181	2.5300 [†]	(15914) 1997 UM ₃	14.08	0.210	12.8
(1281) Jeanne	11.43	0.114	15.2	(3560) Chenqian	10.86	0.257	18.79	(16681) 1994 EV ₇	14.34	0.337	5.3147
(1288) Santa	11.23	0.143	8.28	(3628) Boznemcova	12.71	0.198	3.3354 [†]	(16886) 1998 BC ₂₆	13.04	0.233	5.9908
(1296) Andree	11.60	0.194	5.1836 [†]	(3751) Kiang	11.56	0.175	8.2421	(17681) Tweedledum	14.53	0.496	75.2
(1299) Mertona	11.48	0.364	4.977	(3823) Yorii	12.91	0.171	6.669	(17822) 1998 FM ₁₃₅	13.52	0.220	4.613
(1310) Villigera	11.49	0.229	7.830	(3907) Kilmartin	11.74	0.224	3.841	(18487) 1996 AU ₃	12.63	0.188	6.512
(1316) Kasan	12.93	0.246	5.82	(3915) Fukushima	11.96	0.082	9.418	(19251) Totziens	13.41	0.124	18.446
(1325) Inanda	12.13	0.236	20.52	(3935) Toatenmongakkai	11.86	0.236	106.3	(20378) 1998 KZ ₄₆	12.84	0.243	5.14
(1335) Demoulina	12.74	0.301	74.86	(3936) Elst	12.89	0.219	6.6322	(20932) 2258 T-1	13.33	0.144	4.3239
(1352) Wawel	11.07	0.233	16.97	(4003) Schumann	11.10	0.149	5.7502	(21594) 1998 VP ₃₁	13.08	0.091	5.5865
(1375) Alfreda	11.45	0.320	19.14	(4006) Sandler	12.55	0.183	3.40	(23200) 2000 SH ₃	12.97	0.156	16.22
(1412) Lagrula	12.24	0.272	5.9176	(4008) Corbin	12.94	0.110	6.203	(23276) 2000 YT ₁₀₁	14.26	0.045	3.661
(1443) Ruppina	10.97	0.287	5.880	(4029) Bridges	12.65	0.241	3.5746	(24101) Cassini	12.89	0.167	3.986
(1452) Hunnia	11.94	0.122	17.2	(4142) Dersu-Uzala	13.18	0.272	140.0	(27851) 1994 VG ₂	13.64	0.125	7.733
(1501) Baade	11.86	0.217	15.132	(4150) Starr	12.70	0.240	4.5179	(28126) Nydegger	15.13	0.154	3.783
(1517) Beograd	10.98	0.147	6.943	(4255) Spacewatch	13.08	0.268	20.0	(30470) 2000 OR ₁₉	13.85	0.153	23.02
(1536) Pielinen	12.57	0.308	66.22	(4264) Karljosephine	13.33	0.180	30.96	(32802) 1990 SK	13.87	0.223	2.427
(1542) Schalen	10.46	0.316	7.516	(4294) Horatius	12.62	0.135	12.499	(33916) 2000 LF ₁₉	14.39	0.138	4.4099
(1565) Lemaitre	12.71	0.321	11.403	(4352) Kyoto	11.62	0.245	21.9352	(41044) 1999 VW ₆	13.12	0.146	2.734
(1567) Alikoski	9.550	0.152	16.405	(4359) Berlage	13.47	0.135	7.413	(41223) 1999 XD ₁₆	13.43	0.066	32.52
(1573) Vaisala	12.23	0.249	252.0	(4363) Sergej	13.29	0.233	13.04	(41288) 1999 XD ₁₀₇	14.19	0.154	4.36
(1577) Reiss	12.65	0.397	4.5050	(4383) Suruga	13.08	0.332	3.4069	(42265) 2001 QL ₆₉	13.24	0.157	8.6
(1628) Strobel	10.01	0.107	9.52	(4528) Berg	12.03	0.271	3.5163	(42946) 1999 TU ₉₅	13.67	0.202	3.42
(1644) Rafita	11.41	0.321	6.800	(4565) Grossman	12.77	0.255	4.7429	(44892) 1999 VJ ₈	12.83	0.259	5.872
(1651) Behrens	12.13	0.364	34.34	(4569) Baerbel	12.13	0.209	2.737	(45436) 2000 AD ₁₇₆	14.22	0.105	18.47
(1655) Comas Sola	10.96	0.243	20.456	(4613) Mamoru	11.61	0.165	5.388	(68216) 2001 CV ₂₆	16.38	0.244	2.4290
(1702) Kalahari	10.92	0.238	21.153	(4713) Steel	13.29	0.339	5.199	(69350) 1993 YP	15.29	0.293	31.79
(1723) Klemola	10.04	0.257	6.2545	(4771) Hayashi	12.48	0.122	9.801	(72675) 2001 FP ₅₄	14.38	0.067	2.50
(1734) Zhongolovich	11.50	0.111	7.171	(4898) Nishiizumi	14.21	0.421	3.289	(90698) Kosciuszko	14.17	0.196	5.014
(1741) Giclas	11.45	0.324	2.943	(4899) Candace	12.75	0.209	40.7				

Note. [†]Indicates a *P_{rot}* value that has been truncated from the reported value at four decimal places.

Table 2: WISE Observation Circumstances and Fluxes

Object	UT Date ^a	$\Delta t_{\text{obs}}^{\text{b}}$	N^{c}	R_{AU}^{d}	$\Delta_{\text{AU}}^{\text{e}}$	α ($^{\circ}$) ^f	$\overline{F_{\text{W}3}}^{\text{g}}$	$\diamond F_{\text{W}3}^{\text{h}}$	$\overline{F_{\text{W}4}}^{\text{g}}$	$\diamond F_{\text{W}4}^{\text{h}}$
(91) Aegina	17 Jan 2010	1.125	12	2.604	2.376	22.19	8604 ± 1238	2721 ± 2350	129200 ± 260	3602 ± 442
	5 Jul 2010	1.258	12	2.772	2.491	-21.43	5539 ± 797	1289 ± 1590	10360 ± 230	2003 ± 393
(155) Scylla	30 Jan 2010	1.125	12	2.860	2.694	20.14	599.0 ± 6.9	155.2 ± 14.7	1388 ± 27	363.3 ± 55.6
	16 Jul 2010	3.902	20	3.252	2.999	-18.12	299.1 ± 3.7	92.30 ± 7.06	858.8 ± 19.0	241.3 ± 36.9
(271) Penthesilea	20 Jan 2010	0.992	10	3.278	3.104	17.46	849.2 ± 9.2	152.4 ± 18.5	2411 ± 45	341.6 ± 73.0
	6 Jul 2010	1.258	15	3.306	3.056	-17.83	789.9 ± 9.3	169.0 ± 18.8	2296 ± 41	493.3 ± 76.6
(295) Theresia	31 Jan 2010	1.125	11	3.122	2.977	18.39	198.6 ± 2.6	22.02 ± 5.41	547.7 ± 12.6	46.63 ± 24.87
	22 Jul 2010	0.992	12	3.257	3.023	-18.12	155.2 ± 2.2	16.47 ± 4.28	457.0 ± 10.0	46.24 ± 19.72
(322) Phaeo	25 Jan 2010	0.992	8	3.445	3.302	16.60	605.1 ± 6.8	188.3 ± 13.3	1858 ± 38	467.2 ± 76.5
	10 Jul 2010	1.121	10	3.281	3.022	-17.95	880.6 ± 9.8	225.6 ± 19.3	2389 ± 46	601.7 ± 109.3
(343) Ostara	12 Jan 2010	0.992	11	2.678	2.443	21.51	165.1 ± 2.3	62.98 ± 4.39	359.4 ± 9.6	234.7 ± 16.7
	25 Jun 2010	1.254	14	2.916	2.656	-20.33	139.0 ± 1.9	51.18 ± 3.62	343.3 ± 9.2	122.7 ± 18.3
(444) Gyptis	30 Jan 2010	1.125	9	3.150	3.005	18.22	7659 ± 1114	3179 ± 2370	14500 ± 2050	2603 ± 4636
	20 Jul 2010	1.258	12	2.925	2.673	-20.27	15060 ± 2180	3594 ± 4736	21640 ± 3100	2781 ± 6289
(463) Lola	7 Jan 2010	0.598	6	2.904	2.659	19.73	182.6 ± 2.5	28.24 ± 4.94	435.4 ± 11.2	40.06 ± 21.72
	14 Jun 2010	1.254	12	2.903	2.616	-20.36	149.7 ± 2.0	28.69 ± 3.88	380.1 ± 9.2	65.19 ± 17.67
(464) Megaira	9 Jan 2010	0.465	6	3.371	3.162	16.92	1033 ± 11	74.80 ± 21.49	3016 ± 39	181.1 ± 60.3
	17 Jun 2010	3.504	26	3.320	3.071	-17.73	1148 ± 149	148.0 ± 285.4	3254 ± 65	369.4 ± 137.7
(493) Griseldis	13 Jan 2010	0.727	9	3.487	3.298	16.36	235.4 ± 2.9	76.84 ± 5.77	737.4 ± 14.5	268.0 ± 33.0
	26 Jun 2010	0.992	9	3.621	3.399	-16.25	199.6 ± 2.5	44.93 ± 4.97	656.6 ± 15.0	153.2 ± 29.1
(500) Selinur	7 Feb 2010	1.258	9	2.951	2.764	19.52	446.7 ± 5.0	115.8 ± 9.4	1218 ± 27	232.3 ± 56.3
	27 Jul 2010	1.125	11	2.785	2.514	-21.30	718.3 ± 8.1	121.6 ± 15.8	1724 ± 28	202.7 ± 58.5
(520) Franziska	19 Jan 2010	0.859	11	3.207	3.029	17.86	107.1 ± 1.7	72.43 ± 3.39	330.1 ± 7.9	189.5 ± 15.5
	5 Jul 2010	1.254	13	3.305	3.056	-17.83	105.0 ± 1.5	58.25 ± 3.30	335.1 ± 8.3	167.9 ± 19.0
(538) Friederike	15 Feb 2010	1.125	12	3.586	3.439	15.99	595.8 ± 6.8	109.7 ± 13.7	1862 ± 43	391.4 ± 104.5
	3 Aug 2010	0.992	11	3.403	3.160	-17.27	840.1 ± 9.4	164.7 ± 17.9	2448 ± 40	396.7 ± 77.0
(558) Carmen	3 Feb 2010	3.906	23	2.937	2.769	19.60	1058 ± 83	444.3 ± 245.3	2514 ± 44	565.0 ± 113.1
	27 Jul 2010	1.258	16	3.000	2.746	-19.71	1048 ± 108	306.9 ± 265.2	2580 ± 44	582.9 ± 80.2
(562) Salome	22 Jan 2010	0.992	13	3.225	3.061	17.76	186.7 ± 2.4	54.54 ± 5.04	591.6 ± 13.7	152.9 ± 24.1
	10 Jul 2010	1.258	15	3.095	2.828	-19.07	246.5 ± 3.4	74.90 ± 7.48	707.0 ± 15.9	199.2 ± 31.9
(567) Eleutheria	20 Jan 2010	0.992	10	2.835	2.637	20.30	3218 ± 465	940.2 ± 901.3	6781 ± 101	1590 ± 188
	10 Jul 2010	1.254	14	2.871	2.588	-20.62	2654 ± 386	1029 ± 802	5886 ± 107	2048 ± 231
(583) Klotilde	26 Jan 2010	0.992	8	2.771	2.595	20.81	2968 ± 426	530.1 ± 876.2	6325 ± 117	1104 ± 165
	21 Jul 2010	0.992	10	3.016	2.769	-19.63	1625 ± 233	278.2 ± 478.3	4226 ± 90	812.8 ± 219.9
(651) Antikleia	29 Jan 2010	1.125	11	3.312	3.172	17.30	162.5 ± 2.1	43.80 ± 4.03	510.6 ± 13.8	117.9 ± 31.7
	17 Jul 2010	3.902	20	3.306	3.059	-17.82	187.1 ± 2.4	52.87 ± 4.69	559.9 ± 12.7	154.1 ± 22.3

Table 2 — continued

Object	UT Date ^a	$\Delta t_{\text{obs}}^{\text{b}}$	N^{c}	R_{AU}^{d}	$\Delta_{\text{AU}}^{\text{e}}$	$\alpha (\circ)^{\text{f}}$	$\bar{W}3^{\text{g}}$	$\diamond W3^{\text{h}}$	$\bar{W}4^{\text{g}}$	$\diamond W4^{\text{h}}$
(656) Beagle	31 Jan 2010	1.258	12	2.824	2.661	20.42	813.7 ± 132.2	1275 ± 281	2342 ± 49	1780 ± 124
	27 Jul 2010	1.125	14	3.031	2.779	-19.50	554.2 ± 7.5	426.9 ± 15.4	1593 ± 29	1303 ± 62
(662) Newtonia	17 Jan 2010	0.992	10	2.681	2.462	21.51	214.6 ± 2.8	122.5 ± 6.1	498.4 ± 11.8	242.7 ± 26.3
	7 Jul 2010	1.391	18	2.289	1.961	-26.24	532.2 ± 7.0	395.5 ± 14.3	1029 ± 21	478.6 ± 38.8
(668) Dora	17 Jan 2010	0.992	9	3.219	3.033	17.78	104.8 ± 1.5	42.35 ± 2.97	291.0 ± 8.4	107.8 ± 16.5
	2 Jul 2010	1.258	15	2.895	2.626	-20.47	156.6 ± 2.1	84.84 ± 3.96	384.6 ± 11.2	203.1 ± 24.4
(670) Ottegebe	26 Jan 2010	0.996	9	3.332	3.187	17.18	183.5 ± 2.5	40.37 ± 5.03	593.0 ± 12.3	112.4 ± 26.2
	12 Jul 2010	1.125	13	3.206	2.942	-18.38	207.0 ± 2.6	53.42 ± 5.45	638.6 ± 13.6	175.1 ± 23.9
(688) Melanie	25 Jan 2010	0.992	11	2.808	2.629	20.52	645.9 ± 7.4	224.3 ± 15.7	1461 ± 30	571.7 ± 55.9
	15 Jul 2010	4.301	25	2.566	2.269	-23.22	964.6 ± 11.2	291.0 ± 22.2	2012 ± 35	569.2 ± 72.7
(734) Benda	13 Jan 2010	0.727	8	3.237	3.038	17.66	949.1 ± 11.2	310.2 ± 22.8	2624 ± 47	594.0 ± 90.8
	28 Jun 2010	0.992	12	3.363	3.125	-17.53	755.5 ± 8.3	281.2 ± 16.1	2189 ± 45	752.8 ± 99.7
(735) Marghanna	3 Feb 2010	3.770	20	3.313	3.156	17.31	864.6 ± 10.7	173.1 ± 25.5	2374 ± 46	390.9 ± 91.0
	23 Jul 2010	0.594	8	2.873	2.616	-20.64	2161 ± 310	270.2 ± 622.6	4391 ± 78	731.5 ± 175.8
(793) Arizona	1 Feb 2010	0.992	10	3.046	2.897	18.87	159.7 ± 2.2	31.25 ± 4.63	451.8 ± 11.8	76.92 ± 21.93
	23 Jul 2010	1.125	13	2.871	2.613	-20.65	210.8 ± 2.7	22.51 ± 5.66	557.4 ± 13.0	52.99 ± 24.17
(826) Henrika	16 Jan 2010	0.859	8	2.547	2.314	22.70	268.7 ± 3.9	87.78 ± 8.22	594.5 ± 18.9	213.4 ± 44.8
	10 Jul 2010	1.387	14	2.230	1.889	-26.96	491.2 ± 5.9	145.5 ± 11.1	970.3 ± 19.6	249.1 ± 38.7
(829) Academia	17 Jan 2010	0.992	9	2.797	2.587	20.58	654.8 ± 7.9	295.5 ± 15.2	1498 ± 29	598.2 ± 52.8
	3 Jul 2010.	1.258	12	2.835	2.561	-20.92	695.0 ± 8.3	238.3 ± 15.4	1578 ± 32	522.5 ± 59.5
(883) Matterania	16 Jan 2010	0.992	8	2.571	2.341	22.47	27.42 ± 0.79	12.08 ± 1.64	63.19 ± 4.22	29.54 ± 8.82
	3 Jul 2010	1.121	14	2.261	1.933	-26.60	43.37 ± 0.90	26.01 ± 1.80	91.33 ± 4.19	51.78 ± 8.21
(906) Repsolda	13 Feb 2010	1.125	13	3.000	2.821	19.21	1146 ± 158	323.3 ± 310.1	3026 ± 49	478.9 ± 83.8
	3 Aug 2010	1.258	12	2.864	2.589	-20.65	1840 ± 264	350.0 ± 546.8	4302 ± 66	1088 ± 104
(918) Itha	25 Jan 2010	0.992	8	3.286	3.136	17.43	52.28 ± 0.97	14.68 ± 1.94	182.9 ± 5.8	41.91 ± 11.12
	12 Jul 2010	1.125	10	3.058	2.786	-19.31	102.4 ± 1.6	24.24 ± 3.13	306.8 ± 7.5	78.31 ± 13.81
(972) Cohnia	16 Feb 2010	1.125	9	3.662	3.519	15.65	670.6 ± 7.6	101.1 ± 15.4	2081 ± 34	340.1 ± 68.1
	4 Aug 2010	1.125	11	3.426	3.184	-17.14	916.9 ± 10.1	197.6 ± 17.7	2677 ± 53	575.4 ± 120.3
(977) Philippa	19 Jan 2010	0.992	12	3.038	2.850	18.88	1088 ± 137	462.3 ± 279.3	2976 ± 57	1028 ± 149
	7 Jul 2010	1.125	12	3.072	2.809	-19.23	1158 ± 167	510.8 ± 326.7	3285 ± 53	1150 ± 117
(987) Wallia	15 Feb 2010	1.125	11	3.365	3.210	17.07	344.4 ± 4.4	64.07 ± 8.82	1088 ± 19	122.3 ± 42.4
	5 Aug 2010	0.859	6	2.992	2.723	-19.72	737.4 ± 8.6	53.58 ± 17.37	1810 ± 33	64.21 ± 65.66
(998) Bodea	7 Feb 2010	1.125	8	3.727	3.578	15.34	71.80 ± 1.21	43.08 ± 2.29	258.6 ± 6.8	148.0 ± 14.7
	25 Jul 2010	0.992	10	3.560	3.338	-16.52	105.6 ± 1.6	63.93 ± 2.88	354.5 ± 8.6	211.5 ± 16.0
(1018) Arnolda	10 Feb 2010	0.992	10	2.858	2.668	20.20	69.15 ± 1.15	27.09 ± 2.17	190.7 ± 6.3	74.98 ± 13.27
	3 Jul 2010	1.387	10	2.439	2.136	-24.49	151.5 ± 2.1	91.37 ± 3.85	347.0 ± 9.0	183.8 ± 18.6

Table 2 — continued

Object	UT Date ^a	$\Delta t_{\text{obs}}^{\text{b}}$	N^{c}	R_{AU}^{d}	$\Delta_{\text{AU}}^{\text{e}}$	$\alpha (\circ)^{\text{f}}$	$\bar{W}3^{\text{g}}$	$\diamond W3^{\text{h}}$	$\bar{W}4^{\text{g}}$	$\diamond W4^{\text{h}}$
(1047) Geisha	17 Jan 2010	0.992	12	2.651	2.429	21.77	52.48 ± 0.99	19.88 ± 2.07	122.7 ± 4.8	46.02 ± 9.21
	1 Jul 2010	1.391	14	2.637	2.350	-22.58	50.23 ± 0.97	23.05 ± 1.92	120.2 ± 4.9	50.83 ± 8.98
(1051) Merope	26 Jan 2010	0.859	11	3.396	3.254	16.85	587.6 ± 6.4	93.96 ± 13.64	1701 ± 30	320.3 ± 57.5
	13 Jul 2010	1.258	14	3.259	3.000	-18.08	724.2 ± 7.7	134.1 ± 14.7	2024 ± 42	349.1 ± 102.6
(1076) Viola	24 Jan 2010	0.992	10	2.503	2.295	23.15	334.8 ± 4.0	36.84 ± 8.26	677.5 ± 14.0	39.52 ± 29.06
	13 Jul 2010	1.258	14	2.729	2.431	-21.74	247.7 ± 3.1	41.02 ± 5.88	535.4 ± 12.7	76.71 ± 23.36
(1077) Campanula	22 Jan 2010	0.992	10	2.850	2.662	20.19	23.19 ± 0.68	10.91 ± 1.30	69.82 ± 4.21	38.68 ± 8.96
	8 Jul 2010	1.258	11	2.678	2.386	-22.20	28.91 ± 0.70	13.18 ± 1.39	82.05 ± 4.02	31.76 ± 7.44
(1083) Salvia	7 Jan 2010	0.992	11	2.018	1.692	29.08	141.8 ± 2.0	94.99 ± 4.03	264.5 ± 6.8	168.3 ± 14.1
	29 Jun 2010	0.992	13	2.361	2.048	-25.40	86.86 ± 1.39	34.85 ± 2.93	183.5 ± 5.6	68.22 ± 11.41
(1095) Tulipa	12 Jan 2010	0.992	10	2.951	2.733	19.44	215.3 ± 2.7	50.85 ± 5.76	599.9 ± 12.7	140.7 ± 25.3
	29 Jun 2010	1.254	16	2.970	2.709	-19.93	180.1 ± 2.4	53.84 ± 5.06	530.7 ± 12.7	141.0 ± 23.6
(1109) Tata	10 Feb 2010	1.125	12	2.987	2.804	19.29	1318 ± 190	351.9 ± 388.2	3058 ± 59	350.0 ± 111.7
	4 Aug 2010	1.125	8	2.894	2.620	-20.42	1581 ± 227	233.2 ± 464.1	3405 ± 65	722.5 ± 152.6
(1123) Shapleya	9 Feb 2010	1.258	13	2.566	2.352	22.61	71.23 ± 1.28	35.78 ± 3.05	161.9 ± 5.39	66.59 ± 11.27
	29 Jul 2010	1.258	12	2.518	2.223	-23.68	80.40 ± 1.25	43.53 ± 2.43	175.4 ± 6.2	89.60 ± 13.11
(1125) China	12 Feb 2010	1.125	10	3.187	3.017	18.04	111.0 ± 1.5	55.77 ± 3.09	344.5 ± 9.5	168.6 ± 17.8
	1 Aug 2010	0.992	11	3.500	3.263	-16.78	86.05 ± 1.29	36.15 ± 2.67	293.0 ± 7.5	136.1 ± 17.0
(1136) Mercedes	4 Feb 2010	3.770	22	3.079	2.917	18.67	157.2 ± 2.1	54.11 ± 4.11	418.9 ± 10.3	116.9 ± 21.3
	24 Jul 2010	1.121	12	2.745	2.475	-21.64	359.3 ± 4.2	66.54 ± 8.61	780.4 ± 17.3	154.0 ± 29.5
(1142) Aetolia	27 Jan 2010	1.125	10	2.944	2.780	19.54	136.5 ± 1.8	24.48 ± 3.62	369.7 ± 10.7	63.15 ± 21.98
	23 Jul 2010	1.258	11	2.900	2.642	-20.44	149.4 ± 2.0	50.21 ± 4.38	390.6 ± 10.1	114.1 ± 22.8
(1152) Pawona	16 Jan 2010	0.992	12	2.324	2.068	25.02	206.7 ± 2.9	37.61 ± 6.43	440.2 ± 12.4	102.1 ± 26.6
	9 Jul 2010	1.391	14	2.344	2.019	-25.56	243.1 ± 3.2	41.58 ± 6.18	519.9 ± 11.2	87.69 ± 26.02
(1162) Larissa	28 Jan 2010	1.254	12	3.610	3.480	15.83	183.2 ± 2.4	68.91 ± 5.02	607.7 ± 14.2	214.9 ± 33.2
	22 Jul 2010	1.258	10	3.514	3.292	-16.75	224.2 ± 2.9	36.96 ± 5.92	725.8 ± 16.2	121.3 ± 30.9
(1224) Fantasia	8 Feb 2010	0.594	8	2.761	2.563	20.93	83.37 ± 1.31	12.65 ± 2.68	195.8 ± 5.6	29.47 ± 11.26
	26 Jul 2010	0.992	10	2.652	2.372	-22.42	85.89 ± 1.46	14.52 ± 2.79	216.1 ± 6.6	29.33 ± 12.08
(1258) Sicilia	27 Jan 2010	1.125	9	3.303	3.160	17.34	367.0 ± 4.6	55.84 ± 9.12	1073 ± 25	212.8 ± 46.0
	16 Jul 2010	3.902	22	3.283	3.036	-17.95	373.0 ± 7.9	70.47 ± 33.76	1100 ± 35	259.0 ± 139.7
(1281) Jeanne	14 Jan 2010	1.125	12	2.567	2.329	22.51	422.1 ± 5.1	94.81 ± 10.48	851.7 ± 19.6	156.1 ± 37.3
	6 Jul 2010	1.391	15	2.195	1.856	-27.45	698.3 ± 8.4	248.8 ± 15.8	1299 ± 29	402.6 ± 55.7
(1288) Santa	22 Jan 2010	0.992	8	3.052	2.875	18.81	241.4 ± 3.1	177.7 ± 5.6	623.0 ± 15.7	417.9 ± 29.3
	11 Jul 2010	0.992	12	2.993	2.719	-19.75	336.5 ± 4.4	172.9 ± 8.7	827.8 ± 18.7	418.7 ± 40.2
(1296) Andree	20 Jan 2010	0.992	10	2.310	2.069	25.20	720.9 ± 8.4	223.9 ± 14.8	1363 ± 24	361.0 ± 50.6
	10 Jul 2010	1.387	13	2.571	2.266	-23.16	363.2 ± 4.3	108.8 ± 8.5	827.5 ± 18.1	200.9 ± 32.0

Table 2 — continued

Object	UT Date ^a	$\Delta t_{\text{obs}}^{\text{b}}$	N^{c}	R_{AU}^{d}	$\Delta_{\text{AU}}^{\text{e}}$	$\alpha (\circ)^{\text{f}}$	$\bar{W}3^{\text{g}}$	$\diamond W3^{\text{h}}$	$\bar{W}4^{\text{g}}$	$\diamond W4^{\text{h}}$
(1299) Mertona	19 Jan 2010	0.992	8	3.006	2.815	19.09	51.62 ± 1.00	23.62 ± 2.06	146.1 ± 5.3	63.74 ± 11.01
	4 Jul 2010	0.992	12	3.230	2.980	-18.26	31.51 ± 0.75	18.40 ± 1.44	103.5 ± 4.2	50.74 ± 7.51
(1310) Villigera	19 Jan 2010	0.992	10	2.170	1.910	26.95	213.3 ± 2.7	63.98 ± 5.28	385.6 ± 11.2	121.8 ± 19.6
	2 Jul 2010	1.125	12	2.778	2.503	-21.38	61.41 ± 1.08	15.08 ± 2.17	158.6 ± 5.0	41.43 ± 10.28
(1316) Kasan	14 Jan 2010	0.992	9	3.022	2.818	18.97	13.30 ± 0.52	1.927 ± 1.058	32.35 ± 3.00	6.024 ± 5.970
	23 Jun 2010	1.125	10	3.175	2.938	-18.61	11.43 ± 0.51	1.818 ± 1.017	30.25 ± 3.05	10.60 ± 6.30
(1325) Inanda	18 Jan 2010	0.996	13	3.145	2.957	18.22	26.52 ± 0.68	10.39 ± 1.32	74.42 ± 3.66	32.24 ± 6.95
	1 Jul 2010	1.258	13	2.915	2.649	-20.33	30.42 ± 0.76	17.80 ± 1.52	81.33 ± 4.22	59.72 ± 8.96
(1335) Demouolina	8 Jan 2010	0.727	9	2.560	2.300	22.54	28.74 ± 0.72	16.68 ± 1.43	64.39 ± 3.65	38.53 ± 7.52
	21 Jun 2010	1.391	14	2.565	2.284	-23.27	22.71 ± 0.70	26.55 ± 1.32	53.77 ± 3.65	65.49 ± 7.00
(1352) Wawel	1 Feb 2010	1.125	11	2.951	2.797	19.50	97.17 ± 1.41	32.99 ± 2.84	281.2 ± 7.9	95.20 ± 15.20
	25 Jul 2010	0.992	13	2.950	2.693	-20.07	92.12 ± 1.51	48.37 ± 2.98	275.4 ± 7.8	147.9 ± 15.3
(1375) Alfreda	30 Jan 2010	1.258	11	2.501	2.310	23.19	100.9 ± 1.6	21.40 ± 2.82	234.7 ± 7.7	55.63 ± 14.53
	24 Jul 2010	1.258	12	2.599	2.317	-22.93	97.46 ± 1.46	18.57 ± 2.83	235.6 ± 6.9	47.80 ± 13.60
(1412) Lagrula	23 Jan 2010	0.992	12	2.258	2.022	25.83	53.52 ± 1.35	47.35 ± 3.69	111.0 ± 4.3	93.99 ± 8.55
	13 Jul 2010	1.254	11	2.427	2.102	-24.61	52.74 ± 0.94	31.90 ± 1.93	113.7 ± 4.6	82.07 ± 8.25
(1443) Ruppina	11 Feb 2010	1.125	12	3.029	2.851	19.01	52.19 ± 0.98	25.00 ± 1.80	161.9 ± 5.9	71.18 ± 12.14
	3 Aug 2010	0.992	9	2.933	2.666	-20.15	60.26 ± 1.02	20.21 ± 2.26	183.3 ± 5.9	58.84 ± 12.80
(1452) Hunnia	23 Jan 2010	0.996	11	2.849	2.663	20.21	152.4 ± 2.3	97.22 ± 4.84	354.2 ± 10.2	163.4 ± 19.8
	11 Jul 2010	1.254	11	3.183	2.921	-18.52	84.56 ± 1.33	52.23 ± 2.65	247.5 ± 7.3	149.4 ± 16.7
(1501) Baade	17 Feb 2010	1.258	9	3.142	2.977	18.33	16.69 ± 0.65	5.537 ± 1.308	55.98 ± 3.59	17.40 ± 6.76
	5 Aug 2010	0.398	5	2.962	2.691	-19.93	25.35 ± 0.66	7.139 ± 1.298	75.87 ± 3.57	23.11 ± 7.11
(1517) Beograd	30 Jan 2010	0.859	9	2.718	2.545	21.24	657.0 ± 8.1	95.67 ± 15.35	1456 ± 34	186.3 ± 61.5
	25 Jul 2010	1.258	13	2.645	2.366	-22.50	741.0 ± 8.8	139.9 ± 17.9	1576 ± 37	311.5 ± 90.9
(1536) Pielinen	17 Jan 2010	0.992	9	2.634	2.412	21.92	25.52 ± 0.70	21.03 ± 1.41	61.29 ± 3.33	52.30 ± 6.64
	2 Jul 2010	1.391	16	2.534	2.236	-23.55	37.30 ± 0.86	26.51 ± 1.71	82.11 ± 3.85	61.70 ± 8.21
(1542) Schalen	21 Jan 2010	0.996	10	3.439	3.279	16.62	298.4 ± 4.1	154.9 ± 8.6	899.9 ± 17.2	445.2 ± 32.8
	7 Jul 2010	1.254	12	3.406	3.157	-17.28	337.2 ± 4.168	156.4 ± 8.062	991.6 ± 19.96	416.9 ± 40.93
(1565) Lemaitre	20 Feb 2010	0.992	12	3.092	2.927	18.65	14.22 ± 0.56	3.013 ± 1.117	38.54 ± 3.27	7.218 ± 6.449
	4 Aug 2010	1.258	11	2.690	2.403	-22.05	30.19 ± 0.74	3.058 ± 1.446	66.17 ± 3.53	9.524 ± 7.161
(1567) Alikoski	16 Jan 2010	0.992	11	2.951	2.745	19.45	1790 ± 258	385.6 ± 531.5	3970 ± 64	611.1 ± 108.1
	3 Jul 2010	0.727	8	3.027	2.763	-19.53	1619 ± 232	273.7 ± 478.8	3789 ± 78	613.6 ± 160.5
(1573) Vaisala	4 Feb 2010	3.773	21	2.901	2.729	19.87	23.46 ± 0.74	16.20 ± 1.41	61.87 ± 3.71	44.56 ± 7.75
	21 Jul 2010	1.258	17	2.704	2.437	-22.01	40.71 ± 0.87	27.40 ± 1.69	94.12 ± 3.84	82.24 ± 8.28
(1577) Reiss	8 Feb 2010	0.992	10	2.599	2.388	22.30	12.12 ± 0.59	5.103 ± 1.189	31.64 ± 3.49	14.16 ± 7.78
	28 Jul 2010	0.594	6	2.516	2.228	-23.72	10.80 ± 0.54	6.998 ± 1.078	26.82 ± 3.13	4.533 ± 6.230

Table 2 — continued

Object	UT Date ^a	$\Delta t_{\text{obs}}^{\text{b}}$	N^{c}	R_{AU}^{d}	$\Delta_{\text{AU}}^{\text{e}}$	$\alpha (\circ)^{\text{f}}$	$\bar{W}3^{\text{g}}$	$\diamond W3^{\text{h}}$	$\bar{W}4^{\text{g}}$	$\diamond W4^{\text{h}}$
(1628) Strobel	26 Jan 2010	0.992	10	2.983	2.820	19.27	872.0 ± 9.6	221.8 ± 20.5	2158 ± 43	519.6 ± 107.9
	14 Jul 2010	0.664	9	3.093	2.819	-19.07	890.3 ± 11.3	148.7 ± 21.7	2318 ± 48	370.9 ± 100.8
(1644) Rafita	19 Jan 2010	1.125	11	2.394	2.160	24.25	155.3 ± 2.2	37.28 ± 4.27	310.8 ± 9.1	57.83 ± 16.32
	9 Jul 2010	1.391	13	2.676	2.383	-22.21	117.9 ± 1.7	14.21 ± 3.28	252.6 ± 7.0	34.16 ± 15.97
(1651) Behrens	24 Jan 2010	1.258	11	2.041	1.785	28.83	156.3 ± 2.2	86.55 ± 4.50	259.0 ± 8.5	134.0 ± 20.2
	27 Jul 2010	1.523	15	2.147	1.813	-28.12	105.6 ± 1.6	79.34 ± 3.11	197.0 ± 6.5	182.6 ± 12.3
(1655) Comas Sola	22 Jan 2010	0.992	12	2.951	2.771	19.48	419.4 ± 4.9	75.71 ± 9.21	1039 ± 21	169.0 ± 36.3
	8 Jul 2010	1.125	11	3.258	3.003	-18.09	249.8 ± 3.0	63.90 ± 6.30	707.2 ± 15.6	144.6 ± 35.0
(1702) Kalahari	26 Jan 2010	0.996	13	3.182	3.027	18.02	242.0 ± 3.1	82.62 ± 6.17	660.2 ± 15.8	164.2 ± 41.6
	13 Jul 2010	1.125	13	3.009	2.732	-19.63	384.6 ± 4.6	149.2 ± 9.3	944.4 ± 21.6	257.4 ± 42.6
(1723) Klemola	1 Feb 2010	1.258	15	2.919	2.762	19.72	301.7 ± 3.7	102.7 ± 7.5	809.2 ± 16.3	265.4 ± 38.4
	26 Jul 2010	1.254	16	2.990	2.736	-19.79	339.9 ± 4.38	94.55 ± 8.98	888.4 ± 18.0	207.2 ± 37.2
(1734) Zhongolovich	5 Feb 2010	3.770	16	3.345	3.189	17.14	107.1 ± 1.7	27.52 ± 3.61	331.2 ± 9.4	80.04 ± 18.30
	25 Jul 2010	0.992	11	3.112	2.865	-18.98	200.9 ± 2.8	37.73 ± 5.28	522.1 ± 12.6	93.76 ± 24.87
(1741) Giclas	14 Feb 2010	1.258	12	3.082	2.910	18.69	26.54 ± 0.71	4.530 ± 1.426	86.16 ± 4.08	16.84 ± 8.32
	5 Aug 2010	1.258	10	3.050	2.785	-19.33	43.04 ± 0.89	9.065 ± 1.767	118.1 ± 4.9	27.52 ± 10.04
(1759) Kienle	31 Jan 2010	1.125	11	3.387	3.253	16.91	5.260 ± 0.534	3.971 ± 1.069	15.57 ± 3.60	23.29 ± 6.90
	16 Jul 2010	3.902	21	3.079	2.810	-19.17	11.24 ± 0.58	6.387 ± 1.162	33.22 ± 3.50	24.74 ± 7.19
(1768) Appenzella	16 Feb 2010	0.859	8	2.886	2.706	20.01	128.3 ± 1.9	33.28 ± 3.97	313.4 ± 6.7	72.51 ± 13.66
	4 Aug 2010	0.992	12	2.766	2.484	-21.41	143.8 ± 2.1	45.99 ± 3.85	341.9 ± 9.5	113.6 ± 17.5
(01807) Slovakia	28 Jan 2010	1.125	13	2.622	2.437	22.05	42.82 ± 0.89	29.57 ± 1.67	97.08 ± 4.58	101.0 ± 10.4
	16 Jul 2010	4.168	21	2.511	2.202	-23.74	44.36 ± 1.02	41.55 ± 2.35	94.07 ± 4.35	89.33 ± 9.19
(1896) Beer	24 Jan 2010	1.125	10	2.872	2.692	20.04	3.668 ± 0.551	2.372 ± 1.110	12.89 ± 3.43	8.372 ± 6.634
	10 Jul 2010	1.121	10	2.674	2.377	-22.22	5.898 ± 0.544	2.684 ± 1.109	18.74 ± 3.16	8.696 ± 6.395
(1936) Lugano	29 Jan 2010	1.258	12	2.357	2.152	24.70	847.6 ± 10.4	84.61 ± 20.44	$1510. \pm 24.79$	115.8 ± 56.66
	28 Jul 2010	1.254	11	2.577	2.290	-23.11	754.0 ± 8.8	72.25 ± 16.44	1375 ± 24	99.09 ± 48.34
(1979) Sakharov	3 Feb 2010	0.598	9	2.542	2.362	22.80	11.48 ± 0.61	3.270 ± 1.205	27.33 ± 3.41	18.20 ± 6.96
	27 Jul 2010	1.258	13	2.611	2.327	-22.80	7.480 ± 0.530	2.513 ± 1.069	18.85 ± 3.27	9.564 ± 6.457
(2005) Hencke	13 Feb 2010	1.125	9	3.055	2.880	18.86	12.46 ± 0.53	2.008 ± 1.088	39.10 ± 3.33	9.072 ± 6.557
	1 Aug 2010	0.992	9	3.019	2.759	-19.56	15.26 ± 0.56	2.762 ± 1.138	48.41 ± 3.43	11.77 ± 6.98
(2072) Kosmodemyanskaya	29 Jan 2010	1.254	13	2.695	2.517	21.43	4.511 ± 0.524	1.488 ± 1.040	14.38 ± 3.28	7.749 ± 6.683
	20 Jul 2010	1.254	9	2.840	2.582	-20.90	3.577 ± 0.501	0.955 ± 0.958	11.22 ± 4.04	6.158 ± 8.638
(2106) Hugo	15 Feb 2010	0.992	11	2.964	2.785	19.46	58.76 ± 1.13	34.10 ± 2.25	170.1 ± 5.0	83.51 ± 9.25
	5 Aug 2010	1.125	14	2.931	2.661	-20.15	60.07 ± 1.08	38.61 ± 2.44	175.1 ± 6.0	100.3 ± 11.0
(2111) Tselina	26 Jan 2010	0.730	9	3.273	3.124	17.50	68.31 ± 1.19	11.95 ± 2.38	232.0 ± 6.7	39.98 ± 14.02
	13 Jul 2010	1.125	12	3.294	3.034	-17.87	86.34 ± 1.31	24.99 ± 2.48	277.9 ± 8.6	80.77 ± 15.53

Table 2 — continued

Object	UT Date ^a	$\Delta t_{\text{obs}}^{\text{b}}$	N^{c}	R_{AU}^{d}	$\Delta_{\text{AU}}^{\text{e}}$	$\alpha (\circ)^{\text{f}}$	$\bar{W}3^{\text{g}}$	$\diamond W3^{\text{h}}$	$\bar{W}4^{\text{g}}$	$\diamond W4^{\text{h}}$
(2123) Vltava	8 Jan 2010	0.859	9	3.067	2.836	18.65	46.95 ± 0.95	12.40 ± 2.04	138.5 ± 5.3	34.81 ± 10.32
	21 Jun 2010	1.125	12	3.069	2.824	-19.27	52.23 ± 0.99	10.11 ± 1.83	146.8 ± 5.3	27.80 ± 11.82
(2140) Kemerovo	28 Jan 2010	1.125	12	3.144	2.994	18.25	279.8 ± 3.5	20.75 ± 7.63	717.6 ± 14.5	93.83 ± 32.56
	20 Jul 2010	0.992	10	3.145	2.907	-18.79	270.5 ± 3.6	31.82 ± 7.83	709.8 ± 14.1	49.88 ± 31.83
(2144) Marietta	31 Jan 2010	1.258	11	3.014	2.861	19.07	49.88 ± 0.97	18.84 ± 2.01	153.7 ± 4.6	53.90 ± 8.90
	24 Jul 2010	1.125	12	3.049	2.800	-19.39	42.64 ± 0.91	23.29 ± 1.80	144.5 ± 4.7	70.93 ± 9.01
(2177) Oliver	12 Feb 2010	0.992	10	3.259	3.093	17.63	46.64 ± 0.92	23.89 ± 1.83	165.9 ± 5.3	64.19 ± 9.76
	3 Aug 2010	1.258	12	3.101	2.843	-19.01	55.87 ± 1.01	33.25 ± 2.02	192.1 ± 5.9	91.41 ± 11.73
(2203) van Rhijn	31 Jan 2010	1.125	12	3.673	3.554	15.55	38.53 ± 0.84	19.77 ± 1.72	149.3 ± 5.0	69.59 ± 9.86
	21 Jul 2010	1.125	9	3.575	3.357	-16.46	55.17 ± 0.96	24.76 ± 1.80	195.9 ± 5.6	76.99 ± 10.89
(2204) Lyyli	17 Jan 2010	0.992	11	2.289	2.035	25.44	657.6 ± 8.4	210.4 ± 15.4	1187 ± 25	354.1 ± 44.3
	30 Jun 2010	1.258	15	2.974	2.717	-19.91	232.8 ± 3.0	56.45 ± 5.58	571.9 ± 14.6	158.8 ± 31.2
(2214) Carol	14 Feb 2010	1.258	13	3.187	3.021	18.05	129.9 ± 1.8	81.35 ± 4.11	360.0 ± 10.0	206.7 ± 23.3
	5 Aug 2010	0.598	7	2.744	2.457	-21.58	284.6 ± 3.6	151.5 ± 6.4	678.5 ± 11.3	319.6 ± 21.3
(2239) Paracelsus	8 Jan 2010	0.859	11	3.482	3.273	16.36	164.4 ± 2.4	93.39 ± 4.80	538.5 ± 12.8	311.7 ± 24.4
	21 Jun 2010	1.125	13	3.516	3.296	-16.75	154.5 ± 2.2	73.53 ± 4.70	512.6 ± 11.3	203.7 ± 23.8
(2268) Szmytowna	16 Jan 2010	0.992	10	3.137	2.944	18.26	37.24 ± 0.81	8.993 ± 1.600	112.5 ± 4.5	31.58 ± 9.50
	2 Jul 2010	1.258	16	3.246	2.997	-18.18	34.87 ± 0.78	8.080 ± 1.519	105.0 ± 4.5	28.15 ± 9.16
(2275) Cuitlahuac	4 Feb 2010	4.035	21	2.596	2.400	22.31	16.23 ± 0.66	16.04 ± 1.33	42.98 ± 3.39	37.89 ± 6.64
	28 Jul 2010	1.387	12	2.329	2.017	-25.74	35.38 ± 0.81	28.83 ± 1.65	77.37 ± 3.82	51.59 ± 7.38
(2297) Daghestan	13 Jan 2010	1.125	12	2.870	2.650	20.02	229.3 ± 3.0	115.5 ± 6.0	611.7 ± 14.8	233.6 ± 29.5
	4 Jul 2010	1.258	14	2.749	2.467	-21.61	248.6 ± 3.1	110.0 ± 6.2	645.1 ± 15.3	242.5 ± 27.8
(2306) Bauschinger	22 Jan 2010	0.992	10	2.872	2.683	20.03	102.4 ± 1.6	83.73 ± 2.96	252.9 ± 7.6	197.5 ± 14.6
	10 Jul 2010	1.258	13	2.793	2.504	-21.23	142.1 ± 2.1	92.85 ± 4.21	343.7 ± 9.0	204.0 ± 19.4
(2332) Kalm	13 Jan 2010	1.125	12	3.149	2.947	18.18	210.9 ± 2.8	128.3 ± 5.2	625.8 ± 16.4	378.9 ± 37.4
	29 Jun 2010	1.258	16	3.055	2.800	-19.36	229.4 ± 3.2	145.0 ± 6.7	656.6 ± 16.3	442.1 ± 35.3
(2347) Vinata	27 Jan 2010	0.992	7	3.701	3.573	15.43	47.96 ± 0.87	15.21 ± 1.75	185.8 ± 5.8	59.58 ± 13.13
	13 Jul 2010	0.992	9	3.741	3.501	-15.68	38.39 ± 0.78	17.74 ± 1.58	165.7 ± 4.8	56.78 ± 9.16
(2365) Interkosmos	21 Jan 2010	1.121	11	2.351	2.120	24.73	167.2 ± 2.4	46.32 ± 4.76	350.4 ± 9.2	97.27 ± 21.20
	14 Jul 2010	1.391	11	2.561	2.250	-23.24	113.4 ± 1.59	33.54 ± 3.06	268.9 ± 7.1	59.80 ± 14.15
(2375) Radek	20 Jan 2010	1.125	13	2.537	2.320	22.81	751.2 ± 8.5	202.3 ± 14.8	1481 ± 29	315.1 ± 55.0
	21 Jul 2010	1.254	15	2.528	2.244	-23.62	806.1 ± 10.0	306.6 ± 19.6	1549 ± 31	514.5 ± 84.2
(2446) Lunacharsky	25 Jan 2010	1.125	10	2.255	2.027	25.89	139.5 ± 2.0	96.00 ± 4.22	291.9 ± 8.4	187.6 ± 15.5
	29 Jul 2010	1.523	14	1.997	1.639	-30.43	355.2 ± 4.2	181.7 ± 9.1	616.2 ± 14.4	289.7 ± 27.0
(2463) Sterpin	24 Jan 2010	0.730	8	2.672	2.478	21.61	50.35 ± 0.96	12.70 ± 1.89	120.9 ± 5.4	33.40 ± 10.00
	11 Jul 2010	1.258	12	2.895	2.613	-20.44	39.80 ± 0.78	6.104 ± 1.561	107.5 ± 3.8	26.57 ± 7.30

Table 2 — continued

Object	UT Date ^a	$\Delta t_{\text{obs}}^{\text{b}}$	N^{c}	R_{AU}^{d}	$\Delta_{\text{AU}}^{\text{e}}$	$\alpha (\circ)^{\text{f}}$	$\bar{W}3^{\text{g}}$	$\diamond W3^{\text{h}}$	$\bar{W}4^{\text{g}}$	$\diamond W4^{\text{h}}$
(2500) Alascattalo	26 Jan 2010	1.258	13	2.029	1.777	29.03	76.01 ± 1.24	20.93 ± 2.50	141.8 ± 4.8	37.22 ± 9.02
	1 Aug 2010	1.656	15	2.076	1.726	-29.14	62.26 ± 1.13	18.50 ± 2.53	126.2 ± 4.9	30.63 ± 10.05
(2556) Louise	12 Jan 2010	1.121	13	2.119	1.827	27.61	38.05 ± 0.88	20.09 ± 2.02	79.13 ± 3.62	35.15 ± 7.29
	5 Jul 2010	1.391	16	2.192	1.854	-27.50	42.36 ± 0.89	19.98 ± 1.85	83.88 ± 4.23	49.38 ± 8.94
(2567) Elba	14 Jan 2010	1.125	11	3.058	2.850	18.74	56.35 ± 1.08	15.83 ± 2.13	166.1 ± 6.1	40.24 ± 12.44
	28 Jun 2010	1.258	16	2.894	2.629	-20.49	85.75 ± 1.36	20.47 ± 3.05	228.6 ± 6.6	57.51 ± 11.63
(2687) Tortali	18 Jan 2010	0.992	12	2.644	2.427	21.83	66.15 ± 1.12	27.69 ± 2.37	171.8 ± 5.4	60.79 ± 10.84
	8 Jul 2010	1.258	15	2.424	2.109	-24.67	138.6 ± 2.0	44.23 ± 3.73	305.5 ± 8.0	77.63 ± 17.20
(2786) Grinevia	15 Jan 2010	0.992	11	2.998	2.791	19.13	18.59 ± 0.64	7.540 ± 1.257	59.42 ± 3.66	24.17 ± 7.41
	28 Jun 2010	1.258	12	3.063	2.810	-19.31	19.32 ± 0.61	8.310 ± 1.213	61.06 ± 3.48	24.38 ± 6.88
(2855) Bastian	12 Jan 2010	0.992	12	2.431	2.174	23.82	54.29 ± 0.99	8.973 ± 2.048	111.4 ± 4.0	13.21 ± 7.68
	28 Jun 2010	1.391	15	2.706	2.429	-21.98	27.58 ± 0.74	6.113 ± 1.468	68.10 ± 3.55	18.17 ± 6.75
(2870) Haupt	31 Jan 2010	1.258	12	2.862	2.700	20.13	78.11 ± 1.32	90.06 ± 2.87	181.0 ± 6.0	174.9 ± 11.2
	22 Jul 2010	1.125	11	2.639	2.363	-22.56	109.9 ± 1.7	200.6 ± 3.4	240.4 ± 6.7	415.1 ± 14.1
(2947) Kippenhahn	8 Feb 2010	1.258	12	2.392	2.161	24.35	50.12 ± 1.014	20.06 ± 1.85	97.59 ± 4.03	32.89 ± 8.38
	3 Jul 2010	1.125	13	2.562	2.269	-23.24	29.47 ± 0.74	16.39 ± 1.54	69.13 ± 3.83	29.81 ± 7.83
(2985) Shakespeare	15 Jan 2010	0.992	10	2.912	2.702	19.72	25.56 ± 0.69	13.41 ± 1.34	73.05 ± 3.93	40.02 ± 8.02
	3 Jul 2010	1.258	15	2.843	2.569	-20.86	32.71 ± 0.76	19.86 ± 1.53	93.22 ± 4.21	59.42 ± 9.41
(3036) Krat	29 Jan 2010	0.992	10	3.428	3.293	16.70	248.9 ± 3.2	70.68 ± 6.13	805.1 ± 14.5	216.2 ± 24.1
	16 Jul 2010	0.594	8	3.303	3.040	-17.81	364.4 ± 4.1	55.13 ± 8.37	1118 ± 21	170.4 ± 45.5
(3051) Nantong	9 Feb 2010	1.258	11	3.210	3.041	17.90	34.05 ± 0.74	8.057 ± 1.565	112.7 ± 4.6	26.73 ± 9.64
	27 Jul 2010	1.125	10	2.969	2.712	-19.93	52.54 ± 0.95	17.92 ± 1.90	162.4 ± 5.4	52.63 ± 11.51
(3144) Brosche	1 Feb 2010	1.258	13	2.554	2.373	22.69	8.326 ± 0.561	4.752 ± 1.118	19.95 ± 3.23	11.03 ± 6.81
	26 Jul 2010	1.391	11	2.197	1.871	-27.42	15.55 ± 0.62	11.67 ± 1.24	36.06 ± 3.35	25.31 ± 6.91
(3162) Nostalgia	20 Jan 2010	0.992	13	3.229	3.057	17.74	159.0 ± 2.1	53.49 ± 4.12	497.5 ± 12.2	168.8 ± 22.9
	6 Jul 2010	1.258	16	3.444	3.204	-17.10	100.3 ± 1.54	55.76 ± 2.89	358.6 ± 8.6	183.4 ± 17.3
(3249) Musashino	23 Jan 2010	0.992	11	2.898	2.717	19.85	4.707 ± 0.529	2.929 ± 1.062	17.00 ± 3.25	20.34 ± 6.79
	7 Jul 2010	1.258	14	2.890	2.614	-20.49	5.565 ± 0.515	3.013 ± 1.063	18.80 ± 3.27	14.11 ± 6.51
(3267) Glo	14 Jan 2010	1.125	15	2.505	2.264	23.10	27.12 ± 0.68	8.897 ± 1.297	61.87 ± 3.31	20.61 ± 6.73
	25 Jun 2010	1.387	15	2.882	2.628	-20.59	15.33 ± 0.54	4.989 ± 1.044	38.84 ± 3.04	12.64 ± 6.21
(3305) Ceadams	17 Jan 2010	1.125	12	2.540	2.310	22.77	38.17 ± 0.86	14.24 ± 1.67	97.26 ± 3.98	43.10 ± 8.79
	8 Jul 2010	1.391	15	2.286	1.955	-26.27	88.30 ± 1.39	26.51 ± 2.77	185.5 ± 5.64	55.21 ± 9.96
(3411) Debetencourt	13 Jan 2010	1.258	13	2.062	1.766	28.44	41.86 ± 0.89	15.87 ± 1.75	74.06 ± 3.88	24.00 ± 7.97
	6 Jul 2010	1.520	17	2.289	1.961	-26.23	21.55 ± 0.67	12.87 ± 1.38	44.50 ± 3.53	24.07 ± 7.42
(3438) Inarradas	30 Jan 2010	1.125	7	3.512	3.384	16.28	62.88 ± 1.01	30.53 ± 2.06	204.9 ± 6.8	99.42 ± 13.96
	17 Jul 2010	3.902	19	3.274	3.026	-18.00	108.1 ± 1.6	61.82 ± 3.62	320.8 ± 8.6	168.0 ± 13.9

Table 2 — continued

Object	UT Date ^a	$\Delta t_{\text{obs}}^{\text{b}}$	N^{c}	R_{AU}^{d}	$\Delta_{\text{AU}}^{\text{e}}$	$\alpha (\circ)^{\text{f}}$	$\bar{W}3^{\text{g}}$	$\diamond W3^{\text{h}}$	$\bar{W}4^{\text{g}}$	$\diamond W4^{\text{h}}$
(3483) Svetlov	27 Jan 2010	1.258	14	2.172	1.944	26.95	3.713 ± 0.493	1.402 ± 1.024	10.10 ± 3.24	7.199 ± 6.372
	17 Jul 2010	4.562	31	2.043	1.689	-29.68	7.883 ± 0.556	4.366 ± 1.214	17.52 ± 3.28	14.94 ± 6.46
(3509) Sanshui	25 Jan 2010	0.992	9	2.972	2.804	19.34	22.41 ± 0.67	2.700 ± 1.285	62.35 ± 3.50	11.10 ± 7.33
	12 Jul 2010	1.125	14	2.830	2.541	-20.93	25.73 ± 0.69	5.474 ± 1.376	72.92 ± 3.48	15.84 ± 6.78
(3536) Schleicher	28 Jan 2010	1.258	10	2.354	2.145	24.73	6.651 ± 0.548	4.957 ± 1.088	13.61 ± 3.47	8.149 ± 6.769
	24 Jul 2010	1.391	10	2.436	2.139	-24.55	7.737 ± 0.547	6.560 ± 1.108	17.74 ± 3.30	13.40 ± 6.83
(3544) Borodino	19 Jan 2010	1.125	12	2.485	2.259	23.31	28.95 ± 0.78	21.15 ± 1.44	72.49 ± 3.72	50.44 ± 7.26
	12 Jul 2010	1.391	17	2.065	1.701	-29.32	96.77 ± 1.55	67.70 ± 3.20	186.1 ± 5.7	125.2 ± 10.7
(3554) Amun	13 Jan 2010	1.125	13	1.081	0.423	65.40	326.4 ± 3.9	32.85 ± 7.64	487.2 ± 11.0	55.47 ± 21.07
	4 May 2010	1.391	15	1.219	0.606	-55.47	163.9 ± 2.08	22.62 ± 4.25	227.6 ± 6.6	25.38 ± 13.63
(3560) Chenqian	9 Feb 2010	0.992	10	3.362	3.198	17.06	89.43 ± 1.40	23.33 ± 2.83	261.1 ± 7.8	59.87 ± 15.99
	29 Jul 2010	1.125	13	3.296	3.056	-17.88	83.81 ± 1.32	25.49 ± 2.72	260.9 ± 6.8	65.88 ± 12.07
(3628) Boznemcova	14 Jan 2010	0.859	8	3.215	3.019	17.79	6.446 ± 0.522	1.830 ± 1.047	24.54 ± 3.15	6.930 ± 6.136
	26 Jun 2010	1.125	11	2.923	2.663	-20.28	12.63 ± 0.54	3.554 ± 1.079	36.71 ± 3.75	18.92 ± 6.79
(3751) Kiang	3 Feb 2010	3.508	19	3.072	2.914	18.71	129.0 ± 1.8	42.73 ± 3.85	365.4 ± 8.8	121.0 ± 16.1
	28 Jul 2010	1.125	12	2.920	2.658	-20.27	136.9 ± 1.9	64.81 ± 3.82	384.9 ± 8.0	152.2 ± 15.4
(3823) Yorii	10 Feb 2010	1.125	12	2.779	2.583	20.79	49.46 ± 0.94	13.25 ± 1.90	127.9 ± 4.5	41.89 ± 8.49
	3 Jul 2010	1.258	12	3.201	2.951	-18.41	27.60 ± 0.68	5.931 ± 1.314	87.56 ± 3.69	23.22 ± 7.53
(3907) Kilmartin	15 Jan 2010	0.992	8	3.126	2.930	18.32	5.885 ± 0.466	2.361 ± 0.940	20.80 ± 3.14	12.48 ± 6.26
	30 Jun 2010	1.258	11	3.096	2.844	-19.09	5.257 ± 0.494	1.349 ± 0.989	24.74 ± 3.05	9.624 ± 6.331
(3915) Fukushima	25 Jan 2010	1.125	13	2.491	2.287	23.27	300.7 ± 4.0	208.9 ± 8.0	597.0 ± 15.1	403.9 ± 29.5
	16 Jul 2010	4.434	29	2.419	2.110	-24.73	406.4 ± 5.2	334.3 ± 12.5	798.6 ± 16.8	536.0 ± 32.7
(3935) Toatenmongakkai	24 Jan 2010	0.992	8	3.016	2.846	19.05	33.96 ± 0.75	13.93 ± 1.47	87.38 ± 4.24	31.12 ± 7.45
	9 Jul 2010	1.125	11	3.130	2.866	-18.85	21.76 ± 0.63	12.57 ± 1.28	61.19 ± 3.73	41.06 ± 8.15
(3936) Elst	17 Jan 2010	0.730	9	2.430	2.190	23.87	13.10 ± 0.57	2.377 ± 1.124	28.45 ± 3.18	8.861 ± 6.194
	10 Jul 2010	1.391	16	2.200	1.856	-27.36	23.03 ± 0.68	6.897 ± 1.396	47.59 ± 3.32	18.13 ± 6.57
(4003) Schumann	2 Feb 2010	1.125	11	3.388	3.258	16.91	198.2 ± 2.6	17.49 ± 5.11	608.6 ± 14.0	86.85 ± 26.49
	27 Jul 2010	0.992	11	3.236	2.993	-18.22	237.4 ± 3.1	31.78 ± 5.92	684.8 ± 11.4	92.83 ± 23.05
(4006) Sandler	9 Feb 2010	1.125	11	2.904	2.715	19.85	64.50 ± 1.13	12.84 ± 2.37	176.4 ± 6.5	39.92 ± 11.75
	28 Jul 2010	0.859	8	2.976	2.718	-19.87	71.91 ± 1.33	16.76 ± 2.38	201.7 ± 6.1	29.41 ± 12.53
(4008) Corbin	20 Jan 2010	1.125	13	1.967	1.684	30.00	56.17 ± 1.11	8.653 ± 2.043	97.93 ± 4.21	14.80 ± 9.03
	12 Jul 2010	1.520	19	2.357	2.038	-25.43	29.72 ± 0.71	4.143 ± 1.376	65.33 ± 3.26	13.30 ± 6.68
(4029) Bridges	23 Jan 2010	0.996	11	2.261	2.026	25.80	42.03 ± 0.94	12.01 ± 1.93	86.08 ± 4.00	29.35 ± 8.48
	26 Jul 2010	1.391	15	2.202	1.876	-27.36	64.65 ± 1.15	21.69 ± 2.34	126.3 ± 4.8	38.47 ± 10.49
(4142) Dersu-Uzala	20 Jan 2010	1.520	17	1.709	1.381	35.14	123.8 ± 1.8	54.08 ± 3.60	180.4 ± 5.2	75.45 ± 10.90
	12 Jul 2010	1.387	14	2.020	1.647	-30.03	77.67 ± 1.28	20.18 ± 2.52	125.2 ± 4.9	42.65 ± 10.45

Table 2 — continued

Object	UT Date ^a	$\Delta t_{\text{obs}}^{\text{b}}$	N^{c}	R_{AU}^{d}	$\Delta_{\text{AU}}^{\text{e}}$	$\alpha (\circ)^{\text{f}}$	$\bar{W}3^{\text{g}}$	$\diamond W3^{\text{h}}$	$\bar{W}4^{\text{g}}$	$\diamond W4^{\text{h}}$
(4150) Starr	12 Jan 2010	0.859	9	2.509	2.257	23.04	29.67 ± 0.75	7.640 ± 1.519	65.79 ± 3.67	24.41 ± 7.31
	28 Jun 2010	1.387	16	2.244	1.920	-26.83	42.35 ± 0.94	20.17 ± 1.85	86.43 ± 4.17	50.59 ± 9.20
(4255) Spacewatch	2 Feb 2010	0.996	11	3.532	3.407	16.20	37.30 ± 0.81	6.879 ± 1.630	110.6 ± 4.3	21.65 ± 9.13
	27 Jul 2010	1.254	13	3.389	3.153	-17.37	44.81 ± 0.85	8.374 ± 1.660	128.7 ± 5.0	25.72 ± 10.56
(4264) Karljosephine	8 Jan 2010	0.727	6	2.980	2.748	19.22	7.801 ± 0.531	2.536 ± 1.049	24.18 ± 3.34	14.50 ± 6.90
	16 Jun 2010	1.258	14	3.104	2.829	-18.98	5.458 ± 0.506	3.895 ± 1.015	16.24 ± 3.28	22.71 ± 6.80
(4294) Horatius	20 Jan 2010	0.992	7	2.861	2.666	20.11	27.32 ± 0.70	3.314 ± 1.406	63.28 ± 3.59	10.76 ± 6.91
	9 Jul 2010	1.121	13	2.850	2.567	-20.78	29.54 ± 0.73	3.008 ± 1.478	70.75 ± 3.68	16.80 ± 7.64
(4352) Kyoto	9 Feb 2010	1.125	11	3.226	3.056	17.81	24.46 ± 0.67	8.892 ± 1.351	75.66 ± 4.03	28.66 ± 8.01
	27 Jul 2010	1.125	10	3.306	3.068	-17.82	19.25 ± 0.60	8.777 ± 1.258	62.06 ± 3.53	25.29 ± 7.73
(4359) Berlage	22 Jan 2010	0.992	10	2.502	2.288	23.15	8.399 ± 0.553	6.148 ± 1.109	19.48 ± 3.31	15.73 ± 6.96
	10 Jul 2010	1.258	13	2.342	2.014	-25.59	15.79 ± 0.61	15.57 ± 1.19	35.92 ± 3.58	27.31 ± 7.56
(4363) Sergej	14 Feb 2010	1.125	10	2.877	2.694	20.07	6.078 ± 0.529	5.389 ± 1.071	16.62 ± 3.24	16.32 ± 6.72
	2 Aug 2010	0.859	10	2.638	2.347	-22.52	12.88 ± 0.59	4.870 ± 1.241	32.20 ± 3.52	15.26 ± 6.99
(4383) Suruga	28 Jan 2010	1.258	13	2.554	2.365	22.68	19.62 ± 0.66	4.328 ± 1.316	48.79 ± 3.42	18.51 ± 7.05
	22 Jul 2010	1.391	13	2.575	2.295	-23.16	15.83 ± 0.61	3.655 ± 1.180	40.31 ± 3.44	18.18 ± 7.15
(4528) Berg	12 Jan 2010	0.727	8	2.331	2.059	24.92	70.31 ± 1.12	21.56 ± 2.27	146.4 ± 5.5	44.33 ± 11.93
	1 Jul 2010	1.258	16	2.571	2.279	-23.19	48.99 ± 0.92	12.52 ± 1.85	112.5 ± 4.2	28.01 ± 9.16
(4565) Grossman	15 Jan 2010	0.992	11	2.281	2.017	25.51	35.05 ± 0.85	17.22 ± 1.76	76.72 ± 3.62	34.40 ± 7.65
	10 Jul 2010	1.520	16	2.253	1.919	-26.68	49.35 ± 0.96	29.84 ± 2.04	103.4 ± 4.0	52.14 ± 9.26
(4569) Baerbel	15 Jan 2010	1.125	10	2.490	2.249	23.25	63.22 ± 1.13	17.11 ± 2.45	140.9 ± 5.1	44.79 ± 11.46
	5 Jul 2010	1.391	16	2.425	2.114	-24.67	50.45 ± 1.00	21.14 ± 2.33	122.3 ± 4.6	50.47 ± 10.07
(4613) Mamoru	20 Jan 2010	0.992	10	3.307	3.137	17.31	13.48 ± 0.57	5.676 ± 1.127	48.24 ± 3.37	24.84 ± 7.12
	3 Jul 2010	1.125	14	3.464	3.225	-17.00	11.81 ± 0.52	4.811 ± 1.029	45.53 ± 3.31	22.44 ± 6.58
(4713) Steel	20 Jan 2010	1.523	18	1.885	1.589	31.45	83.95 ± 1.35	34.06 ± 2.64	139.5 ± 4.7	47.43 ± 9.36
	29 Jul 2010	1.785	20	1.784	1.389	-34.53	103.3 ± 1.6	33.78 ± 2.94	172.2 ± 5.7	41.74 ± 11.41
(4771) Hayashi	30 Jan 2010	1.125	10	2.919	2.761	19.72	27.99 ± 0.71	7.902 ± 1.465	92.22 ± 3.92	22.59 ± 7.29
	23 Jul 2010	1.258	15	2.663	2.387	-22.35	59.64 ± 1.07	25.86 ± 2.28	159.5 ± 5.3	63.37 ± 9.97
(4898) Nishiizumi	15 Jan 2010	1.258	16	1.801	1.469	33.07	11.49 ± 0.60	4.730 ± 1.172	20.19 ± 3.17	9.890 ± 6.578
	12 Jul 2010	1.258	9	1.940	1.558	-31.41	6.246 ± 0.495	2.801 ± 0.943	13.36 ± 3.17	10.74 ± 6.56
(4899) Candace	22 Jan 2010	1.125	10	2.212	1.969	26.42	50.63 ± 0.97	9.938 ± 1.986	92.27 ± 3.93	15.03 ± 7.60
	22 Jul 2010	1.652	20	1.946	1.594	-31.37	89.15 ± 1.40	27.86 ± 2.74	146.0 ± 4.6	41.90 ± 10.10
(4908) Ward	26 Jan 2010	0.992	9	2.657	2.468	21.74	8.856 ± 0.554	7.540 ± 1.116	20.58 ± 3.23	20.30 ± 6.76
	12 Jul 2010	1.258	14	2.384	2.057	-25.09	16.35 ± 0.63	14.56 ± 1.18	35.72 ± 3.20	33.65 ± 6.48
(5035) Swift	22 Jan 2010	1.125	13	2.501	2.287	23.17	44.13 ± 0.91	18.75 ± 1.95	100.8 ± 4.5	35.19 ± 8.73
	11 Jul 2010	0.992	10	2.774	2.482	-21.38	32.33 ± 0.74	10.53 ± 1.50	83.23 ± 4.04	23.79 ± 8.90

Table 2 — continued

Object	UT Date ^a	$\Delta t_{\text{obs}}^{\text{b}}$	N^{c}	R_{AU}^{d}	$\Delta_{\text{AU}}^{\text{e}}$	$\alpha (\circ)^{\text{f}}$	$\bar{W}3^{\text{g}}$	$\diamond W3^{\text{h}}$	$\bar{W}4^{\text{g}}$	$\diamond W4^{\text{h}}$
(5052) Nancyruth	13 Jan 2010	0.992	8	2.700	2.469	21.33	8.125 ± 0.544	8.112 ± 1.080	17.57 ± 3.32	23.64 ± 6.77
	26 Jun 2010	1.258	12	2.618	2.336	-22.77	9.601 ± 0.548	7.922 ± 1.075	21.06 ± 3.16	19.02 ± 6.51
(5080) Oja	23 Jan 2010	1.125	11	2.324	2.097	25.05	52.95 ± 1.02	11.17 ± 2.19	104.9 ± 4.4	22.06 ± 8.96
	13 Jul 2010	1.391	12	2.491	2.175	-23.94	36.35 ± 0.82	6.510 ± 1.715	80.15 ± 3.52	18.21 ± 7.03
(5088) Tancredi	22 Jan 2010	0.859	9	3.133	2.959	18.31	34.74 ± 0.79	19.44 ± 1.59	117.1 ± 4.3	61.54 ± 8.90
	9 Jul 2010	1.125	11	3.363	3.111	-17.51	27.59 ± 0.68	15.11 ± 1.42	102.9 ± 4.1	51.63 ± 8.20
(5104) Skripnichenko	16 Jan 2010	0.996	9	2.345	2.092	24.77	60.30 ± 1.10	12.00 ± 2.23	141.7 ± 5.1	30.49 ± 10.36
	9 Jul 2010	1.391	15	2.332	2.005	-25.71	73.28 ± 1.20	22.82 ± 2.37	160.8 ± 5.38	48.53 ± 9.54
(5226) Pollack	11 Feb 2010	1.125	13	2.416	2.192	24.10	14.31 ± 0.60	6.051 ± 1.203	34.15 ± 3.33	15.58 ± 6.33
	2 Aug 2010	1.125	11	2.532	2.233	-23.52	14.75 ± 0.60	5.527 ± 1.221	37.38 ± 3.23	15.56 ± 6.41
(5333) Kanaya	25 Jan 2010	0.992	11	1.980	1.716	29.80	340.1 ± 4.0	91.72 ± 7.99	556.7 ± 13.0	151.6 ± 22.6
	27 Jul 2010	1.523	15	2.272	1.954	-26.45	180.8 ± 2.4	54.87 ± 4.55	349.7 ± 9.8	91.73 ± 19.76
(5378) Ellyett	2 Feb 2010	4.828	22	1.936	1.670	30.59	11.43 ± 0.56	5.344 ± 1.095	20.25 ± 3.16	16.05 ± 6.42
	30 Jul 2010	1.520	14	2.076	1.729	-29.14	9.506 ± 0.554	8.635 ± 1.149	18.62 ± 3.24	19.97 ± 6.42
(5427) Jensmartin	17 Jan 2010	1.125	12	1.995	1.704	29.53	9.567 ± 0.533	3.948 ± 1.100	20.36 ± 2.98	8.761 ± 5.900
	9 Jul 2010	1.523	17	1.844	1.444	-33.27	16.79 ± 0.60	9.563 ± 1.198	32.63 ± 3.15	18.66 ± 6.04
(5527) 1991 UQ ₃	18 Jan 2010	1.125	10	2.247	1.993	25.95	23.42 ± 0.71	8.223 ± 1.476	47.27 ± 3.56	23.64 ± 7.00
	14 Jul 2010	1.520	18	2.007	1.629	-30.23	45.66 ± 1.44	49.15 ± 6.15	75.11 ± 4.04	83.95 ± 9.06
(5574) Seagrave	14 Jan 2010	0.992	11	2.425	2.175	23.90	50.49 ± 0.95	16.70 ± 1.90	115.9 ± 4.2	33.77 ± 7.41
	5 Jul 2010	1.391	15	2.613	2.322	-22.80	38.57 ± 0.79	7.978 ± 1.718	94.05 ± 4.01	17.90 ± 8.29
(5592) Oshima	21 Jan 2010	0.992	11	3.302	3.133	17.33	70.28 ± 1.24	18.47 ± 2.41	225.6 ± 6.6	73.64 ± 13.26
	8 Jul 2010	1.254	15	3.215	2.957	-18.34	92.71 ± 1.42	28.09 ± 2.97	271.5 ± 7.6	61.14 ± 13.38
(5604) 1992 FE	2 Feb 2010	1.125	10	1.238	0.746	53.03	6.043 ± 0.579	3.292 ± 1.169	8.307 ± 3.503	3.237 ± 7.276
	27 Jun 2010	0.594	8	1.068	0.259	-71.61	57.71 ± 1.04	6.040 ± 2.055	79.07 ± 3.95	11.19 ± 8.10
(5682) Beresford	13 Jan 2010	0.992	10	2.965	2.752	19.34	4.540 ± 0.523	2.370 ± 1.048	14.55 ± 3.32	13.36 ± 6.93
	24 Jun 2010	1.258	15	2.736	2.466	-21.73	8.383 ± 0.536	2.392 ± 1.083	22.11 ± 3.29	9.685 ± 6.515
(5712) Funke	14 Jan 2010	0.992	8	3.158	2.956	18.13	6.310 ± 0.523	2.952 ± 1.067	22.51 ± 3.11	14.58 ± 6.37
	29 Jun 2010	1.258	16	2.967	2.705	-19.96	10.70 ± 0.56	5.643 ± 1.109	32.64 ± 3.16	15.93 ± 6.12
(6091) Mitsuru	18 Jan 2010	1.125	10	2.314	2.069	25.14	23.53 ± 0.69	13.35 ± 1.44	45.77 ± 3.51	33.25 ± 6.81
	13 Jul 2010	1.258	12	1.869	1.470	-32.73	48.73 ± 0.95	40.28 ± 1.89	83.16 ± 4.04	70.19 ± 8.81
(6121) Plachinda	2 Feb 2010	1.254	12	2.655	2.481	21.78	10.79 ± 0.61	5.256 ± 1.221	28.58 ± 3.69	17.50 ± 7.37
	24 Jul 2010	1.258	13	2.433	2.136	-24.58	14.98 ± 0.60	7.243 ± 1.200	38.79 ± 3.22	21.05 ± 7.16
(6139) Naomi	29 Jan 2010	1.125	11	2.255	2.040	25.89	87.33 ± 1.36	25.92 ± 2.79	169.2 ± 5.1	44.10 ± 10.06
	1 Aug 2010	1.254	16	2.401	2.091	-24.89	90.34 ± 1.33	16.73 ± 2.73	175.9 ± 6.1	47.60 ± 10.08
(6170) Levasseur	25 Jan 2010	1.125	13	1.881	1.600	31.55	47.34 ± 0.99	6.329 ± 2.035	87.13 ± 4.22	20.99 ± 9.08
	13 Jul 2010	1.387	12	2.497	2.184	-23.88	17.92 ± 0.60	2.443 ± 1.196	42.32 ± 3.12	8.030 ± 6.088

Table 2 — continued

Object	UT Date ^a	$\Delta t_{\text{obs}}^{\text{b}}$	N^{c}	R_{AU}^{d}	$\Delta_{\text{AU}}^{\text{e}}$	$\alpha (\circ)^{\text{f}}$	$\bar{W}3^{\text{g}}$	$\diamond W3^{\text{h}}$	$\bar{W}4^{\text{g}}$	$\diamond W4^{\text{h}}$
(6185) Mitsuma	16 Jan 2010	1.258	14	2.145	1.871	27.28	117.5 ± 1.7	36.81 ± 3.43	215.0 ± 6.4	70.24 ± 12.45
	7 Jul 2010	1.258	14	2.472	2.161	-24.17	68.60 ± 1.17	17.42 ± 2.15	148.9 ± 5.4	32.82 ± 10.70
(6261) Chione	27 Jan 2010	1.125	13	2.120	1.882	27.66	12.49 ± 0.78	9.822 ± 1.247	24.10 ± 3.19	25.35 ± 6.68
	13 Jul 2010	1.258	14	2.735	2.447	-21.71	4.981 ± 0.485	3.476 ± 0.967	13.99 ± 3.02	7.591 ± 5.965
(6361) Koppel	19 Jan 2010	1.125	13	2.087	1.815	28.11	9.189 ± 0.551	8.545 ± 1.075	20.97 ± 3.24	19.32 ± 6.63
	26 Jul 2010	1.520	15	2.059	1.713	-29.44	14.57 ± 0.62	5.572 ± 1.245	30.59 ± 3.33	11.00 ± 6.59
(6572) Carson	19 Jan 2010	0.992	12	2.998	2.808	19.15	11.94 ± 0.56	4.093 ± 1.114	35.55 ± 3.41	11.44 ± 6.32
	4 Jul 2010	1.258	15	2.610	2.317	-22.82	32.51 ± 0.79	9.702 ± 1.577	79.19 ± 3.99	26.95 ± 8.37
(6838) Okuda	27 Jan 2010	1.258	11	2.378	2.171	24.46	105.5 ± 1.6	18.25 ± 3.07	201.2 ± 6.6	35.31 ± 14.35
	22 Jul 2010	0.992	13	2.694	2.422	-22.08	40.19 ± 0.84	12.70 ± 1.61	107.9 ± 4.3	32.61 ± 8.37
(6870) 1991 OM ₁	26 Jan 2010	1.258	15	2.114	1.873	27.76	4.320 ± 0.534	2.513 ± 1.077	10.12 ± 3.33	5.285 ± 6.667
	16 Jul 2010	4.832	34	2.122	1.786	-28.51	5.289 ± 0.485	4.814 ± 0.937	12.35 ± 3.10	20.77 ± 6.39
(6901) Roybishop	15 Jan 2010	1.258	10	2.046	1.758	28.71	31.04 ± 0.75	4.250 ± 1.488	60.13 ± 3.45	8.725 ± 6.569
	4 Jul 2010	1.652	14	2.158	1.823	-27.99	28.92 ± 0.72	4.024 ± 1.402	58.32 ± 3.12	12.75 ± 6.00
(6905) Miyazaki	10 Feb 2010	1.125	13	2.992	2.810	19.25	52.93 ± 1.01	4.188 ± 1.979	136.2 ± 4.7	26.14 ± 9.42
	29 Jul 2010	1.125	9	2.719	2.441	-21.83	86.22 ± 1.25	4.627 ± 2.556	210.7 ± 5.6	14.07 ± 10.69
(6911) Nancygreen	12 Feb 2010	0.992	10	2.103	1.844	27.99	5.084 ± 0.589	4.853 ± 1.208	16.13 ± 3.49	15.10 ± 8.14
	2 Aug 2010	1.520	17	1.996	1.639	-30.44	12.24 ± 0.53	2.597 ± 1.064	20.43 ± 2.97	12.93 ± 5.96
(7476) Ogilsbie	24 Jan 2010	1.258	13	2.440	2.226	23.78	184.9 ± 2.4	56.39 ± 4.60	441.9 ± 9.0	140.7 ± 17.0
	21 Jul 2010	1.391	14	2.496	2.210	-23.95	107.3 ± 1.6	41.45 ± 3.24	302.7 ± 8.6	101.1 ± 16.8
(7783) 1994 JD	8 Jan 2010	1.258	15	1.830	1.484	32.42	9.217 ± 0.566	8.680 ± 1.088	19.34 ± 3.03	20.95 ± 6.55
	4 Jul 2010	1.785	17	1.990	1.629	-30.58	8.147 ± 0.507	8.284 ± 1.000	16.07 ± 3.00	12.76 ± 6.13
(7829) Jaroff	3 Feb 2010	4.832	24	1.965	1.697	30.10	5.225 ± 0.521	3.737 ± 1.025	12.30 ± 3.27	8.342 ± 6.952
	2 Aug 2010	1.125	10	2.087	1.737	-28.95	5.165 ± 0.558	3.201 ± 1.125	12.01 ± 3.35	10.83 ± 6.81
(7832) 1993 FA ₂₇	10 Feb 2010	1.387	12	2.430	2.205	23.96	7.306 ± 0.548	3.404 ± 1.108	13.99 ± 3.58	10.91 ± 7.47
	5 Aug 2010	0.859	9	2.013	1.647	-30.09	16.65 ± 0.62	2.196 ± 1.224	31.07 ± 3.33	12.56 ± 6.56
(7949) 1992 SU	31 Jan 2010	1.125	14	3.284	3.145	17.46	73.15 ± 1.22	8.732 ± 2.361	201.3 ± 5.4	20.66 ± 12.20
	17 Jul 2010	3.902	26	3.595	3.364	-16.35	42.64 ± 0.86	10.15 ± 1.69	134.8 ± 5.1	37.94 ± 10.93
(8213) 1995 FE	13 Feb 2010	1.391	10	2.095	1.838	28.12	20.94 ± 0.68	10.48 ± 1.33	41.95 ± 3.22	20.21 ± 6.65
	5 Aug 2010	0.465	6	2.506	2.205	-23.76	11.72 ± 0.56	12.21 ± 1.08	28.59 ± 2.99	22.57 ± 6.05
(8862) Takayukiota	25 Jan 2010	0.859	10	3.105	2.944	18.48	5.661 ± 0.534	9.779 ± 1.056	22.68 ± 3.27	48.90 ± 7.03
	11 Jul 2010	1.125	13	3.038	2.766	-19.44	7.192 ± 0.514	6.474 ± 1.038	25.97 ± 3.14	18.76 ± 6.21
(8887) Scheeres	18 Jan 2010	0.992	12	2.717	2.503	21.22	18.43 ± 0.60	7.322 ± 1.170	49.72 ± 3.18	19.43 ± 6.38
	6 Jul 2010	1.387	15	2.495	2.192	-23.94	31.15 ± 0.71	9.841 ± 1.492	75.11 ± 3.50	21.97 ± 7.08
(9297) Marchuk	18 Jan 2010	0.992	8	2.540	2.313	22.78	59.62 ± 1.02	3.412 ± 2.019	127.6 ± 5.0	26.20 ± 10.21
	11 Jul 2010	1.387	14	2.318	1.984	-25.86	95.54 ± 1.51	9.372 ± 2.749	178.5 ± 5.5	20.18 ± 10.73

Table 2 — continued

Object	UT Date ^a	$\Delta t_{\text{obs}}^{\text{b}}$	N^{c}	R_{AU}^{d}	$\Delta_{\text{AU}}^{\text{e}}$	$\alpha (\circ)^{\text{f}}$	$\bar{W}3^{\text{g}}$	$\diamond W3^{\text{h}}$	$\bar{W}4^{\text{g}}$	$\diamond W4^{\text{h}}$
(10936) 1998 FN ₁₁	20 Jan 2010	0.594	8	3.063	2.878	18.73	26.78 ± 0.70	10.65 ± 1.35	73.49 ± 3.33	30.24 ± 6.57
	2 Jul 2010	1.258	13	3.079	2.822	-19.20	25.75 ± 0.69	11.25 ± 1.34	73.55 ± 4.03	31.29 ± 8.02
(11549) 1992 YY	28 Jan 2010	1.391	12	2.352	2.144	24.74	58.82 ± 0.99	11.14 ± 1.93	129.9 ± 4.6	23.26 ± 9.48
	28 Jul 2010	1.391	11	2.311	1.996	-25.96	106.8 ± 1.6	12.68 ± 2.93	211.4 ± 6.1	24.19 ± 11.53
(11780) Thunder Bay	4 Feb 2010	3.773	19	3.193	3.036	17.98	8.406 ± 0.576	4.809 ± 1.267	25.13 ± 3.32	15.68 ± 6.76
	23 Jul 2010	1.258	15	2.941	2.686	-20.14	9.865 ± 0.523	12.38 ± 1.04	26.26 ± 3.02	39.95 ± 5.84
(12376) Cochabamba	9 Jan 2010	0.859	6	2.111	1.807	27.69	28.01 ± 0.74	15.44 ± 1.50	60.31 ± 3.17	26.64 ± 6.26
	19 Jul 2010	1.785	21	1.961	1.609	-31.11	46.08 ± 0.96	20.08 ± 1.93	84.25 ± 4.09	33.62 ± 8.21
(12753) Povenmire	16 Jan 2010	1.125	13	2.269	2.008	25.67	44.33 ± 0.87	45.86 ± 1.70	89.20 ± 4.13	86.18 ± 7.79
	13 Jul 2010	1.523	17	2.273	1.934	-26.41	53.90 ± 1.03	46.73 ± 2.06	108.6 ± 4.4	86.52 ± 8.40
(13474) V'yus	14 Jan 2010	0.992	8	3.359	3.170	17.01	3.968 ± 0.510	2.708 ± 0.990	15.88 ± 3.35	10.08 ± 6.93
	26 Jun 2010	1.125	7	3.158	2.912	-18.70	6.015 ± 0.518	2.656 ± 1.036	20.15 ± 3.12	6.408 ± 6.123
(13856) 1999 XZ ₁₀₅	25 Jan 2010	0.992	9	3.172	3.014	18.08	38.65 ± 0.86	12.37 ± 1.65	111.5 ± 4.1	43.64 ± 8.51
	11 Jul 2010	1.125	10	3.138	2.871	-18.80	36.35 ± 0.79	15.33 ± 1.64	107.0 ± 4.4	45.06 ± 9.62
(14342) Iglika	18 Feb 2010	0.992	11	3.500	3.354	16.40	24.87 ± 0.64	15.85 ± 1.27	85.08 ± 3.70	54.86 ± 7.42
	4 Aug 2010	0.992	12	3.237	2.985	-18.18	36.10 ± 0.79	24.83 ± 1.59	109.8 ± 4.4	74.95 ± 9.81
(14950) 1996 BE ₂	12 Jan 2010	0.465	5	2.034	1.725	28.85	45.35 ± 0.94	28.75 ± 1.89	84.25 ± 3.49	55.54 ± 6.95
	9 Jul 2010	1.523	17	2.130	1.779	-28.35	53.34 ± 1.01	17.01 ± 2.06	98.47 ± 4.37	27.07 ± 9.47
(15362) 1996 ED	25 Jan 2010	0.992	10	2.393	2.181	24.29	14.99 ± 0.61	7.519 ± 1.249	31.96 ± 3.21	18.14 ± 6.44
	14 Jul 2010	1.121	13	2.597	2.287	-22.90	10.31 ± 0.56	5.461 ± 1.134	27.12 ± 3.37	18.29 ± 6.71
(15430) 1998 UR ₃₁	21 Jan 2010	1.258	16	1.985	1.709	29.71	13.89 ± 0.66	3.658 ± 1.334	28.99 ± 3.19	10.17 ± 6.60
	3 Aug 2010	1.656	13	1.863	1.474	-32.82	27.48 ± 0.75	5.109 ± 1.470	45.91 ± 3.36	9.144 ± 6.666
(15499) Cloyd	31 Jan 2010	1.125	13	3.151	3.007	18.22	14.68 ± 0.60	3.882 ± 1.159	44.52 ± 3.39	14.21 ± 7.30
	23 Jul 2010	1.258	14	3.249	3.014	-18.16	11.91 ± 0.53	2.456 ± 1.038	39.45 ± 3.28	13.30 ± 6.76
(15914) 1997 UM ₃	17 Jan 2010	0.859	9	2.634	2.412	21.92	4.122 ± 0.561	2.081 ± 1.097	11.95 ± 3.77	10.91 ± 7.38
	2 Jul 2010	1.258	11	2.829	2.554	-20.97	4.402 ± 0.534	3.669 ± 1.106	11.16 ± 3.41	9.538 ± 6.748
(16681) 1994 EV ₇	25 Jan 2010	0.280	9	1.984	1.723	29.76	14.62 ± 0.62	13.98 ± 1.25	27.96 ± 3.26	26.19 ± 6.60
	18 Jul 2010	2.110	21	2.005	1.657	-30.35	20.68 ± 0.63	17.65 ± 1.24	38.47 ± 3.10	41.70 ± 6.39
(16886) 1998 BC ₂₆	27 Jan 2010	0.992	12	1.983	1.722	29.75	14.61 ± 0.62	13.97 ± 1.25	27.95 ± 3.26	26.18 ± 6.60
	13 Jul 2010	1.125	13	2.005	1.657	-30.35	20.67 ± 0.63	17.64 ± 1.24	38.46 ± 3.10	41.70 ± 6.39
(17681) Tweedledum	15 Jan 2010	1.387	15	1.823	1.500	32.62	8.785 ± 0.524	8.873 ± 1.010	17.65 ± 3.05	19.37 ± 6.28
	8 Jul 2010	1.656	18	1.875	1.484	-32.66	9.788 ± 0.545	9.385 ± 1.067	17.69 ± 3.18	17.64 ± 6.74
(17822) 1998 FM ₁₃₅	11 Feb 2010	0.992	11	3.394	3.233	16.90	8.588 ± 0.533	3.819 ± 1.058	35.76 ± 3.29	17.78 ± 6.43
	1 Aug 2010	1.258	10	3.206	2.953	-18.37	10.11 ± 0.57	7.016 ± 1.125	40.97 ± 3.44	21.69 ± 7.41
(18487) 1996 AU ₃	28 Jan 2010	1.125	13	2.893	2.727	19.90	11.33 ± 0.56	5.905 ± 1.104	34.19 ± 3.16	17.80 ± 6.29
	17 Jul 2010	4.297	29	2.595	2.301	-22.95	25.49 ± 0.71	16.21 ± 1.52	63.00 ± 3.62	38.62 ± 7.07

Table 2 — continued

Object	UT Date ^a	$\Delta t_{\text{obs}}^{\text{b}}$	N^{c}	R_{AU}^{d}	$\Delta_{\text{AU}}^{\text{e}}$	$\alpha (\circ)^{\text{f}}$	$\bar{W}3^{\text{g}}$	$\diamond W3^{\text{h}}$	$\bar{W}4^{\text{g}}$	$\diamond W4^{\text{h}}$
(19251) Totziens	17 Jan 2010	0.727	10	3.319	3.135	17.22	5.190 ± 0.514	1.550 ± 1.046	16.63 ± 3.29	21.65 ± 6.37
	28 Jun 2010	1.125	13	3.066	2.814	-19.29	7.170 ± 0.502	3.314 ± 1.014	19.58 ± 3.13	10.54 ± 6.36
(20378) 1998 KZ ₄₆	17 Jan 2010	0.992	7	2.850	2.645	20.18	15.38 ± 0.57	4.956 ± 1.144	42.17 ± 3.24	13.92 ± 6.37
	3 Jul 2010	1.258	14	2.905	2.637	-20.40	11.08 ± 0.53	4.326 ± 1.059	33.74 ± 3.07	15.09 ± 5.98
(20932) 2258 T-1	27 Jan 2010	1.125	12	2.999	2.840	19.16	4.276 ± 0.543	1.721 ± 1.090	14.18 ± 3.39	12.10 ± 6.77
	13 Jul 2010	1.121	13	2.746	2.449	-21.60	8.242 ± 0.543	1.509 ± 1.071	24.43 ± 3.30	11.10 ± 6.15
(21594) 1998 VP ₃₁	15 Jan 2010	1.125	12	2.324	2.065	25.01	101.9 ± 1.6	25.05 ± 2.88	195.0 ± 6.0	48.84 ± 10.75
	14 Jul 2010	1.520	14	2.145	1.786	-28.11	128.9 ± 1.8	35.81 ± 3.57	236.1 ± 6.7	62.09 ± 12.85
(23200) 2000 SH ₃	14 Feb 2010	0.992	12	2.899	2.717	19.91	10.19 ± 0.59	5.215 ± 1.149	28.83 ± 3.54	24.12 ± 7.76
	29 Jul 2010	1.254	11	2.713	2.438	-21.89	17.49 ± 0.59	5.435 ± 1.247	41.90 ± 3.21	16.93 ± 6.66
(23276) 2000 YT ₁₀₁	18 Feb 2010	1.258	16	3.053	2.885	18.88	9.133 ± 0.536	2.327 ± 1.080	26.64 ± 3.18	10.89 ± 6.42
	5 Aug 2010	1.254	13	2.841	2.564	-20.82	13.05 ± 0.56	3.746 ± 1.119	33.64 ± 3.28	15.59 ± 7.06
(24101) Cassini	12 Feb 2010	1.125	11	3.177	3.007	18.10	7.619 ± 0.521	1.978 ± 1.065	26.03 ± 3.13	9.564 ± 6.221
	28 Jul 2010	1.258	15	3.418	3.186	-17.22	5.375 ± 0.473	2.015 ± 0.935	16.95 ± 3.19	10.82 ± 7.14
(27851) 1994 VG ₂	12 Feb 2010	1.125	11	2.439	2.218	23.87	72.08 ± 1.21	33.75 ± 2.32	144.3 ± 5.0	65.09 ± 9.48
	29 Jul 2010	1.258	16	2.713	2.436	-21.89	45.48 ± 0.91	17.59 ± 1.66	102.5 ± 4.43	37.68 ± 9.27
(28126) Nydegger	12 Jan 2010	1.125	12	2.183	1.899	26.73	5.353 ± 0.538	1.819 ± 1.098	11.64 ± 3.42	10.97 ± 7.14
	2 Jul 2010	1.387	15	2.387	2.074	-25.10	3.473 ± 0.561	2.717 ± 1.123	8.427 ± 3.483	4.742 ± 7.075
(30470) 2000 OR ₁₉	21 Jan 2010	0.992	11	2.879	2.689	19.99	17.86 ± 0.65	18.34 ± 1.38	50.23 ± 3.73	47.43 ± 7.29
	13 Jul 2010	1.254	15	2.550	2.237	-23.36	44.44 ± 0.91	33.35 ± 1.73	100.7 ± 4.4	75.48 ± 8.27
(32802) 1990 SK	3 Feb 2010	3.773	13	2.884	2.710	19.98	3.279 ± 0.569	1.359 ± 1.124	10.75 ± 3.51	9.590 ± 7.345
	20 Jul 2010	1.125	10	2.664	2.393	-22.36	7.376 ± 0.927	12.24 ± 2.79	16.13 ± 3.50	14.01 ± 6.97
(33916) 2000 LF ₁₉	18 Jan 2010	0.992	12	2.582	2.357	22.38	8.188 ± 0.594	3.047 ± 1.185	19.98 ± 3.43	16.95 ± 7.08
	5 Jul 2010	1.387	15	2.129	1.783	-28.38	20.21 ± 0.66	10.88 ± 1.30	37.56 ± 3.30	21.97 ± 6.83
(41044) 1999 VW ₆	3 Feb 2010	3.641	25	3.024	2.857	19.02	4.948 ± 0.550	5.743 ± 1.205	16.10 ± 3.38	15.95 ± 6.87
	24 Jul 2010	1.258	15	2.833	2.572	-20.94	9.724 ± 0.515	2.008 ± 1.034	27.86 ± 3.07	12.29 ± 6.15
(41223) 1999 XD ₁₆	16 Jan 2010	0.992	11	3.616	3.441	15.77	11.49 ± 0.54	4.047 ± 1.07	42.23 ± 3.43	17.29 ± 7.48
	26 Jun 2010	1.125	13	3.417	3.186	-17.24	14.63 ± 0.57	7.231 ± 1.159	45.49 ± 3.28	20.30 ± 6.55
(41288) 1999 XD ₁₀₇	21 Jan 2010	0.465	7	2.450	2.226	23.67	6.753 ± 0.496	1.614 ± 0.990	15.83 ± 3.04	4.988 ± 6.510
	11 Jul 2010	1.391	15	2.249	1.910	-26.72	14.80 ± 0.60	7.317 ± 1.19	29.64 ± 3.25	19.04 ± 6.64
(42265) 2001 QL ₆₉	28 Jan 2010	1.258	11	2.980	2.821	19.30	8.709 ± 0.561	8.867 ± 1.140	24.45 ± 3.50	33.65 ± 7.05
	22 Jul 2010	1.258	11	2.910	2.654	-20.36	11.54 ± 0.56	5.215 ± 1.121	33.46 ± 3.33	12.31 ± 6.90
(42946) 1999 TU ₉₅	1 Feb 2010	1.258	11	2.380	2.180	24.45	11.44 ± 0.59	2.488 ± 1.162	25.16 ± 3.64	10.31 ± 6.60
	3 Jul 2010	1.254	14	2.449	2.145	-24.38	11.03 ± 0.56	4.083 ± 1.123	26.30 ± 3.19	11.11 ± 6.39
(44892) 1999 VJ ₈	12 Feb 2010	0.992	7	3.148	2.975	18.27	10.07 ± 0.53	4.346 ± 1.125	31.40 ± 3.18	32.40 ± 6.12
	3 Jul 2010	1.258	11	2.912	2.646	-20.31	12.30 ± 0.54	2.464 ± 1.083	33.34 ± 3.15	8.932 ± 6.319

Table 2 — continued

Object	UT Date ^a	$\Delta t_{\text{obs}}^{\text{b}}$	N^{c}	R_{AU}^{d}	$\Delta_{\text{AU}}^{\text{e}}$	$\alpha (\text{°})^{\text{f}}$	$\bar{W}3^{\text{g}}$	$\diamond W3^{\text{h}}$	$\bar{W}4^{\text{g}}$	$\diamond W4^{\text{h}}$
(45436) 2000 AD ₁₇₆	28 Jan 2010	1.523	16	2.252	2.034	25.93	12.08 ± 0.60	8.163 ± 1.183	24.66 ± 3.49	20.57 ± 6.98
	3 Jul 2010	0.465	5	2.455	2.148	-24.31	7.309 ± 0.520	5.159 ± 1.056	17.28 ± 3.18	12.32 ± 6.22
(68216) 2001 CV ₂₆	23 Jan 2010	0.992	13	1.102	0.486	63.28	48.96 ± 0.97	8.693 ± 2.139	68.47 ± 3.52	14.70 ± 7.31
	25 Jun 2010	1.520	16	1.698	1.287	-36.64	6.617 ± 0.561	2.597 ± 1.115	11.23 ± 3.46	7.553 ± 7.134
(69350) 1993 YP	10 Feb 2010	1.520	17	2.076	1.813	28.38	5.645 ± 0.529	4.560 ± 1.071	13.47 ± 3.15	10.29 ± 6.37
	4 Aug 2010	1.652	17	1.939	1.574	-31.43	12.33 ± 0.54	10.29 ± 1.09	24.20 ± 2.96	16.48 ± 6.00
(72675) 2001 FP ₅₄	17 Jan 2010	0.992	10	2.533	2.301	22.83	5.848 ± 0.577	2.085 ± 1.179	14.92 ± 3.30	6.007 ± 6.648
	8 Jul 2010	1.391	11	2.571	2.269	-23.17	6.495 ± 0.534	0.983 ± 1.059	14.79 ± 3.15	5.238 ± 6.434
(90698) Kosciuszko	27 Jan 2010	1.258	10	1.970	1.714	29.98	21.99 ± 0.68	5.908 ± 1.336	34.16 ± 3.21	7.188 ± 6.564
	24 Jul 2010	1.391	13	2.470	2.185	-24.21	6.606 ± 0.502	2.078 ± 1.021	14.66 ± 3.09	13.31 ± 6.12

Notes. All mean flux and range values are in units of mJy = 10^{29} Wm² Hz⁻¹.

^aUT date of the first observation.

^bTime spanned by observations (days).

^cNumber of observations used.

^dMean Heliocentric distance.

^eMean WISE-centric distance.

^fMean solar phase angle.

^gLightcurve-averaged mean flux.

^hPhotometric range of lightcurve.

Table 3: TPM Results

Object	D_{eff} (km)	p_V	Γ^a	T_c (K)	$\bar{\theta}(\circ)$	a/b^b	Spin ^c
(91) Aegina	101.40 ± 13.85	$0.052^{+0.007}_{-0.007}$	19^{+31}_{-19}	250 ± 16	17 ± 12	1.08 ± 0.19	↑
(155) Scylla	38.41 ± 0.54	$0.054^{+0.002}_{-0.003}$	16^{+15}_{-5}	219 ± 12	34 ± 22	1.51 ± 0.27	↑↑
(271) Penthesilea	65.05 ± 2.30	$0.054^{+0.003}_{-0.003}$	16^{+33}_{-16}	210 ± 1	16 ± 4	1.51 ± 0.27	↑↑
(295) Theresia	30.50 ± 1.23	$0.220^{+0.013}_{-0.013}$	24^{+38}_{-17}	211 ± 3	45 ± 20	1.08 ± 0.19	↑↑
(322) Phaeo	59.66 ± 1.29	$0.126^{+0.004}_{-0.009}$	12^{+11}_{-7}	210 ± 6	—	2.16 ± 0.39	↓↓
(343) Ostara	19.65 ± 1.38	$0.113^{+0.009}_{-0.010}$	140^{+120}_{-60}	226 ± 7	—	1.51 ± 0.27	↓↓
(444) Gyptis	162.3 ± 22.9	$0.049^{+0.007}_{-0.008}$	74^{+74}_{-74}	253 ± 25	—	1.08 ± 0.19	↓↓
(463) Lola	20.27 ± 1.48	$0.115^{+0.009}_{-0.010}$	70^{+30}_{-30}	221 ± 4	44 ± 15	2.16 ± 0.39	↑↑
(464) Megaira	69.56 ± 6.38	$0.053^{+0.006}_{-0.006}$	120^{+120}_{-120}	209 ± 2	15 ± 11	2.16 ± 0.39	—
(493) Griseldis	40.86 ± 1.13	$0.054^{+0.003}_{-0.004}$	56^{+25}_{-32}	203 ± 2	—	1.51 ± 0.27	—
(500) Selinur	41.15 ± 0.37	$0.196^{+0.004}_{-0.017}$	16^{+7}_{-8}	218 ± 7	—	1.51 ± 0.27	↓↓
(520) Franziska	27.42 ± 1.00	$0.149^{+0.008}_{-0.011}$	12^{+24}_{-5}	204 ± 2	—	1.51 ± 0.27	—
(538) Friederike	66.45 ± 1.42	$0.073^{+0.003}_{-0.003}$	35^{+12}_{-11}	207 ± 3	—	1.51 ± 0.27	—
(558) Carmen	59.71 ± 3.15	$0.117^{+0.007}_{-0.011}$	$7.7^{+26.9}_{-7.7}$	222 ± 3	—	1.08 ± 0.19	↓↓
(562) Salome	36.99 ± 1.90	$0.145^{+0.009}_{-0.011}$	23^{+12}_{-20}	206 ± 5	19 ± 10	1.08 ± 0.19	↑↑
(567) Eleutheria	87.45 ± 7.81	$0.056^{+0.005}_{-0.007}$	19^{+30}_{-11}	234 ± 4	—	1.08 ± 0.19	↑↑
(583) Klotilde	80.78 ± 6.25	$0.067^{+0.006}_{-0.006}$	30^{+12}_{-19}	224 ± 11	49 ± 35	1.08 ± 0.19	↑↑
(651) Antikleia	34.07 ± 1.92	$0.159^{+0.010}_{-0.014}$	37^{+16}_{-26}	206 ± 2	48 ± 40	1.08 ± 0.19	↓↓
(656) Beagle	55.14 ± 3.02	$0.068^{+0.005}_{-0.004}$	32^{+14}_{-14}	210 ± 1	—	1.51 ± 0.27	↑↑
(662) Newtonia	24.04 ± 1.41	$0.211^{+0.014}_{-0.022}$	35^{+23}_{-25}	235 ± 11	47 ± 39	1.51 ± 0.27	↓↓
(668) Dora	23.18 ± 0.48	$0.062^{+0.004}_{-0.003}$	52^{+8}_{-8}	216 ± 7	52 ± 8	1.51 ± 0.27	↑↑
(670) Ottegebe	35.08 ± 0.76	$0.258^{+0.009}_{-0.018}$	44^{+14}_{-18}	203 ± 2	46 ± 10	1.51 ± 0.27	↑↑
(688) Melanie	38.44 ± 2.49	$0.070^{+0.006}_{-0.007}$	41^{+44}_{-19}	230 ± 6	45 ± 13	1.51 ± 0.27	↑↑
(734) Benda	66.30 ± 2.75	$0.045^{+0.002}_{-0.003}$	13^{+8}_{-13}	211 ± 2	17 ± 11	1.51 ± 0.27	↑↑
(735) Marghanna	65.09 ± 3.93	$0.063^{+0.004}_{-0.005}$	17^{+88}_{-17}	214 ± 24	48 ± 29	1.51 ± 0.27	↑↑
(793) Arizona	26.94 ± 1.33	$0.237^{+0.013}_{-0.020}$	32^{+16}_{-13}	215 ± 4	50 ± 24	1.08 ± 0.19	↑↑
(826) Henrika	23.11 ± 0.97	$0.096^{+0.006}_{-0.005}$	45^{+16}_{-21}	237 ± 8	29 ± 24	1.08 ± 0.19	↑↑
(829) Academia	37.20 ± 1.49	$0.063^{+0.003}_{-0.004}$	15^{+7}_{-15}	228 ± 1	23 ± 17	2.16 ± 0.39	↓↓
(883) Matterania	7.60 ± 0.81	$0.304^{+0.034}_{-0.038}$	36^{+37}_{-24}	232 ± 6	—	1.51 ± 0.27	↑↑
(906) Repsolda	71.08 ± 6.05	$0.070^{+0.007}_{-0.007}$	47^{+115}_{-28}	225 ± 9	—	1.08 ± 0.19	↓↓
(918) Itha	21.59 ± 0.37	$0.222^{+0.009}_{-0.017}$	37^{+10}_{-10}	203 ± 7	—	1.51 ± 0.27	↓↓
(972) Cohnia	73.12 ± 0.79	$0.055^{+0.002}_{-0.003}$	19^{+38}_{-13}	206 ± 3	40 ± 12	1.51 ± 0.27	↑↑
(977) Philippa	76.87 ± 6.35	$0.040^{+0.004}_{-0.004}$	27^{+84}_{-21}	211 ± 3	—	1.08 ± 0.19	↓↓
(987) Wallia	43.05 ± 1.91	$0.161^{+0.009}_{-0.012}$	46^{+64}_{-46}	211 ± 13	—	2.16 ± 0.39	↓↓
(998) Bodea	31.14 ± 1.87	$0.052^{+0.004}_{-0.005}$	20^{+16}_{-7}	198 ± 3	—	1.08 ± 0.19	↓↓
(1018) Arnolda	16.31 ± 1.74	$0.260^{+0.029}_{-0.037}$	43^{+47}_{-43}	221 ± 10	—	1.51 ± 0.27	↑↑
(1047) Geisha	10.53 ± 0.41	$0.283^{+0.015}_{-0.024}$	35^{+58}_{-14}	225 ± 1	31 ± 10	1.51 ± 0.27	↑↑
(1051) Merope	53.46 ± 1.81	$0.066^{+0.004}_{-0.006}$	48^{+81}_{-25}	210 ± 2	—	2.16 ± 0.39	↑↑
(1076) Viola	22.22 ± 1.49	$0.054^{+0.004}_{-0.005}$	24^{+44}_{-24}	235 ± 4	—	1.51 ± 0.27	↓↓
(1077) Campanula	10.12 ± 0.80	$0.230^{+0.020}_{-0.022}$	56^{+40}_{-34}	209 ± 3	56 ± 31	1.51 ± 0.27	↑↑
(1083) Salvia	11.22 ± 1.12	$0.209^{+0.024}_{-0.029}$	54^{+17}_{-30}	240 ± 8	16 ± 10	1.51 ± 0.27	↓↓
(1095) Tulipa	31.05 ± 1.36	$0.143^{+0.008}_{-0.010}$	23^{+13}_{-13}	211 ± 3	—	1.08 ± 0.19	↑↑
(1109) Tata	64.10 ± 2.59	$0.049^{+0.003}_{-0.002}$	10^{+46}_{-10}	229 ± 4	—	1.08 ± 0.19	↑↑
(1123) Shapleya	11.97 ± 0.55	$0.304^{+0.019}_{-0.027}$	14^{+33}_{-14}	230 ± 3	16 ± 14	1.51 ± 0.27	—
(1125) China	26.87 ± 1.09	$0.060^{+0.004}_{-0.004}$	34^{+8}_{-7}	201 ± 4	54 ± 24	1.51 ± 0.27	↓↓

Table 3 — continued

Object	D_{eff} (km)	p_V	Γ^a	T_c (K)	$\bar{\theta}^c$ (°)	a/b^b	Spin ^c
(1136) Mercedes	24.66 ± 1.81	$0.123^{+0.010}_{-0.012}$	54^{+81}_{-34}	226 ± 12	—	2.16 ± 0.39	↓
(1142) Aetolia	23.91 ± 1.28	$0.260^{+0.018}_{-0.022}$	$8.0^{+29.7}_{-8.0}$	216 ± 2	37 ± 25	1.08 ± 0.19	↑↑
(1152) Pawona	17.47 ± 0.90	$0.203^{+0.012}_{-0.017}$	26^{+35}_{-14}	233 ± 1	—	1.08 ± 0.19	↓
(1162) Larissa	41.15 ± 2.27	$0.152^{+0.011}_{-0.014}$	19^{+15}_{-19}	201 ± 1	52 ± 44	1.51 ± 0.27	↑↑
(1224) Fantasia	13.65 ± 0.22	$0.252^{+0.013}_{-0.022}$	58^{+16}_{-12}	222 ± 4	> 58	1.51 ± 0.27	↑↑
(1258) Sicilia	44.05 ± 2.62	$0.060^{+0.004}_{-0.004}$	61^{+76}_{-31}	209 ± 1	—	1.51 ± 0.27	↑↑
(1281) Jeanne	24.38 ± 0.94	$0.079^{+0.004}_{-0.004}$	90^{+44}_{-25}	242 ± 5	53 ± 27	1.51 ± 0.27	↑↑
(1288) Santa	30.68 ± 1.27	$0.060^{+0.004}_{-0.003}$	15^{+23}_{-5}	220 ± 3	33 ± 28	2.16 ± 0.39	↓
(1296) Andree	23.28 ± 2.12	$0.074^{+0.007}_{-0.008}$	40^{+74}_{-12}	238 ± 12	—	2.16 ± 0.39	↑↑
(1299) Mertona	15.22 ± 1.18	$0.194^{+0.017}_{-0.024}$	15^{+29}_{-8}	207 ± 7	—	1.51 ± 0.27	↑↑
(1310) Villigera	14.63 ± 1.28	$0.209^{+0.021}_{-0.026}$	40^{+23}_{-30}	224 ± 26	50 ± 31	1.08 ± 0.19	↑↑
(1316) Kasan	6.54 ± 0.50	$0.277^{+0.033}_{-0.041}$	10^{+34}_{-10}	221 ± 5	51 ± 26	1.51 ± 0.27	↓
(1325) Inanda	11.42 ± 1.57	$0.189^{+0.027}_{-0.030}$	76^{+50}_{-36}	214 ± 3	> 40	2.16 ± 0.39	↑↑
(1335) Demoulinia	7.65 ± 0.78	$0.241^{+0.027}_{-0.031}$	130^{+90}_{-100}	227 ± 3	—	2.16 ± 0.39	↑↑
(1352) Wawel	21.72 ± 1.68	$0.139^{+0.012}_{-0.012}$	97^{+28}_{-71}	209 ± 2	—	1.51 ± 0.27	↑↑
(1375) Alfreda	14.46 ± 0.55	$0.222^{+0.012}_{-0.022}$	30^{+48}_{-18}	224 ± 2	< 42	1.08 ± 0.19	↓
(1412) Lagrula	9.13 ± 0.50	$0.267^{+0.019}_{-0.027}$	37^{+23}_{-9}	234 ± 2	—	1.51 ± 0.27	↓
(1443) Ruppina	16.68 ± 1.03	$0.259^{+0.018}_{-0.020}$	40^{+18}_{-14}	205 ± 1	—	1.51 ± 0.27	↑↑
(1452) Hunnia	21.22 ± 1.99	$0.065^{+0.007}_{-0.008}$	24^{+34}_{-20}	216 ± 12	—	1.51 ± 0.27	↑↑
(1501) Baade	11.48 ± 0.88	$0.240^{+0.020}_{-0.022}$	34^{+48}_{-34}	205 ± 5	—	1.08 ± 0.19	↓
(1517) Beograd	34.21 ± 2.25	$0.061^{+0.004}_{-0.004}$	19^{+55}_{-5}	231 ± 3	—	1.51 ± 0.27	↑↑
(1536) Pielinen	8.53 ± 0.19	$0.225^{+0.013}_{-0.019}$	74^{+23}_{-35}	227 ± 5	23 ± 36	1.51 ± 0.27	—
(1542) Schalen	46.48 ± 1.54	$0.053^{+0.003}_{-0.004}$	10^{+15}_{-10}	208 ± 1	38 ± 19	1.51 ± 0.27	↓
(1565) Lemaitre	8.44 ± 0.96	$0.204^{+0.026}_{-0.033}$	24^{+53}_{-24}	227 ± 14	48 ± 30	1.08 ± 0.19	↑↑
(1567) Alikoski	71.15 ± 4.24	$0.053^{+0.004}_{-0.005}$	$7.2^{+73.4}_{-7.2}$	228 ± 3	45 ± 38	1.08 ± 0.19	↓
(1573) Vaisala	10.31 ± 0.64	$0.213^{+0.022}_{-0.033}$	130^{+120}_{-80}	223 ± 8	46 ± 28	1.51 ± 0.27	↓
(1577) Reiss	5.72 ± 0.57	$0.468^{+0.052}_{-0.066}$	25^{+36}_{-20}	217 ± 4	—	1.51 ± 0.27	↑↑
(1628) Strobel	53.71 ± 1.21	$0.060^{+0.003}_{-0.005}$	47^{+12}_{-30}	219 ± 3	51 ± 36	1.51 ± 0.27	↓
(1644) Rafita	13.49 ± 0.84	$0.263^{+0.019}_{-0.031}$	28^{+25}_{-14}	235 ± 4	48 ± 15	1.51 ± 0.27	↓
(1651) Behrens	10.09 ± 0.46	$0.242^{+0.015}_{-0.025}$	59^{+29}_{-19}	250 ± 9	43 ± 36	1.51 ± 0.27	↑↑
(1655) Comas Sola	35.09 ± 1.30	$0.059^{+0.003}_{-0.005}$	40^{+37}_{-30}	215 ± 7	14 ± 7	1.51 ± 0.27	↑↑
(1702) Kalahari	34.16 ± 1.23	$0.065^{+0.003}_{-0.006}$	28^{+40}_{-9}	217 ± 6	46 ± 8	1.51 ± 0.27	↓
(1723) Klemola	33.77 ± 0.91	$0.148^{+0.007}_{-0.011}$	30^{+11}_{-10}	216 ± 1	37 ± 10	1.51 ± 0.27	↓
(1734) Zhongolovich	25.33 ± 0.71	$0.069^{+0.004}_{-0.004}$	35^{+31}_{-10}	210 ± 9	42 ± 28	2.16 ± 0.39	↓
(1741) Giclas	13.17 ± 0.56	$0.266^{+0.093}_{-0.015}$	33^{+20}_{-10}	207 ± 8	—	1.51 ± 0.27	↓
(1759) Kienle	7.73 ± 1.17	$0.184^{+0.029}_{-0.030}$	52^{+88}_{-52}	208 ± 1	—	1.51 ± 0.27	↓
(1768) Appenzella	18.91 ± 0.59	$0.058^{+0.004}_{-0.003}$	31^{+18}_{-12}	223 ± 2	—	1.51 ± 0.27	↑↑
(1807) Slovakia ^d	9.83 ± 1.19	$0.229^{+0.030}_{-0.033}$	200^{+240}_{-50}	231 ± 4	—	1.51 ± 0.27	↑↑
(1896) Beer	5.07 ± 0.96	$0.229^{+0.045}_{-0.045}$	80^{+335}_{-80}	201 ± 5	—	1.51 ± 0.27	↑↑
(1936) Lugano	24.03 ± 0.27	$0.083^{+0.005}_{-0.007}$	120^{+70}_{-80}	249 ± 2	49 ± 13	2.94 ± 0.53	—
(1979) Sakharov	4.69 ± 0.77	$0.282^{+0.048}_{-0.062}$	58^{+269}_{-27}	223 ± 3	—	1.51 ± 0.27	↑↑
(2005) Hencke	8.99 ± 0.95	$0.315^{+0.037}_{-0.046}$	40^{+48}_{-34}	204 ± 1	—	1.08 ± 0.19	↓
(2072) Kosmodemyanskaya	4.74 ± 1.44	$0.657^{+0.201}_{-0.207}$	19^{+129}_{-19}	204 ± 1	—	1.08 ± 0.19	↑↑
(2106) Hugo	16.15 ± 1.50	$0.091^{+0.009}_{-0.010}$	22^{+36}_{-9}	209 ± 1	—	1.51 ± 0.27	↑↑
(2111) Tselina	24.05 ± 2.19	$0.195^{+0.020}_{-0.026}$	47^{+36}_{-24}	201 ± 2	46 ± 13	1.51 ± 0.27	↓

Table 3 — continued

Object	D_{eff} (km)	p_V	Γ^a	T_c (K)	$\bar{\theta}^c$ (°)	a/b^b	Spin ^c
(2123) Vltava	16.05 ± 0.68	$0.179^{+0.011}_{-0.010}$	56^{+37}_{-22}	210 ± 2	—	1.08 ± 0.19	↓
(2140) Kemerovo	33.56 ± 2.05	$0.050^{+0.004}_{-0.005}$	20^{+39}_{-14}	217 ± 1	46 ± 13	1.08 ± 0.19	↑↑
(2144) Marietta	17.26 ± 0.45	$0.203^{+0.009}_{-0.010}$	53^{+10}_{-8}	203 ± 4	39 ± 14	1.51 ± 0.27	↑↑
(2177) Oliver	19.52 ± 0.50	$0.085^{+0.005}_{-0.003}$	42^{+10}_{-10}	197 ± 1	< 18	1.51 ± 0.27	↑↑
(2203) van Rhijn	22.31 ± 1.08	$0.087^{+0.005}_{-0.005}$	55^{+55}_{-27}	194 ± 4	—	2.16 ± 0.39	↓↓
(2204) Lyyli	25.05 ± 0.95	$0.047^{+0.003}_{-0.004}$	90^{+36}_{-50}	237 ± 20	49 ± 22	2.16 ± 0.39	↓↓
(2214) Carol	26.28 ± 1.60	$0.061^{+0.003}_{-0.005}$	21^{+15}_{-9}	220 ± 8	42 ± 31	1.51 ± 0.27	↑↑
(2239) Paracelsus	37.53 ± 2.48	$0.054^{+0.004}_{-0.006}$	18^{+7}_{-18}	201 ± 1	—	1.51 ± 0.27	↑↑
(2268) Szmytowna	15.18 ± 1.46	$0.190^{+0.020}_{-0.019}$	30^{+32}_{-30}	207 ± 1	—	1.08 ± 0.19	↓↓
(2275) Cuitlahuac	7.29 ± 0.19	$0.342^{+0.017}_{-0.028}$	13^{+24}_{-13}	227 ± 12	< 13	1.51 ± 0.27	↓↓
(2297) Daghestan	25.06 ± 0.89	$0.086^{+0.005}_{-0.004}$	58^{+23}_{-18}	217 ± 1	34 ± 25	2.16 ± 0.39	↑↑
(2306) Bauschinger	19.24 ± 0.97	$0.072^{+0.005}_{-0.005}$	18^{+14}_{-10}	222 ± 1	15 ± 8	1.51 ± 0.27	↓↓
(2332) Kalm	36.52 ± 2.55	$0.060^{+0.005}_{-0.005}$	77^{+15}_{-48}	209 ± 2	—	1.51 ± 0.27	↑↑
(2347) Vinata	23.63 ± 1.27	$0.103^{+0.008}_{-0.008}$	35^{+20}_{-14}	187 ± 4	12 ± 11	2.16 ± 0.39	↑↑
(2365) Interkosmos	16.62 ± 1.41	$0.195^{+0.018}_{-0.021}$	41^{+10}_{-41}	234 ± 9	—	1.08 ± 0.19	↑↑
(2375) Radek	32.19 ± 1.60	$0.123^{+0.008}_{-0.010}$	11^{+14}_{-11}	241 ± 2	45 ± 15	1.51 ± 0.27	↓↓
(2446) Lunacharsky	12.43 ± 0.31	$0.078^{+0.003}_{-0.004}$	33^{+12}_{-10}	244 ± 13	< 21	2.16 ± 0.39	↓↓
(2463) Sterpin	11.93 ± 0.69	$0.221^{+0.016}_{-0.023}$	17^{+43}_{-17}	217 ± 7	—	1.08 ± 0.19	↓↓
(2500) Alascattalo	7.99 ± 0.27	$0.278^{+0.013}_{-0.020}$	41^{+18}_{-28}	242 ± 6	33 ± 20	1.08 ± 0.19	↑↑
(2556) Louise	5.96 ± 0.55	$0.252^{+0.025}_{-0.031}$	61^{+37}_{-33}	238 ± 3	—	2.16 ± 0.39	↓↓
(2567) Elba	18.40 ± 1.27	$0.110^{+0.008}_{-0.009}$	50^{+11}_{-36}	212 ± 5	—	1.08 ± 0.19	↓↓
(2687) Tortali	14.91 ± 0.21	$0.148^{+0.005}_{-0.011}$	59^{+16}_{-10}	226 ± 10	< 27	1.08 ± 0.19	↓↓
(2786) Grinevia	11.07 ± 0.98	$0.237^{+0.023}_{-0.029}$	12^{+19}_{-12}	203 ± 1	< 23	1.08 ± 0.19	↓↓
(2855) Bastian	8.78 ± 0.57	$0.151^{+0.012}_{-0.012}$	17^{+42}_{-7}	226 ± 12	< 41	1.08 ± 0.19	↑↑
(2870) Haupt ^d	15.51 ± 2.28	$0.057^{+0.009}_{-0.009}$	130^{+180}_{-130}	229 ± 3	—	2.94 ± 0.53	—
(2947) Kippenhahn	7.80 ± 0.29	$0.267^{+0.014}_{-0.017}$	32^{+18}_{-11}	236 ± 12	> 28	1.51 ± 0.27	↑↑
(2985) Shakespeare	10.64 ± 0.92	$0.260^{+0.025}_{-0.024}$	41^{+49}_{-13}	211 ± 1	—	2.16 ± 0.39	↓↓
(3036) Krat	41.41 ± 1.28	$0.090^{+0.006}_{-0.005}$	15^{+57}_{-9}	204 ± 2	< 43	2.16 ± 0.39	↓↓
(3051) Nantong	16.79 ± 1.60	$0.081^{+0.008}_{-0.009}$	27^{+28}_{-14}	203 ± 3	< 38	1.08 ± 0.19	↑↑
(3144) Brosche	4.80 ± 0.53	$0.219^{+0.026}_{-0.027}$	59^{+56}_{-45}	226 ± 2	—	1.51 ± 0.27	↑↑
(3162) Nostalgia	28.88 ± 1.48	$0.064^{+0.005}_{-0.006}$	29^{+51}_{-15}	199 ± 6	—	3.49 ± 0.63	↑↑
(3249) Musashino	6.44 ± 1.22	$0.185^{+0.036}_{-0.036}$	93^{+132}_{-73}	197 ± 3	—	1.51 ± 0.27	↓↓
(3267) Glo	7.37 ± 1.28	$0.262^{+0.049}_{-0.053}$	23^{+43}_{-13}	225 ± 6	43 ± 29	1.08 ± 0.19	↓↓
(3305) Ceadams	10.37 ± 0.12	$0.218^{+0.007}_{-0.013}$	21^{+6}_{-3}	228 ± 11	> 26	1.08 ± 0.19	↓↓
(3411) Debetencourt	5.18 ± 0.21	$0.294^{+0.017}_{-0.020}$	22^{+83}_{-12}	244 ± 10	14 ± 13	1.51 ± 0.27	↑↑
(3438) Inarradas	25.18 ± 0.68	$0.058^{+0.003}_{-0.003}$	54^{+15}_{-15}	206 ± 5	49 ± 11	1.51 ± 0.27	↓↓
(3483) Svetlov	2.96 ± 0.48	$0.496^{+0.107}_{-0.114}$	110^{+400}_{-50}	222 ± 11	—	1.51 ± 0.27	↓↓
(3509) Sanshui	9.93 ± 0.84	$0.243^{+0.023}_{-0.028}$	62^{+27}_{-34}	212 ± 1	—	1.08 ± 0.19	↑↑
(3536) Schleicher	3.67 ± 1.14	$0.375^{+0.118}_{-0.119}$	32^{+182}_{-10}	230 ± 8	—	1.51 ± 0.27	↓↓
(3544) Borodino	9.29 ± 0.81	$0.241^{+0.024}_{-0.027}$	72^{+14}_{-45}	237 ± 18	—	1.51 ± 0.27	↓↓
(3554) Amun	2.71 ± 0.02	$0.140^{+0.027}_{-0.028}$	1400^{+700}_{-200}	274 ± 6	< 14	1.08 ± 0.19	↓↓
(3560) Chenqian	22.84 ± 0.56	$0.152^{+0.007}_{-0.011}$	44^{+22}_{-10}	206 ± 3	50 ± 7	1.51 ± 0.27	↑↑
(3628) Boznemcova	8.07 ± 0.80	$0.223^{+0.023}_{-0.024}$	32^{+23}_{-32}	201 ± 12	—	1.08 ± 0.19	↓↓
(3751) Kiang	22.38 ± 0.68	$0.083^{+0.005}_{-0.007}$	62^{+20}_{-16}	211 ± 1	35 ± 6	2.46 ± 0.44	↑↑
(3823) Yorii	13.66 ± 1.47	$0.064^{+0.007}_{-0.008}$	49^{+22}_{-49}	209 ± 10	—	1.08 ± 0.19	↓↓

Table 3 — continued

Object	D_{eff} (km)	p_V	Γ^a	T_c (K)	$\bar{\theta}^c$ (°)	a/b^b	Spin ^c
(3907) Kilmartin	8.16 ± 1.12	$0.530^{+0.076}_{-0.083}$	26^{+47}_{-26}	183 ± 14	—	1.08 ± 0.19	↑↑
(3915) Fukushima	22.18 ± 0.39	$0.059^{+0.004}_{-0.003}$	22^{+13}_{-7}	240 ± 1	41 ± 18	1.51 ± 0.27	↓↓
(3935) Toatenmongakkai	12.02 ± 0.82	$0.219^{+0.017}_{-0.021}$	120^{+90}_{-60}	215 ± 5	51 ± 27	1.51 ± 0.27	↑↑
(3936) Elst	5.00 ± 0.68	$0.490^{+0.069}_{-0.074}$	22^{+56}_{-22}	235 ± 3	—	1.08 ± 0.19	↓↓
(4003) Schumann	31.92 ± 0.41	$0.063^{+0.003}_{-0.002}$	32^{+35}_{-11}	208 ± 3	—	2.16 ± 0.39	↑↑
(4006) Sandler	16.89 ± 0.64	$0.059^{+0.003}_{-0.003}$	36^{+7}_{-11}	212 ± 1	47 ± 14	1.08 ± 0.19	↓↓
(4008) Corbin	6.18 ± 0.31	$0.307^{+0.025}_{-0.035}$	67^{+37}_{-25}	240 ± 16	39 ± 15	1.08 ± 0.19	↓↓
(4029) Bridges	7.87 ± 0.62	$0.246^{+0.021}_{-0.025}$	32^{+26}_{-18}	240 ± 3	46 ± 25	1.08 ± 0.19	↓↓
(4142) Dersu-Uzala	6.31 ± 0.52	$0.236^{+0.048}_{-0.049}$	110^{+140}_{-30}	263 ± 10	—	1.08 ± 0.19	↓↓
(4150) Starr	6.93 ± 0.39	$0.304^{+0.021}_{-0.024}$	29^{+16}_{-14}	231 ± 6	—	1.51 ± 0.27	↑↑
(4255) Spacewatch	15.71 ± 0.45	$0.042^{+0.003}_{-0.002}$	24^{+22}_{-17}	209 ± 2	42 ± 19	1.51 ± 0.27	↑↑
(4264) Karljosephine	6.37 ± 1.83	$0.202^{+0.059}_{-0.059}$	110^{+300}_{-110}	206 ± 2	—	1.51 ± 0.27	—
(4294) Horatius	8.07 ± 0.66	$0.242^{+0.023}_{-0.023}$	12^{+77}_{-12}	225 ± 2	—	1.51 ± 0.27	—
(4352) Kyoto	11.33 ± 1.31	$0.308^{+0.038}_{-0.041}$	47^{+64}_{-32}	204 ± 2	—	2.16 ± 0.39	↑↑
(4359) Berlage	4.98 ± 0.69	$0.289^{+0.042}_{-0.042}$	40^{+71}_{-26}	228 ± 1	—	1.51 ± 0.27	↓↓
(4363) Sergej	5.48 ± 0.48	$0.282^{+0.026}_{-0.031}$	27^{+94}_{-27}	218 ± 5	—	1.51 ± 0.27	↓↓
(4383) Suruga	6.79 ± 1.03	$0.223^{+0.035}_{-0.040}$	37^{+53}_{-17}	220 ± 1	—	1.08 ± 0.19	↑↑
(4528) Berg	10.45 ± 0.96	$0.247^{+0.024}_{-0.033}$	26^{+20}_{-26}	231 ± 6	—	1.08 ± 0.19	↓↓
(4565) Grossman	7.57 ± 0.37	$0.240^{+0.017}_{-0.022}$	51^{+36}_{-12}	233 ± 3	53 ± 35	1.51 ± 0.27	↓↓
(4569) Baerbel	9.21 ± 0.73	$0.292^{+0.026}_{-0.028}$	48^{+45}_{-9}	225 ± 5	49 ± 17	2.16 ± 0.39	↑↑
(4613) Mamoru	11.96 ± 1.48	$0.280^{+0.036}_{-0.037}$	$9.4^{+22.6}_{-9.4}$	194 ± 3	< 22	1.08 ± 0.19	↓↓
(4713) Steel	6.58 ± 0.18	$0.196^{+0.025}_{-0.037}$	40^{+28}_{-13}	258 ± 1	—	1.08 ± 0.19	↑↑
(4771) Hayashi	13.32 ± 0.96	$0.101^{+0.008}_{-0.008}$	61^{+37}_{-29}	208 ± 10	—	1.08 ± 0.19	↓↓
(4898) Nishiizumi	2.46 ± 0.22	$0.600^{+0.073}_{-0.103}$	34^{+445}_{-34}	243 ± 13	—	1.26 ± 0.23	↑↑
(4899) Candace	7.17 ± 0.57	$0.271^{+0.028}_{-0.039}$	79^{+104}_{-60}	255 ± 8	—	1.08 ± 0.19	↑↑
(4908) Ward	4.91 ± 0.71	$0.262^{+0.040}_{-0.042}$	12^{+68}_{-12}	229 ± 4	—	1.51 ± 0.27	—
(5035) Swift	10.22 ± 1.06	$0.211^{+0.023}_{-0.025}$	26^{+35}_{-20}	223 ± 7	—	1.08 ± 0.19	↓↓
(5052) Nancyruth	4.66 ± 0.78	$0.167^{+0.029}_{-0.032}$	10^{+72}_{-10}	231 ± 1	—	1.51 ± 0.27	—
(5080) Oja	7.98 ± 0.53	$0.243^{+0.018}_{-0.026}$	26^{+50}_{-17}	235 ± 7	—	1.08 ± 0.19	↑↑
(5088) Tancredi	16.17 ± 1.02	$0.066^{+0.005}_{-0.005}$	40^{+12}_{-19}	197 ± 4	—	1.51 ± 0.27	↓↓
(5104) Skripnichenko	9.49 ± 0.48	$0.329^{+0.021}_{-0.026}$	41^{+31}_{-22}	229 ± 4	—	1.51 ± 0.27	↓↓
(5226) Pollack	5.74 ± 1.03	$0.303^{+0.056}_{-0.062}$	24^{+51}_{-18}	221 ± 3	—	1.08 ± 0.19	↓↓
(5333) Kanaya	13.86 ± 1.32	$0.066^{+0.007}_{-0.007}$	23^{+32}_{-7}	249 ± 12	—	1.08 ± 0.19	↑↑
(5378) Ellyett	2.77 ± 0.25	$0.776^{+0.095}_{-0.119}$	75^{+455}_{-62}	246 ± 7	—	2.16 ± 0.39	↓↓
(5427) Jensmartin	3.13 ± 0.14	$0.622^{+0.055}_{-0.084}$	19^{+76}_{-19}	239 ± 6	—	1.08 ± 0.19	↓↓
(5527) 1991 UQ ₃	5.30 ± 0.56	$0.233^{+0.026}_{-0.029}$	120^{+130}_{-80}	254 ± 17	—	2.16 ± 0.39	↓↓
(5574) Seagrave	9.72 ± 1.05	$0.225^{+0.027}_{-0.032}$	34^{+34}_{-34}	225 ± 3	—	1.08 ± 0.19	↓↓
(5592) Oshima	23.91 ± 1.16	$0.065^{+0.004}_{-0.005}$	34^{+23}_{-27}	206 ± 4	—	1.08 ± 0.19	↓↓
(5604) 1992 FE	0.67 ± 0.01	$0.447^{+0.077}_{-0.086}$	1100^{+2200}_{-600}	281 ± 1	—	1.51 ± 0.27	↑↑
(5682) Beresford	5.37 ± 1.83	$0.233^{+0.080}_{-0.082}$	29^{+152}_{-29}	212 ± 10	—	1.08 ± 0.19	↓↓
(5712) Funke	7.22 ± 1.60	$0.269^{+0.061}_{-0.062}$	33^{+50}_{-33}	202 ± 7	—	1.51 ± 0.27	↓↓
(6091) Mitsuru	4.94 ± 0.75	$0.423^{+0.068}_{-0.070}$	45^{+25}_{-13}	253 ± 11	> 26	2.46 ± 0.44	↑↑
(6121) Plachinda	5.83 ± 0.82	$0.250^{+0.036}_{-0.038}$	56^{+63}_{-34}	217 ± 1	—	1.51 ± 0.27	↑↑
(6139) Naomi	10.68 ± 0.36	$0.207^{+0.014}_{-0.025}$	66^{+31}_{-36}	242 ± 1	53 ± 32	1.08 ± 0.19	↓↓
(6170) Levasseur	5.57 ± 0.63	$0.238^{+0.031}_{-0.040}$	76^{+161}_{-56}	239 ± 16	—	1.08 ± 0.19	↓↓

Table 3 — continued

Object	D_{eff} (km)	p_V	Γ^a	T_c (K)	$\bar{\theta}^c$ (°)	a/b^b	Spin ^c
(6185) Mitsuma	10.36 ± 1.00	$0.113^{+0.012}_{-0.013}$	66^{+61}_{-45}	240 ± 11	41 ± 16	1.08 ± 0.19	↓
(6261) Chione	3.91 ± 0.56	$0.270^{+0.046}_{-0.052}$	41^{+52}_{-41}	230 ± 22	—	1.51 ± 0.27	↓
(6361) Koppel	3.59 ± 0.19	$0.728^{+0.049}_{-0.062}$	20^{+172}_{-20}	232 ± 5	—	1.51 ± 0.27	↓
(6572) Carson	8.56 ± 1.21	$0.262^{+0.038}_{-0.038}$	21^{+33}_{-15}	218 ± 11	—	1.08 ± 0.19	↓
(6838) Okuda	11.88 ± 0.28	$0.185^{+0.010}_{-0.014}$	47^{+13}_{-10}	230 ± 20	53 ± 16	1.08 ± 0.19	↑
(6870) 1991 OM ₁	2.80 ± 0.66	$0.647^{+0.180}_{-0.193}$	59^{+330}_{-59}	226 ± 1	—	1.51 ± 0.27	↓
(6901) Roybishop	5.05 ± 0.44	$0.337^{+0.054}_{-0.058}$	59^{+83}_{-40}	241 ± 3	—	1.08 ± 0.19	↓
(6905) Miyazaki	14.30 ± 0.73	$0.222^{+0.015}_{-0.019}$	26^{+66}_{-26}	220 ± 3	43 ± 36	1.08 ± 0.19	↑
(6911) Nancygreen	2.90 ± 0.32	$0.515^{+0.068}_{-0.081}$	210^{+1220}_{-180}	230 ± 38	—	1.51 ± 0.27	↓
(7476) Ogilsbie ^d	18.41 ± 1.21	$0.146^{+0.013}_{-0.015}$	70^{+30}_{-20}	219 ± 9	—	1.08 ± 0.19	↑
(7783) 1994 JD	2.78 ± 0.33	$0.461^{+0.098}_{-0.104}$	170^{+190}_{-110}	237 ± 4	—	1.51 ± 0.27	↓
(7829) Jaroff	2.55 ± 0.50	$0.430^{+0.117}_{-0.133}$	32^{+176}_{-32}	225 ± 1	—	1.08 ± 0.19	↓
(7832) 1993 FA ₂₇	3.55 ± 0.53	$0.444^{+0.070}_{-0.073}$	46^{+160}_{-46}	245 ± 2	—	1.08 ± 0.19	↑
(7949) 1992 SU	18.26 ± 1.36	$0.066^{+0.006}_{-0.006}$	37^{+28}_{-27}	209 ± 7	32 ± 29	1.51 ± 0.27	↑
(8213) 1995 FE ^d	4.80 ± 1.02	$0.287^{+0.063}_{-0.068}$	36^{+167}_{-18}	228 ± 12	—	1.51 ± 0.27	↓
(8862) Takayukiota	7.76 ± 2.35	$0.229^{+0.070}_{-0.070}$	43^{+195}_{-43}	193 ± 4	10 ± 10	2.16 ± 0.39	↑
(8887) Scheeres	7.56 ± 0.81	$0.275^{+0.032}_{-0.037}$	21^{+52}_{-21}	220 ± 6	< 43	1.51 ± 0.27	↑
(9297) Marchuk	9.55 ± 0.57	$0.260^{+0.019}_{-0.020}$	22^{+120}_{-22}	240 ± 9	39 ± 27	1.08 ± 0.19	↑
(10936) 1998 FN ₁₁	11.75 ± 0.50	$0.127^{+0.008}_{-0.010}$	13^{+22}_{-13}	212 ± 2	< 5	1.08 ± 0.19	↑
(11549) 1992 YY	10.30 ± 0.44	$0.247^{+0.017}_{-0.030}$	30^{+18}_{-5}	236 ± 7	—	1.08 ± 0.19	↓
(11780) Thunder Bay	7.82 ± 2.43	$0.214^{+0.067}_{-0.067}$	130^{+450}_{-130}	212 ± 6	—	1.51 ± 0.27	↑
(12376) Cochabamba	5.93 ± 0.97	$0.245^{+0.041}_{-0.046}$	120^{+60}_{-110}	240 ± 11	—	1.51 ± 0.27	↓
(12753) Povenmire	8.00 ± 0.19	$0.249^{+0.015}_{-0.027}$	17^{+23}_{-11}	238 ± 1	< 8	1.51 ± 0.27	↓
(13474) V'yus	6.63 ± 1.41	$0.146^{+0.032}_{-0.033}$	64^{+123}_{-44}	196 ± 8	—	1.26 ± 0.23	—
(13856) 1999 XZ ₁₀₅	14.79 ± 1.23	$0.059^{+0.005}_{-0.006}$	20^{+12}_{-10}	209 ± 1	—	1.08 ± 0.19	↑
(14342) Iglika	16.22 ± 1.11	$0.079^{+0.006}_{-0.007}$	24^{+8}_{-14}	202 ± 5	—	1.51 ± 0.27	↑
(14950) 1996 BE ₂	6.66 ± 1.01	$0.145^{+0.023}_{-0.024}$	54^{+49}_{-34}	246 ± 1	—	1.51 ± 0.27	↓
(15362) 1996 ED	4.95 ± 1.01	$0.275^{+0.058}_{-0.058}$	110^{+120}_{-110}	226 ± 12	—	1.51 ± 0.27	↑
(15430) 1998 UR ₃₁	3.78 ± 0.43	$0.297^{+0.037}_{-0.039}$	72^{+127}_{-63}	249 ± 16	—	1.08 ± 0.19	↓
(15499) Cloyd	9.67 ± 1.25	$0.146^{+0.020}_{-0.020}$	33^{+36}_{-33}	203 ± 4	—	1.08 ± 0.19	↑
(15914) 1997 UM ₃	4.20 ± 0.95	$0.234^{+0.054}_{-0.054}$	88^{+188}_{-72}	214 ± 7	—	1.51 ± 0.27	↓
(16681) 1994 EV ₇	3.94 ± 0.34	$0.209^{+0.037}_{-0.038}$	63^{+74}_{-30}	245 ± 2	—	1.51 ± 0.27	↓
(16886) 1998 BC ₂₆	7.11 ± 0.78	$0.211^{+0.025}_{-0.027}$	33^{+49}_{-18}	220 ± 3	49 ± 33	1.08 ± 0.19	—
(17681) Tweedledum	2.48 ± 0.31	$0.441^{+0.071}_{-0.098}$	130^{+320}_{-110}	243 ± 7	—	1.51 ± 0.27	↓
(17822) 1998 FM ₁₃₅	10.92 ± 1.43	$0.058^{+0.008}_{-0.008}$	79^{+53}_{-52}	188 ± 1	—	1.51 ± 0.27	↑
(18487) 1996 AU ₃	7.78 ± 0.79	$0.259^{+0.030}_{-0.035}$	46^{+36}_{-26}	216 ± 11	—	1.51 ± 0.27	↓
(19251) Totziens	6.24 ± 2.14	$0.196^{+0.068}_{-0.069}$	32^{+121}_{-32}	209 ± 8	—	1.08 ± 0.19	↑
(20378) 1998 KZ ₄₆	7.78 ± 0.80	$0.212^{+0.026}_{-0.035}$	34^{+23}_{-14}	210 ± 5	—	1.08 ± 0.19	↑
(20932) 2258 T-1	5.76 ± 1.32	$0.247^{+0.037}_{-0.058}$	41^{+111}_{-41}	206 ± 6	—	1.08 ± 0.19	↓
(21594) 1998 VP ₃₁	10.30 ± 0.26	$0.097^{+0.005}_{-0.005}$	44^{+16}_{-12}	246 ± 3	50 ± 17	1.08 ± 0.19	↑
(23200) 2000 SH ₃	7.20 ± 1.10	$0.219^{+0.035}_{-0.037}$	17^{+66}_{-17}	220 ± 10	—	1.08 ± 0.19	↓
(23276) 2000 YT ₁₀₁	7.01 ± 0.96	$0.071^{+0.010}_{-0.010}$	27^{+30}_{-27}	214 ± 6	—	1.08 ± 0.19	↑
(24101) Cassini	7.40 ± 1.43	$0.224^{+0.045}_{-0.045}$	15^{+38}_{-15}	200 ± 4	—	1.08 ± 0.19	—
(27851) 1994 VG ₂	10.43 ± 0.98	$0.057^{+0.006}_{-0.006}$	11^{+14}_{-11}	234 ± 7	< 20	1.08 ± 0.19	—
(28126) Nydegger	2.63 ± 0.76	$0.226^{+0.066}_{-0.067}$	33^{+205}_{-33}	229 ± 7	—	1.08 ± 0.19	—

Table 3 — continued

Object	D_{eff} (km)	p_V	Γ^a	T_c (K)	$\bar{\theta}(\circ)$	a/b^b	Spin ^c
(30470) 2000 OR ₁₉	9.42 ± 0.28	$0.057^{+0.004}_{-0.004}$	45^{+43}_{-22}	224 ± 13	< 11	1.51 ± 0.27	↓
(32802) 1990 SK	4.27 ± 1.76	$0.273^{+0.114}_{-0.116}$	20^{+162}_{-20}	219 ± 22	—	1.51 ± 0.27	↓
(33916) 2000 LF ₁₉	4.08 ± 0.41	$0.185^{+0.020}_{-0.020}$	38^{+51}_{-38}	240 ± 19	—	1.51 ± 0.27	↑
(41044) 1999 VW ₆	5.79 ± 1.58	$0.297^{+0.082}_{-0.083}$	14^{+157}_{-14}	209 ± 7	—	1.51 ± 0.27	↓
(41223) 1999 XD ₁₆	11.61 ± 1.15	$0.055^{+0.006}_{-0.006}$	23^{+43}_{-23}	201 ± 8	—	1.08 ± 0.19	↑
(41288) 1999 XD ₁₀₇	4.22 ± 0.98	$0.207^{+0.050}_{-0.051}$	41^{+86}_{-34}	234 ± 10	—	1.08 ± 0.19	↓
(42265) 2001 QL ₆₉	7.07 ± 1.35	$0.177^{+0.035}_{-0.036}$	25^{+89}_{-25}	210 ± 2	—	1.51 ± 0.27	↓
(42946) 1999 TU ₉₅	4.74 ± 0.79	$0.266^{+0.046}_{-0.047}$	37^{+60}_{-37}	227 ± 5	—	1.08 ± 0.19	↓
(44892) 1999 VJ ₈	7.80 ± 1.66	$0.213^{+0.046}_{-0.048}$	32^{+93}_{-32}	210 ± 7	—	1.08 ± 0.19	↑
(45436) 2000 AD ₁₇₆	3.89 ± 1.54	$0.240^{+0.098}_{-0.099}$	75^{+482}_{-75}	231 ± 9	—	1.51 ± 0.27	↑
(68216) 2001 CV ₂₆	1.24 ± 0.05	$0.322^{+0.022}_{-0.030}$	430^{+1210}_{-280}	278 ± 22	—	1.08 ± 0.19	↓
(69350) 1993 YP	2.87 ± 0.69	$0.162^{+0.041}_{-0.044}$	240^{+490}_{-150}	235 ± 13	—	1.51 ± 0.27	↓
(72675) 2001 FP ₅₄	3.77 ± 1.32	$0.219^{+0.078}_{-0.078}$	29^{+367}_{-29}	223 ± 6	—	1.08 ± 0.19	↓
(90698) Kosciuszko	3.55 ± 0.25	$0.298^{+0.028}_{-0.034}$	16^{+49}_{-16}	258 ± 29	—	1.08 ± 0.19	↑

^aThermal inertia values are in SI units ($J m^{-2} K^{-1} s^{-1/2}$).

^b a/b values are adjusted downward by 16% to account for the overestimation as described in MacLennan and Emery (2019).

^cIndicates either prograde (↑) or retrograde (↓) spin direction.

^dTPM results with $\chi^2_{min} > 8$ and thus should be used with caution.

Table 4: Literature TPM Results

Object	H_V	G_V	P_{rot} (hr)	D_{eff} (km)	p_V	Γ^a	T_c (K)	Source(s)
(1) Ceres	3.21	0.02	9.0742	951 ± 8	$0.100^{+0.004}_{-0.006}$	25^{+15}_{-10}	238 ± 15	[1]
(2) Pallas	4.08	0.08	7.8132 [†]	536 ± 5	$0.142^{+0.006}_{-0.005}$	30^{+15}_{-15}	234 ± 15	[1]
(3) Juno	5.29	0.34	7.2095	254 ± 4	$0.209^{+0.02}_{-0.019}$	70^{+30}_{-40}	245 ± 15	[1]
(4) Vesta	3.00	0.23	5.3421	530 ± 24	$0.394^{+0.011}_{-0.024}$	30^{+10}_{-10}	230 ± 10	[2]
(6) Hebe	5.71	0.27	7.2744 [†]	198 ± 3	$0.24^{+0.01}_{-0.01}$	50^{+40}_{-35}	205 ± 15	[14]
(8) Flora	6.35	0.24	12.865	142 ± 2	$0.252^{+0.014}_{-0.014}$	50^{+35}_{-30}	243 ± 15	[1]
(10) Hygeia	5.38	0.11	27.63	441 ± 6	$0.063^{+0.002}_{-0.002}$	50^{+20}_{-25}	210 ± 15	[1]
(16) Psyche	5.84	0.11	4.1959 [†]	242.5 ± 25	$0.138^{+0.015}_{-0.015}$	120^{+40}_{-40}	212 ± 10	[15]
(18) Melpomene	6.54	0.32	11.57	135 ± 3	$0.233^{+0.018}_{-0.017}$	50^{+15}_{-44}	236 ± 15	[1]
(19) Fortuna	7.23	0.21	7.4432	219 ± 3	$0.047^{+0.001}_{-0.001}$	40^{+30}_{-15}	232 ± 15	[1]
(20) Massalia	6.43	0.23	8.098	147 ± 2	$0.217^{+0.012}_{-0.012}$	35^{+25}_{-10}	234 ± 15	[1]
(21) Lutetia	7.34	0.21	8.1655 [†]	95.76 ± 4	$0.221^{+0.011}_{-0.015}$	20^{+10}_{-12}	215 ± 15	[1][9]
(22) Kalliope	6.54	0.27	4.1482	167 ± 17	$0.152^{+0.006}_{-0.012}$	125^{+125}_{-120}	241 ± 10	[3]
(29) Amphitrite	5.85	0.20	5.3921	202 ± 3	$0.197^{+0.011}_{-0.011}$	25^{+10}_{-13}	227 ± 15	[1]
(32) Pomona	7.52	0.23	9.4477 [†]	85 ± 1	$0.240^{+0.007}_{-0.011}$	112^{+8}_{-92}	215 ± 10	[3]
(41) Daphne	7.21	0.09	5.988	189 ± 1	$0.065^{+0.002}_{-0.002}$	50^{+0}_{-49}	263 ± 10	[3]
(44) Nysa	6.99	0.42	6.4214 [†]	81 ± 1	$0.429^{+0.012}_{-0.041}$	115^{+45}_{-35}	212 ± 10	[3]
(45) Eugenia	7.43	0.15	5.6991 [†]	198 ± 20	$0.048^{+0.002}_{-0.003}$	45^{+40}_{-40}	236 ± 10	[3]
(52) Europa	6.22	0.10	5.6304	317 ± 4	$0.057^{+0.002}_{-0.001}$	10^{+25}_{-10}	209 ± 15	[1]
(54) Alexandra	7.68	0.17	7.024	153 ± 2	$0.063^{+0.003}_{-0.003}$	10^{+22}_{-10}	225 ± 15	[1]
(63) Ausonia	7.55	—	9.282	94.6 ± 2.4	$0.189^{+0.010}_{-0.009}$	50^{+12}_{-24}	303 ± 50	[8]
(65) Cybele	6.82	0.23	6.0814	275 ± 4	$0.044^{+0.002}_{-0.003}$	25^{+15}_{-20}	215 ± 15	[1][16]
(73) Klytia	9.08	0.4	8.2831 [†]	44.8 ± 1.7	$0.189^{+0.019}_{-0.019}$	14^{+15}_{-13}	224 ± 5	[7]
(82) Alkmene	8.19	0.23	13.0008 [†]	58.2 ± 1.3	$0.256^{+0.026}_{-0.026}$	30^{+14}_{-16}	207 ± 2	[6]
(87) Sylvia	6.86	0.23	5.1836 [†]	300 ± 30	$0.035^{+0.001}_{-0.002}$	70^{+60}_{-60}	233 ± 10	[3]
(88) Thisbe	7.12	0.17	6.042	221 ± 2	$0.051^{+0.001}_{-0.001}$	60^{+15}_{-25}	211 ± 15	[1]
(93) Minerva	7.82	0.20	5.982	167 ± 3	$0.046^{+0.003}_{-0.003}$	25^{+30}_{-10}	210 ± 15	[1]
(99) Dike	9.3	0.11	18.1191 [†]	66.5 ± 0.9	$0.072^{+0.027}_{-0.027}$	35^{+19}_{-19}	216 ± 3	[7]
(100) Hekate	7.54	0.22	27.0703 [†]	87 ± 5	$0.220^{+0.030}_{-0.030}$	4^{+66}_{-2}	239 ± 7	[13]
(107) Camilla	7.02	0.13	4.8439 [†]	245 ± 25	$0.046^{+0.002}_{-0.002}$	25^{+10}_{-10}	213 ± 10	[3]
(109) Felicitas	8.84	0.11	13.1906 [†]	85 ± 6	$0.065^{+0.008}_{-0.010}$	40^{+100}_{-40}	222 ± 5	[11]
(110) Lydia	7.79	0.29	10.9258 [†]	93.5 ± 3.5	$0.153^{+0.007}_{-0.012}$	95^{+105}_{-25}	217 ± 10	[3]
(115) Thyra	7.59	0.31	7.2400 [†]	92 ± 2	$0.191^{+0.003}_{-0.013}$	75^{+25}_{-50}	231 ± 10	[3]
(121) Hermione	7.21	0.16	5.5509 [†]	220 ± 22	$0.047^{+0.002}_{-0.002}$	35^{+25}_{-30}	224 ± 10	[3]
(125) Liberatrix	8.83	0.26	3.9682	50.7 ± 1.7	$0.184^{+0.021}_{-0.021}$	71^{+24}_{-26}	206 ± 2	[7]
(130) Elektra	7.09	0.20	5.2246 [†]	197 ± 20	$0.066^{+0.003}_{-0.006}$	35^{+30}_{-30}	223 ± 10	[3]
(155) Scylla	10.8	0.09	7.9588 [†]	38.1 ± 1	$0.049^{+0.029}_{-0.029}$	24^{+16}_{-14}	220 ± 12	[7]
(159) Aemilia	8.1	0.09	24.486	137 ± 8	$0.054^{+0.015}_{-0.015}$	50^{+50}_{-50}	200 ± 10	[12]
(167) Urda	9.13	0.28	13.0613 [†]	40.1 ± 0.6	$0.240^{+0.011}_{-0.011}$	80^{+40}_{-40}	217 ± 4	[7][11]
(183) Istria	9.49	0.22	11.77	31.43 ± 3.06	$0.288^{+0.030}_{-0.034}$	21^{+13}_{-11}	192 ± 2	[11]
(188) Menippe	9.16	0.14	11.9765 [†]	35.6 ± 1	$0.275^{+0.054}_{-0.054}$	17^{+17}_{-11}	209 ± 3	[7]
(193) Ambrosia	9.62	0.33	6.5817 [†]	30.5 ± 1	$0.225^{+0.031}_{-0.031}$	49^{+20}_{-14}	197 ± 34	[7]
(195) Eurykleia	8.89	0.09	16.5218 [†]	87 ± 10	$0.060^{+0.020}_{-0.020}$	15^{+55}_{-15}	231 ± 3	[13]

Table 4 — continued

Object	H_V	G_V	P_{rot} (hr)	D_{eff} (km)	p_V	Γ^a	T_c (K)	Source(s)
(208) Lacrimosa	9.08	0.23	14.085	40.4 ± 0.7	$0.253^{+0.009}_{-0.012}$	77^{+23}_{-18}	212 ± 4	[11]
(220) Stephania	11.0	0.2	18.2087	29.8 ± 0.6	$0.066^{+0.023}_{-0.023}$	4^{+6}_{-4}	230 ± 2	[7]
(226) Weringia	9.83	0.25	11.1485 [†]	28.7 ± 0.2	$0.230^{+0.022}_{-0.022}$	30^{+10}_{-10}	213 ± 2	[7]
(227) Philosophia	9.1	0.15	26.468	101 ± 5	$0.041^{+0.005}_{-0.005}$	125^{+90}_{-90}	225 ± 10	[12]
(263) Dresden	10.2	0.27	16.8139 [†]	23.9 ± 0.9	$0.230^{+0.039}_{-0.039}$	26^{+24}_{-26}	210 ± 3	[7]
(272) Antonia	10.5	0.16	3.8548	30.5 ± 1.1	$0.104^{+0.025}_{-0.025}$	75^{+10}_{-10}	209 ± 3	[7]
(274) Philagoria	9.8	0.17	17.9410 [†]	28.5 ± 0.9	$0.238^{+0.025}_{-0.025}$	93^{+8}_{-13}	227 ± 1	[7]
(277) Elvira	9.76	0.23	29.6922 [†]	38 ± 2	$0.152^{+0.006}_{-0.005}$	190^{+210}_{-90}	230 ± 10	[3]
(281) Lucretia	11.8	0.32	4.3497 [†]	11.2 ± 0.2	$0.247^{+0.030}_{-0.029}$	48^{+12}_{-13}	226 ± 3	[7]
(283) Emma	8.47	0.15	6.8953 [†]	135 ± 15	$0.040^{+0.002}_{-0.002}$	110^{+105}_{-105}	237 ± 10	[3]
(290) Bruna	12.0	0.4	13.8055 [†]	9.8 ± 0.2	$0.259^{+0.032}_{-0.032}$	21^{+39}_{-21}	237 ± 18	[7]
(301) Bavaria	10.1	0.11	12.2409	55 ± 2	$0.047^{+0.004}_{-0.003}$	45^{+60}_{-30}	240 ± 2	[13]
(306) Unitas	8.75	0.21	8.7387 [†]	56 ± 1	$0.178^{+0.007}_{-0.009}$	200^{+60}_{-100}	248 ± 10	[3]
(311) Claudia	9.88	0.25	7.5314 [†]	26.2 ± 0.7	$0.252^{+0.027}_{-0.027}$	17^{+13}_{-17}	211 ± 4	[7]
(329) Svea	9.34	0.04	22.777	78 ± 4	$0.055^{+0.015}_{-0.015}$	75^{+50}_{-50}	234 ± 10	[12]
(340) Eduarda	9.85	0.27	8.0061 [†]	27.2 ± 0.4	$0.241^{+0.032}_{-0.031}$	25^{+19}_{-25}	216 ± 1	[7]
(349) Dembowska	5.93	0.37	4.701	155.8 ± 7.1	$0.309^{+0.026}_{-0.038}$	20^{+12}_{-7}	226 ± 7	[21]
(351) Yrsa	8.95	0.22	13.3120 [†]	42.5 ± 1.3	$0.230^{+0.030}_{-0.030}$	50^{+19}_{-20}	207 ± 4	[7]
(352) Gisela	10.1	0.3	7.4801 [†]	24.5 ± 0.5	$0.227^{+0.027}_{-0.027}$	10^{+24}_{-10}	243 ± 4	[7]
(355) Gabriella	10.1	0.29	4.8290 [†]	24.5 ± 0.8	$0.230^{+0.031}_{-0.031}$	35^{+5}_{-5}	239 ± 7	[7]
(378) Holmia	9.79	0.26	4.4404 [†]	28.8 ± 0.7	$0.241^{+0.023}_{-0.023}$	13^{+12}_{-12}	217 ± 2	[7]
(380) Fiducia	9.34	0.11	13.7172 [†]	72 ± 8	$0.057^{+0.009}_{-0.012}$	10^{+140}_{-10}	242 ± 3	[13]
(382) Dodona	8.62	0.19	4.1132 [†]	75 ± 1	$0.111^{+0.004}_{-0.005}$	60^{+90}_{-45}	232 ± 10	[3]
(390) Alma	10.0	0.27	3.7412 [†]	24.9 ± 0.5	$0.234^{+0.034}_{-0.033}$	37^{+13}_{-29}	235 ± 5	[7]
(394) Arduina	9.63	0.25	16.6217 [†]	30.9 ± 0.9	$0.234^{+0.025}_{-0.024}$	83^{+17}_{-28}	218 ± 2	[7]
(400) Ducrosa	10.3	0.17	6.8679 [†]	34.6 ± 0.8	$0.093^{+0.025}_{-0.025}$	38^{+16}_{-13}	198 ± 3	[7]
(413) Edburga	9.92	0.30	15.7715 [†]	33.8 ± 0.6	$0.158^{+0.018}_{-0.020}$	100^{+60}_{-60}	211 ± 10	[7][11]
(423) Diotima	7.29	0.27	4.775	200 ± 4	$0.053^{+0.004}_{-0.003}$	40^{+30}_{-20}	208 ± 15	[1]
(430) Hybris	10.8	0.05	7.2166 [†]	33.2 ± 0.7	$0.069^{+0.031}_{-0.031}$	55^{+9}_{-5}	197 ± 2	[7]
(433) Eros	10.6	0.43	5.27	17.8 ± 0.5	$0.315^{+0.024}_{-0.034}$	150^{+50}_{-50}	278 ± 10	[3]
(468) Lina	9.60	0.19	16.4784 [†]	69 ± 10	$0.052^{+0.006}_{-0.014}$	20^{+280}_{-20}	221 ± 4	[13]
(478) Tergeste	7.96	0.15	16.105	87 ± 6	$0.150^{+0.020}_{-0.020}$	75^{+45}_{-45}	201 ± 10	[12]
(482) Petrina	9.1	0.58	11.7921 [†]	44.2 ± 0.8	$0.185^{+0.019}_{-0.019}$	4^{+20}_{-4}	209 ± 2	[7]
(484) Pittsburghia	9.83	0.39	10.6498 [†]	29.2 ± 0.7	$0.202^{+0.025}_{-0.025}$	6^{+5}_{-5}	218 ± 3	[7]
(487) Venetia	8.14	0.15	13.342	70 ± 4	$0.210^{+0.020}_{-0.020}$	100^{+75}_{-75}	214 ± 10	[12]
(497) Iva	9.75	0.15	4.6209 [†]	37.4 ± 0.7	$0.139^{+0.026}_{-0.026}$	70^{+19}_{-25}	191 ± 2	[7]
(509) Iolanda	8.48	0.38	12.2909 [†]	55.1 ± 1.8	$0.222^{+0.02}_{-0.026}$	9.0^{+12}_{-9}	204 ± 3	[7][11]
(511) Davida	6.14	0.00	5.1297	307 ± 6	$0.065^{+0.003}_{-0.002}$	35^{+15}_{-17}	200 ± 15	[1]
(512) Taurinensis	10.7	0.31	5.5820 [†]	18 ± 0.7	$0.234^{+0.020}_{-0.020}$	4^{+4}_{-4}	241 ± 6	[7]
(520) Franziska	10.4	0.25	16.5045 [†]	28.1 ± 1	$0.123^{+0.027}_{-0.026}$	33^{+37}_{-27}	205 ± 3	[7]
(532) Herculina	5.94	0.33	9.4049	207.3 ± 12	$0.172^{+0.012}_{-0.024}$	15^{+10}_{-10}	221 ± 10	[3]
(537) Pauly	8.77	0.4	16.2961 [†]	41.9 ± 1	$0.276^{+0.027}_{-0.026}$	7^{+9}_{-7}	200 ± 2	[7]

Table 4 — continued

Object	H_V	G_V	P_{rot} (hr)	D_{eff} (km)	p_V	Γ^a	T_c (K)	Source(s)
(538) Friederike	9.34	0.08	46.739	76 ± 4	0.060 ^{+0.010} _{-0.010}	20 ⁺²⁵ ₋₂₀	207 ± 3	[13]
(544) Jetta	9.99	0.25	7.7453 [†]	26.9 ± 1.3	0.210 ^{+0.027} _{-0.026}	28 ⁺¹⁶ ₋₁₈	212 ± 3	[7]
(550) Senta	9.26	0.31	20.5726 [†]	37.8 ± 0.9	0.223 ^{+0.024} _{-0.024}	26 ⁺³⁴ ₋₂₆	211 ± 3	[7]
(556) Phyllis	9.56	—	4.923	35.6 ± 0.9	0.209 ^{+0.010} _{-0.010}	30 ⁺¹² ₋₁₁	235 ± 7	[8]
(562) Salome	9.87	0.19	6.3503 [†]	33.8 ± 0.7	0.158 ^{+0.024} _{-0.024}	7 ⁺³ ₋₇	206 ± 5	[7]
(573) Recha	9.35	0.2	7.1659 [†]	40.1 ± 1.1	0.172 ^{+0.023} _{-0.023}	45 ⁺¹⁵ ₋₁₅	225 ± 4	[7]
(590) Tomyris	9.98	0.25	5.5525 [†]	32.1 ± 1.2	0.154 ^{+0.029} _{-0.028}	18 ⁺²⁶ ₋₁₈	209 ± 2	[7]
(617) Patroclus	7.95	0.12	103.02	106 ± 11	0.103 ^{+0.007} _{-0.004}	20 ⁺¹⁵ ₋₁₅	155 ± 10	[3]
(624) Hektor	7.3	0.33	6.9205 [†]	186 ± 20	0.058 ^{+0.017} _{-0.007}	6 ⁺⁴ ₋₆	167 ± 3	[5]
(644) Cosima	10.7	0.32	7.5571 [†]	19.4 ± 0.5	0.205 ^{+0.030} _{-0.030}	46 ⁺²⁴ ₋₂₁	208 ± 3	[7]
(653) Berenike	9.19	0.21	12.4836 [†]	46 ± 3	0.180 ^{+0.020} _{-0.030}	40 ⁺¹²⁰ ₋₄₀	217 ± 1	[13]
(669) Kypria	9.82	0.12	14.2789 [†]	30.4 ± 1.1	0.195 ^{+0.034} _{-0.033}	33 ⁺²² ₋₃₀	206 ± 2	[7]
(673) Edda	9.90	0.14	22.3341 [†]	38 ± 5	0.130 ^{+0.030} _{-0.050}	3 ⁺³³ ₋₃	225 ± 2	[13]
(687) Tinette	11.4	0.17	7.3971	21.8 ± 0.6	0.087 ^{+0.025} _{-0.025}	50 ⁺¹⁵ ₋₁₅	204 ± 2	[7]
(694) Ekard	8.97	0.10	5.9220 [†]	109.5 ± 1.5	0.038 ^{+0.002} _{-0.002}	120 ⁺²⁰ ₋₂₀	166 ± 10	[3]
(720) Bohlina	9.54	0.22	8.9186 [†]	41 ± 1	0.160 ^{+0.005} _{-0.004}	100 ⁺¹⁰⁰ ₋₃₀	217 ± 10	[3]
(731) Sorga	9.62	0.31	8.1863 [†]	37.2 ± 1.4	0.161 ^{+0.020} _{-0.020}	76 ⁺⁴⁴ ₋₃₆	198 ± 2	[7]
(749) Malzovia	11.5	0.21	5.9275 [†]	13.5 ± 0.5	0.207 ^{+0.028} _{-0.028}	63 ⁺³⁷ ₋₂₈	237 ± 5	[7]
(756) Lilliania	9.67	0.06	7.8325	61 ± 1.3	0.059 ^{+0.030} _{-0.030}	9 ⁺⁷ ₋₉	206 ± 2	[7]
(757) Portlandia	9.92	0.16	6.5811 [†]	32.9 ± 0.5	0.158 ^{+0.025} _{-0.025}	56 ⁺⁸ ₋₁₁	237 ± 6	[7]
(771) Libera	10.3	0.32	5.8904 [†]	30.3 ± 2.8	0.154 ^{+0.022} _{-0.024}	65 ⁺⁸⁵ ₋₃₅	206 ± 8	[5][11]
(784) Pickeringia	9.15	0.13	13.1700 [†]	78.4 ± 1.7	0.054 ^{+0.026} _{-0.026}	41 ⁺²³ ₋₂₁	197 ± 1	[7]
(787) Moskva	9.75	0.37	6.0558 [†]	30.5 ± 0.5	0.213 ^{+0.018} _{-0.018}	21 ⁺²³ ₋₁₉	220 ± 3	[7]
(789) Lena	11.1	0.19	5.8423 [†]	21.5 ± 0.8	0.116 ^{+0.025} _{-0.024}	33 ⁺²¹ ₋₃₃	216 ± 3	[7]
(802) Epyaxa	12.6	0.24	4.3901 [†]	7.2 ± 0.5	0.268 ^{+0.040} _{-0.040}	62 ⁺⁷ ₋₇	225 ± 11	[7]
(808) Merxia	9.74	0.28	30.6297	28.9 ± 0.5	0.229 ^{+0.021} _{-0.021}	112 ⁺²⁸ ₋₂₂	219 ± 4	[7]
(810) Atossa	12.4	0.29	4.3855 [†]	8.1 ± 0.3	0.242 ^{+0.051} _{-0.051}	68 ⁺²⁷ ₋₃₃	223 ± 7	[7]
(816) Juliania	10.2	0.09	10.5627 [†]	48.8 ± 0.7	0.054 ^{+0.028} _{-0.028}	13 ⁺²⁷ ₋₁₃	229 ± 3	[7]
(832) Karin	11.1	0.16	18.3512	17 ± 2	0.230 ^{+0.050} _{-0.060}	65 ⁺²¹⁵ ₋₆₅	212 ± 3	[5]
(834) Burnhamia	9.34	0.23	13.8760 [†]	67 ± 7	0.074 ^{+0.014} _{-0.016}	22 ⁺³⁰ ₋₂₀	217 ± 3	[13]
(852) Wladilena	10.1	0.39	4.6133	26.6 ± 0.3	0.205 ^{+0.023} _{-0.022}	53 ⁺²⁶ ₋₂₃	225 ± 1	[7]
(857) Glasenappia	11.3	0.25	8.2076 [†]	12.2 ± 0.5	0.297 ^{+0.022} _{-0.024}	45 ⁺⁴² ₋₅₀	244 ± 8	[7][11]
(867) Kovacia	11.2	0.13	8.6781 [†]	24.5 ± 1	0.075 ^{+0.026} _{-0.026}	17 ⁺²³ ₋₁₇	198 ± 3	[7]
(873) Mechthild	11.2	0.14	11.0064 [†]	31.8 ± 0.5	0.053 ^{+0.026} _{-0.026}	46 ⁺⁵³ ₋₄₆	234 ± 1	[7]
(874) Rotraut	9.9	0.14	14.3007 [†]	51.7 ± 0.7	0.066 ^{+0.026} _{-0.026}	49 ⁺¹⁰ ₋₁₄	210 ± 2	[7]
(890) Waltraut	10.3	0.2	12.5831 [†]	29.2 ± 1.1	0.125 ^{+0.032} _{-0.032}	94 ⁺²⁶ ₋₃₄	211 ± 3	[7]
(900) Rosalinde	11.4	0.19	16.6868 [†]	20.5 ± 0.7	0.099 ^{+0.024} _{-0.024}	7 ⁺⁷ ₋₇	221 ± 3	[7]
(915) Cosette	11.5	0.34	4.4697 [†]	12.4 ± 0.4	0.237 ^{+0.031} _{-0.030}	36 ⁺³⁸ ₋₃₆	225 ± 7	[7]
(934) Thuringia	9.88	0.12	8.1653 [†]	52.3 ± 1	0.061 ^{+0.027} _{-0.027}	5 ⁺⁵ ₋₅	203 ± 3	[7]
(956) Elisa	12.0	0.25	16.494	10.6 ± 0.8	0.228 ^{+0.020} _{-0.024}	100 ⁺⁵⁰ ₋₇₀	270 ± 10	[3]
(958) Asplinda	10.2	0.36	25.305	46 ± 0.9	0.054 ^{+0.019} _{-0.019}	1 ⁺³ ₋₁	200 ± 2	[7]
(984) Gretia	9.53	0.38	5.7780 [†]	33.9 ± 0.9	0.223 ^{+0.017} _{-0.019}	21 ⁺¹⁶ ₋₁₅	202 ± 3	[7][11]

Table 4 — continued

Object	H_V	G_V	P_{rot} (hr)	D_{eff} (km)	p_V	Γ^a	T_c (K)	Source(s)
(998) Bodea	11.3	0.15	8.5741 [†]	29.4 ± 0.5	$0.052^{+0.025}_{-0.025}$	12^{+4}_{-9}	198 ± 3	[7]
(1013) Tombecka	10.0	0.22	6.0502 [†]	33.7 ± 0.8	$0.132^{+0.023}_{-0.023}$	52^{+18}_{-12}	209 ± 3	[7]
(1017) Jacqueline	10.8	0.1	7.8715 [†]	37.8 ± 1.3	$0.046^{+0.028}_{-0.028}$	38^{+31}_{-38}	223 ± 2	[7]
(1036) Ganymed	9.24	0.31	10.31	36 ± 1	$0.230^{+0.100}_{-0.100}$	30^{+70}_{-20} 24^{+8}_{-8} 47^{+17}_{-17} 96^{+21}_{-21}	192 ± 6 180 ± 10 204 ± 10 240 ± 10	[5][11][20] [20] [20] [20]
(1056) Azalea	11.5	0.2	15.0276	11.5 ± 0.3	$0.272^{+0.029}_{-0.028}$	4^{+4}_{-4}	230 ± 4	[7]
(1087) Arabis	9.68	0.21	5.795	34.4 ± 0.5	$0.174^{+0.023}_{-0.023}$	1^{+1}_{-1}	205 ± 3	[7]
(1102) Pepita	9.28	0.24	5.1053 [†]	35.5 ± 0.5	$0.246^{+0.023}_{-0.022}$	9^{+11}_{-9}	204 ± 3	[7]
(1119) Euboea	11.2	0.24	11.3981 [†]	30.2 ± 0.6	$0.054^{+0.022}_{-0.022}$	9^{+6}_{-6}	241 ± 2	[7]
(1127) Mimi	10.4	0.15	12.7456 [†]	46.9 ± 0.8	$0.045^{+0.025}_{-0.025}$	8^{+2}_{-2}	213 ± 4	[7]
(1130) Skuld	11.8	0.22	4.8076 [†]	9.7 ± 0.3	$0.301^{+0.023}_{-0.023}$	3^{+3}_{-3}	242 ± 4	[7]
(1140) Crimea	9.62	0.21	9.7869 [†]	29.6 ± 0.9	$0.259^{+0.022}_{-0.024}$	23^{+15}_{-23}	211 ± 2	[7][11]
(1173) Anchises	8.66	0.24	11.6095	136 ± 18	$0.033^{+0.003}_{-0.002}$	50^{+50}_{-25}	171 ± 10	[3]
(1188) Gothlandia	11.5	0.25	3.4918 [†]	13.2 ± 0.1	$0.237^{+0.020}_{-0.021}$	45^{+25}_{-25}	222 ± 7	[7][11]
(1210) Morosovia	9.83	0.11	15.2609 [†]	34.7 ± 1	$0.153^{+0.027}_{-0.027}$	65^{+25}_{-35}	219 ± 4	[7]
(1241) Dysona	9.49	0.22	8.6074 [†]	76.8 ± 2.3	$0.043^{+0.023}_{-0.023}$	23^{+22}_{-23}	205 ± 3	[7]
(1276) Ucclia	10.6	0.04	4.9075 [†]	36 ± 0.9	$0.068^{+0.032}_{-0.032}$	63^{+17}_{-18}	206 ± 3	[7]
(1291) Phryne	10.3	0.25	5.5841 [†]	26.7 ± 1.3	$0.168^{+0.020}_{-0.020}$	20^{+18}_{-20}	206 ± 4	[7][11]
(1301) Yvonne	11.1	0.17	7.3197 [†]	21.2 ± 0.9	$0.111^{+0.025}_{-0.025}$	1^{+1}_{-1}	209 ± 4	[7]
(1339) Desagneauxa	10.7	0.22	9.3751	25.4 ± 1.1	$0.122^{+0.025}_{-0.024}$	63^{+17}_{-23}	207 ± 9	[7]
(1360) Tarka	11.2	0.07	8.8661 [†]	29.4 ± 0.4	$0.059^{+0.030}_{-0.030}$	40^{+5}_{-5}	217 ± 3	[7]
(1386) Storeria	13.1	0.19	8.6780 [†]	10.1 ± 0.7	$0.069^{+0.024}_{-0.024}$	52^{+12}_{-51}	217 ± 3	[7]
(1388) Aphrodite	10.7	0.16	11.9439	21.1 ± 0.5	$0.182^{+0.025}_{-0.025}$	69^{+21}_{-24}	206 ± 2	[7]
(1401) Lavonne	11.9	0.27	3.9326 [†]	9.3 ± 0.4	$0.304^{+0.032}_{-0.032}$	52^{+58}_{-52}	226 ± 4	[7]
(1419) Danzig	11.2	0.19	8.1196 [†]	14.2 ± 0.6	$0.239^{+0.025}_{-0.025}$	54^{+31}_{-42}	253 ± 7	[7]
(1424) Sundmania	9.73	0.14	94.5371 [†]	61.6 ± 2.9	$0.047^{+0.026}_{-0.026}$	14^{+17}_{-14}	221 ± 2	[7]
(1432) Ethiopia	12.0	0.28	9.8458	7.15 ± 0.67	$0.535^{+0.058}_{-0.070}$	71^{+180}_{-65}	218 ± 8	[11]
(1436) Salonta	10.1	0.16	8.8699 [†]	55.9 ± 0.9	$0.047^{+0.025}_{-0.025}$	2^{+6}_{-2}	209 ± 3	[7]
(1472) Muonio	12.4	0.35	8.7054 [†]	9.1 ± 1.3	$0.230^{+0.090}_{-0.060}$	25^{+65}_{-25}	216 ± 6	[5]
(1495) Helsinki	11.4	0.36	5.3312 [†]	12.8 ± 0.3	$0.285^{+0.040}_{-0.040}$	19^{+13}_{-13}	229 ± 5	[7][11]
(1508) Kemi	11.7	0.12	9.1918 [†]	14.8 ± 0.2	$0.146^{+0.027}_{-0.027}$	16^{+8}_{-6}	191 ± 6	[7]
(1545) Thernoe	11.5	0.12	17.203	17.29 ± 0.86	$0.124^{+0.027}_{-0.027}$	27^{+27}_{-27}	209 ± 4	[7]
(1568) Aisleen	11.5	0.13	6.68	11.8 ± 0.04	$0.268^{+0.030}_{-0.030}$	51^{+30}_{-15}	212 ± 8	[7][11]
(1580) Betulia	14.8	0.15	6.1383 [†]	5.4 ± 0.54	$0.070^{+0.010}_{-0.010}$	175^{+51}_{-51} 193^{+40}_{-33} 200^{+10}_{-10}	261 ± 10 332 ± 10 336 ± 10	[3][20] [20] [20]
(1607) Mavis	11.3	0.26	6.1478 [†]	13.7 ± 0.7	$0.265^{+0.032}_{-0.032}$	60^{+50}_{-45}	204 ± 4	[7][11]
(1618) Dawn	11.1	0.31	43.2191	16.3 ± 0.6	$0.186^{+0.020}_{-0.020}$	5^{+5}_{-5}	214 ± 4	[7]
(1620) Geographos	14.8	0.11	5.2233 [†]	2.46 ± 0.03	$0.344^{+0.060}_{-0.062}$	340^{+140}_{-100}	332 ± 10	[3]
(1627) Ivar	12.6	0.33	4.7952 [†]	8 ± 0.7	$0.255^{+0.020}_{-0.014}$	100^{+120}_{-40}	244 ± 4	[5]

Table 4 — continued

Object	H_V	G_V	P_{rot} (hr)	D_{eff} (km)	p_V	Γ^a	T_c (K)	Source(s)
(1672) Gezelle	11.3	0.19	40.6825 [†]	25 ± 0.9	$0.064^{+0.024}_{-0.024}$	10^{+10}_{-10}	205 ± 2	[7]
(1691) Oort	10.7	0.16	10.2684 [†]	36.2 ± 1.7	$0.054^{+0.025}_{-0.025}$	32^{+17}_{-32}	197 ± 3	[7]
(1701) Okavango	10.4	0.13	13.1918 [†]	20.1 ± 1.2	$0.241^{+0.027}_{-0.027}$	35^{+35}_{-35}	231 ± 3	[7]
(1704) Wachmann	12.9	0.3	3.3139 [†]	6.6 ± 0.1	$0.235^{+0.023}_{-0.023}$	110^{+50}_{-50}	240 ± 7	[7]
(1723) Klemola	10.0	0.26	6.2561	31.6 ± 0.9	$0.151^{+0.021}_{-0.021}$	34^{+15}_{-9}	216 ± 3	[7]
(1738) Oosterhoff	12.4	0.24	4.4490 [†]	8 ± 0.2	$0.261^{+0.065}_{-0.065}$	60^{+49}_{-20}	230 ± 10	[7]
(1742) Schaifers	11.1	0.18	8.5327 [†]	15.3 ± 0.6	$0.229^{+0.056}_{-0.056}$	91^{+18}_{-21}	202 ± 5	[7]
(1789) Dobrovolsky	12.1	0.23	4.8111	8.6 ± 0.2	$0.284^{+0.035}_{-0.035}$	15^{+5}_{-9}	233 ± 7	[7]
(1820) Lohmann	13.1	0.16	14.0449 [†]	6.1 ± 0.3	$0.234^{+0.041}_{-0.041}$	118^{+22}_{-8}	226 ± 9	[7]
(1837) Osita	12.7	0.21	3.8188	6.9 ± 0.3	$0.264^{+0.025}_{-0.025}$	111^{+19}_{-21}	244 ± 7	[7]
(1862) Apollo	15.9	0.22	3.0654 [†]	1.55 ± 0.07	$0.316^{+0.031}_{-0.042}$	140^{+140}_{-100}	352 ± 10	[19]
(1865) Cerberus	16.6	0.37	6.8033 [†]	1.2 ± 0.1	$0.280^{+0.035}_{-0.034}$	300^{+2200}_{-0}	250 ± 15	[5]
(1902) Shaposhnikov	9.24	0.2	20.9958 [†]	79 ± 3.2	$0.045^{+0.023}_{-0.023}$	15^{+15}_{-15}	177 ± 2	[7]
(1906) Neaf	12.7	—	11.01	7.728 ± 0.41	$0.246^{+0.014}_{-0.024}$	70^{+19}_{-16}	230 ± 6	[8]
(1930) Lucifer	10.9	0.25	13.0536	30.7 ± 1.3	$0.081^{+0.022}_{-0.022}$	60^{+50}_{-25}	210 ± 3	[7]
(1980) Tezcatlipoca	13.6	0.18	7.2523 [†]	5.6 ± 0.7	$0.210^{+0.080}_{-0.080}$	200^{+400}_{-190}	227 ± 8	[5][11]
(1987) Kaplan	11.4	0.26	12.5964 [†]	25.7 ± 0.7	$0.122^{+0.026}_{-0.025}$	27^{+16}_{-19}	216 ± 3	[7]
(2156) Kate	12.4	0.19	5.6228	8.04 ± 0.45	$0.294^{+0.021}_{-0.025}$	56^{+23}_{-23}	215 ± 1	[11]
(2511) Patterson	12.7	—	4.141	9.034 ± 1.12	$0.180^{+0.055}_{-0.034}$	90^{+58}_{-43}	220 ± 6	[8]
(2606) Odessa	11.7	0.21	8.2444	17 ± 2.5	$0.13^{+0.04}_{-0.04}$	90^{+80}_{-40}	180 ± 7	[5]
(2617) Jiangxi	10.3	0.17	11.7730 [†]	51.3 ± 2.9	$0.039^{+0.025}_{-0.025}$	6^{+6}_{-6}	230 ± 3	[7]
(2659) Millis	11.5	0.12	6.1246 [†]	27.2 ± 0.8	$0.052^{+0.027}_{-0.027}$	36^{+18}_{-20}	202 ± 2	[7]
(2867) Steins	12.8	0.23	6.0468 [†]	5.3 ± 0.4	$0.450^{+0.037}_{-0.052}$	210^{+30}_{-30}	230 ± 10	[10]
(3200) Phaethon	14.3	0.15	3.6040 [†]	5.1 ± 0.2	$0.122^{+0.008}_{-0.008}$	600^{+200}_{-200}	311 ± 10	[6]
(3281) Maupertuis	12.7	—	6.73	5.509 ± 0.44	$0.484^{+0.051}_{-0.074}$	60^{+58}_{-31}	232 ± 12	[8]
(3428) Roberts	11.9	0.16	3.2784 [†]	17.3 ± 0.6	$0.086^{+0.025}_{-0.025}$	66^{+14}_{-21}	198 ± 2	[7]
(3544) Borodino	12.3	0.19	5.4346	8.3 ± 0.3	$0.261^{+0.037}_{-0.037}$	61^{+28}_{-26}	237 ± 18	[7]
(3678) Mongmanwai	12.5	0.18	4.1830 [†]	8.5 ± 0.3	$0.183^{+0.069}_{-0.069}$	72^{+17}_{-17}	205 ± 8	[7]
(4077) Asuka	10.8	0.11	7.9231	19.3 ± 0.4	$0.189^{+0.032}_{-0.032}$	10^{+4}_{-4}	202 ± 3	[7]
(4265) Kani	12.9	0.21	5.7276 [†]	14 ± 0.7	$0.048^{+0.023}_{-0.023}$	6^{+6}_{-6}	218 ± 4	[7]
(4606) Saheki	12.9	0.2	4.9735 [†]	6.8 ± 0.4	$0.211^{+0.040}_{-0.040}$	9^{+11}_{-9}	225 ± 13	[7]
(4611) Vulkaneifel	11.9	0.27	3.756	12.1 ± 1.12	$0.216^{+0.023}_{-0.028}$	32^{+23}_{-32}	202 ± 1	[11]
(4800) Veveri	11.7	0.12	6.2157	13.3 ± 0.6	$0.173^{+0.027}_{-0.027}$	39^{+25}_{-29}	218 ± 7	[7]
(5489) Oberkochen	11.5	0.24	5.6244	14.6 ± 0.4	$0.191^{+0.027}_{-0.027}$	18^{+16}_{-12}	214 ± 3	[7]
(5625) Jamesferguson	12.8	0.17	6.671	14.46 ± 0.86	$0.062^{+0.005}_{-0.006}$	52^{+14}_{-15}	204 ± 1	[11]
(6136) Gryphon	11.5	0.2	16.4684 [†]	15.3 ± 0.5	$0.160^{+0.023}_{-0.023}$	38^{+17}_{-13}	213 ± 4	[7]
(6159) Andreseloy	13.4	0.18	10.639	5.65 ± 1.37	$0.246^{+0.061}_{-0.061}$	61^{+177}_{-61}	222 ± 2	[11]
(6635) Zuber	14.0	0.21	5.5356 [†]	3.6 ± 0.1	$0.326^{+0.060}_{-0.060}$	52^{+48}_{-49}	237 ± 11	[7]
(7001) Neother	13.3	—	9.581	5.923 ± 0.38	$0.241^{+0.034}_{-0.013}$	20^{+21}_{-20}	235 ± 7	[8]
(8359) 1989 WD	13.2	0.2	2.8910 [†]	8.1 ± 0.5	$0.116^{+0.031}_{-0.031}$	86^{+64}_{-41}	218 ± 11	[7]
(9158) Plate	13.6	—	5.165	4.113 ± 0.14	$0.379^{+0.026}_{-0.024}$	10^{+19}_{-10}	227 ± 21	[8]
(12088) Macalintal	14.0	—	3.342	3.591 ± 0.330	$0.340^{+0.051}_{-0.052}$	70^{+68}_{-53}	210 ± 22	[8]

Table 4 — continued

Object	H_V	G_V	P_{rot} (hr)	D_{eff} (km)	p_V	Γ^a	T_c (K)	Source(s)
(15032) Alexlevin	14.5	—	4.405	2.832 ± 0.15	$0.349^{+0.024}_{-0.035}$	20^{+15}_{-20}	229 ± 12	[8]
(19848) Yeungchuchiu	12.0	0.09	3.4510^\dagger	11.05 ± 1.14	$0.170^{+0.078}_{-0.078}$	18^{+17}_{-17}	211 ± 5	[7]
(25143) Itokawa	19.4	0.21	12.132	0.32 ± 0.03	$0.300^{+0.04}_{-0.037}$	700^{+100}_{-100}	337 ± 10	[3]
(29075) 1950 DA	16.7	0.23	2.1216	1.3 ± 0.13	$0.200^{+0.026}_{-0.031}$	24^{+20}_{-14}	280 ± 10	[3]
(33342) 1998 WT24	18.5	0.4	3.697	0.35 ± 0.04	$0.56^{+0.20}_{-0.20}$	200^{+100}_{-100}	315 ± 10	[3]
(54509) YORP	23.4	1.24	0.2029	0.092 ± 0.01	$0.086^{+0.185}_{-0.060}$	700^{+500}_{-500}	360 ± 10	[3]
(99942) Apophis	19.7	0.25	30.56	0.375 ± 0.014	$0.166^{+0.043}_{-0.035}$	150^{+350}_{-100}	362 ± 10	[3]
(101955) Bennu	20.1	-0.0	4.2975^\dagger	0.484 ± 0.01	$0.063^{+0.005}_{-0.005}$	310^{+70}_{-70}	338 ± 10	[3]
(155140) 2005 UD	17.5	—	5.235	1.3 ± 0.2	$0.100^{+0.020}_{-0.020}$	300^{+120}_{-110}	343 ± 18	[4]
(162173) Ryugu	19.3	0.15	7.63	0.87 ± 0.03	$0.044^{+0.007}_{-0.006}$	350^{+250}_{-250}	250 ± 10	[3]
(175706) 1996 FG3	18.4	0.15	3.5942	1.63 ± 0.04	$0.029^{+0.004}_{-0.004}$	80^{+40}_{-40}	328 ± 15	[3]
(276049) 2002 CE26	15.8	-0.2	3.2931	3.5 ± 0.4	$0.07^{+0.02}_{-0.02}$	54^{+27}_{-27}	208 ± 10	[20]
						102^{+30}_{-30}	260 ± 10	[20]
						172^{+34}_{-34}	304 ± 10	[20]
(308635) 2005 YU55	21.9	-0.1	19.31	0.31 ± 0.025	$0.032^{+0.004}_{-0.005}$	550^{+250}_{-200}	325 ± 10	[3]
(341843) 2008 EV5	20	0.4	3.725	0.31 ± 0.006	$0.184^{+0.082}_{-0.057}$	450^{+60}_{-60}	321 ± 15	[3]
2002 NY40	19.2	0.15	19.98	0.28 ± 0.03	$0.34^{+0.06}_{-0.06}$	100^{+50}_{-50}	363 ± 15	[17]

Note and References. † Indicates that the reported P_{rot} value has been rounded to four decimal places.

- [1] Alí-Lagoa et al. (2020)
- [2] Capria et al. (2014)
- [3] Delbo' et al. (2015)
- [4] Devogèle et al. (2020)
- [5] Hanuš et al. (2015)
- [6] Hanuš et al. (2016)
- [7] Hanuš et al. (2018)
- [8] Jiang et al. (2020)
- [9] Keihm et al. (2012)
- [10] Leyrat et al. (2011)
- [11] MacLennan and Emery (2019)
- [12] Marciniak et al. (2018)
- [13] Marciniak et al. (2019)
- [14] Marsset et al. (2017)
- [15] Matter et al. (2013)
- [16] Müller and Blommaert (2004)
- [17] Müller, T. G. et al. (2004)
- [18] Pravec et al. (2019)
- [19] Rozitis et al. (2013)
- [20] Rozitis et al. (2018)
- [21] Yu et al. (2017)